

Department of Civil Engineering
Professional Paper P73-1

CONTRIBUTIONS TO THE FIFTH WORLD CONFERENCE
ON EARTHQUAKE ENGINEERING

To Be Held
June 25-29, 1973
In Rome, Italy

by

Members of the Structures Division
Robert V. Whitman, Editor

Any opinions, findings, conclusions
or recommendations expressed in this
publication are those of the author(s)
and do not necessarily reflect the views
of the National Science Foundation.

P73-1

Structures Publication No. 360

January 1973

ACKNOWLEDGEMENTS

The research reported in the first eight Contributions to the Fifth World Conference on Earthquake Engineering was supported in part by four National Science Foundation Grants: GK-27955, GK-26296, GI-29936 and GI-35139.

The ninth paper was prepared by members of the Laboratório Nacional de Engenharia Civil in Lisbon, Portugal.



TABLE OF CONTENTS

1. EARTHQUAKE DAMAGE PROBABILITY MATRICES
by Robert V. Whitman, John W. Reed and Sheu-Tien Hong
2. METHODOLOGY FOR OPTIMUM SEISMIC DESIGN
by E.H. Vanmarcke, C.A. Cornell, R.V. Whitman and J.W. Reed
3. PROBABILISTIC SEISMIC RESPONSE OF SIMPLE INELASTIC SYSTEMS
by E.H. Vanmarcke and D. Veneziano
4. PROBABILISTIC SEISMIC ANALYSIS OF LIGHT EQUIPMENT WITHIN BUILDINGS
by M.K. Chakravorty and E.H. Vanmarcke
5. AFTERSHOCKS IN ENGINEERING SEISMIC RISK ANALYSIS
by Hans A. Merz and C.A. Cornell
6. NONLINEAR DYNAMIC ANALYSIS OF BUILDINGS WITH TORSIONAL EFFECTS
by S.A. Anagnostopoulos, J.M. Roesset and J.M. Biggs
7. DUCTILITY REQUIREMENTS FOR SOME NONLINEAR SYSTEMS SUBJECTED TO EARTHQUAKES
by S.A. Anagnostopoulos and J.M. Roesset
8. A COMPARISON OF LINEAR AND EXACT NONLINEAR ANALYSES OF SOIL AMPLIFICATION
by I.V. Constantopoulos, J.M. Roesset and J.T. Christian
9. SEISMIC STUDIES OF PARQUE CENTRAL BUILDINGS
by M. Paparoni, J. Ferry Borges, A. Ravara and R.V. Whitman
(Prepared in the Laboratório Nacional de Engenharia Civil,
in Lisbon, Portugal)

EARTHQUAKE DAMAGE PROBABILITY MATRICES

by

Robert V. Whitman^I, John W. Reed^{II} and Sheu-Tien Hong^{III}

SYNOPSIS

A format is presented for organizing and portraying statistical data concerning damage to buildings caused by earthquake. This format uses 9 categories of damage, identified both by subjective word descriptions and by ratio of damage cost to building replacement cost. The form of such statistical damage information is illustrated by data collected for damage caused by the 1971 San Fernando earthquake, and the trends brought out by these data are discussed.

INTRODUCTION

In any systematic analysis of earthquake risk or optimum seismic protection (1, 5, 6), it is necessary to express the degree of damage that will be experienced by a set of buildings when these buildings are exposed to different intensities of ground shaking. Even similar buildings will respond somewhat differently to a given ground shaking. Moreover, minor details in the pattern of ground motion can significantly influence the response of a building, and these details vary among ground motions all having the same nominal intensity. Hence the degree of damage must be expressed in probabilistic terms. Fig. 1 shows the form of the damage probability matrix (DPM) used in this study. Each number in the matrix is the probability that a building will experience a particular level of damage as the result of a particular intensity. The probabilities in each column must sum to unity or to 100%.

Two general approaches may be used to develop DPMs. One approach is to compile statistics empirically from experiences during actual earthquakes. This first approach relates damage directly to some measure of intensity. Alternatively, the response (and damage) of buildings to various ground motions may be predicted by theoretical dynamic analysis.

This paper presents empirical DPMs compiled from a survey of damage to buildings, having 5 or more stories, shaken by the San Fernando

^I Professor of Civil Engineering and Head of Structural Engineering, Massachusetts Institute of Technology, Cambridge, Massachusetts, USA.

^{II} Senior Research Engineer, URS/John A. Blume Associates Research Division, Las Vegas, Nevada, USA.

^{III} Research Associate, Department of Civil Engineering, Massachusetts Institute of Technology, Cambridge, Massachusetts, USA.

earthquake of 9 February 1971.

DAMAGE STATES

To describe and categorize the damage that a building might experience, a set of damage states has been developed. This scale of damage, shown in Figs. 1 and 3, runs from 0 to 8. Each damage state is identified by: (a) a subjective description of physical damage, and (b) an objective ratio of repair cost to replacement cost. The relationship between the two identifiers has been developed from experience during the San Fernando earthquake, but is believed to have general applicability. While the DPMs presented in this paper are based upon actual repair costs; for other earthquakes, only the more qualitative damage information may be available. More specific and detailed damage descriptions have been developed, but must vary for different classes of buildings based upon the details of construction.

It must be emphasized that the cost ratios in Fig. 1 are primarily a means for identifying a damage state, and in general are not the true cost of a particular level of damage. Replacement cost at the time of the earthquake has been used since it is a more-or-less definite quantity and independent of changable factors such as assessing practice, market conditions and inflation. For certain types of risk studies, the ratio of repair cost to market value might be a more meaningful statistic; such a conversion can always be made by the user of the DPMs. More importantly, there may be important monetary, human and social costs in addition to the direct repair cost: injuries and death, loss of income, etc. Such associated costs, while linked to the damage state, vary depending upon the value attached to human and social losses.

A probability damage matrix is a set of probability mass functions for damage, given the intensity. As is true for most probability mass functions, it is difficult to evaluate with confidence each number in a column of a damage probability matrix. For some applications, it may suffice to use mean damage ratios (MDRs): that is, for each intensity, evaluate only the expected value of damage. If only repair costs were of interest, then the MDR as a function of intensity (plus possibly some measure of the variance from this mean) would provide essentially all of the information needed for risk studies. However, associated costs usually will be determined by the likelihood that high damage states will occur, and hence it usually is necessary to assume the specific probabilities for these higher states. However, MDR is at least a useful indication of the relative damage to different types of buildings during different earthquakes.

SAN FERNANDO EARTHQUAKE DAMAGE SURVEY

The ideal way to prepare damage statistics is to start with a complete list of buildings, together with their pertinent characteristics, and then determine the nature, and actual cost of repair, of damage. Buildings that were strongly shaken but had little or no damage are of as much interest as heavily damaged buildings, since they indicate a measure

of success in earthquake resistant design.

The MIT survey of damage caused by the San Fernando earthquake specifically covered buildings having 5 or more stories. There were several reasons for these restrictions: (a) others were studying damage to low residential buildings, and (b) there was a desire to focus upon buildings in which engineering design plays an important role. No list of such buildings was available at the start of the survey; hence it was necessary to piece together a list from various sources.

It was determined that there were approximately 1600 such buildings within area of the map in Fig. 2. About 40% of these buildings were built prior to 1933 when building codes did not specifically require earthquake resistant design. Another 56% were built since 1947 under modern code provisions. Ignoring the relatively few tall buildings constructed during the Depression and World War II (1933 - 1947), the distribution of these buildings according to age, height and intensity zone is given in Table 1. Thus far in the study, intensity of ground shaking has been represented by the modified Mercalli (MM) scale. Most of the buildings were within the zone of MM VII, where the measured peak horizontal ground accelerations ranged from about 0.1g to about 0.2g. (In a subsequent stage of the study, a more quantitative measure of the intensity of ground shaking will be used.) This final list undoubtedly still is not entirely correct, containing some structures that do not belong and omitting some that belong. However, this list gives a very adequate picture of the number and type of buildings shaken by the earthquake.

While considerable information was already available concerning buildings with considerable damage (2, 4), it became necessary to utilize a questionnaire to obtain statistics concerning less-damaged buildings. A sample, one-page questionnaire was developed, asking owners for data on building characteristics, total repair cost, and breakdown by type of damage (structural, partitions, mechanical, etc.). About 1240 questionnaires were sent, with a covering letter from the Building Owners and Managers Association (BOMA). Unanswered questionnaires were followed up by telephone and visits. By these questionnaires, plus lesser amounts of information from other sources, damage costs were assembled for about 370 buildings. Table 2 gives the breakdown of these buildings by age, intensity zone and height (omitting the few buildings built between 1933 - 1947).

All of the data concerning building characteristics and damage cost was digitized for storing and processing by computer. DPMs and MDRs can be generated by the computer for different building types, different ages of buildings, different assumptions concerning boundaries between intensity zones, different methods for relating replacement cost to building characteristics, etc. The results presented in the following section are based upon the intensity zones in Fig. 2; buildings in areas where the intensity clearly exceeded VIII are excluded from the survey. In constructing DPMs, buildings were assigned to damage states on the basis of damage ratio, using the best estimate for damage cost and the best estimate of replacement cost. Where possible, replacement cost was evaluated as the permit value inflated to the date of the San Fernando earthquake. Alter-

natively, replacement cost was evaluated from building area times an average building cost per unit area. MDRs were computed by averaging the actual, individual damage ratios.

DAMAGE MATRICES AND DAMAGE RATIOS FOR SAN FERNANDO EARTHQUAKE

The damage that occurred in MM VII of the San Fernando earthquake is summarized in Table 3 in the form of damage probabilities. Buildings have been divided into several different categories according to date of construction, height and type of construction (concrete or steel). The results do show clearly that buildings designed under modern codes did fare better than the older buildings. The apparent erratic behavior of the probabilities in any column may be due in part to the range of damage ratios used for each damage state.

Since data was obtained for fewer buildings in intensity MM VI and VIII, it is less meaningful to construct DPMs for different building heights and type of construction. Table 4 presents results when all buildings in an age group are lumped together. The expected increase in damage with increasing intensity is very evident. The damage was very small in MM VI. (Note that modern buildings actually had more damage than old buildings in this zone.) In MM VIII, the damage, especially to concrete buildings, was quite significant.

These trends emerge even more clearly when the mean damage ratios (MDRs) are examined. A few other observations may be made from study of the MDRs:

1. For the newer buildings in MM VII, the MDR decreases as the story height increases above the 8 to 13 story range (see Fig. 4). This may represent confirmation of the frequently heard belief that the current code is more conservative for very tall buildings than for short buildings. Alternatively, it may simply mean that more attention is paid to the design details of unusually tall buildings.
2. For the older steel buildings in MM VII (and also in MM VI although the data are not shown), the damage to steel buildings may indicate an adverse matching between the periods of the older, taller buildings and the predominant period of the ground motion at these moderate distances from an epicenter.
3. Considering all post-1947 buildings, the MDR attenuates more rapidly with distance for 5 to 7 stories than for 8 to 13 stories (see Fig. 5). These trends undoubtedly are related to differences in the rate of attenuation of high and low frequency components of the ground motion.
4. Considering all buildings, concrete buildings in zone VII were slightly more damaged than steel buildings. (However, in their specific groups this pattern might reverse.) The difference was marked in zone VIII: MDR = 16% for concrete vs. 0.4% for steel.

Since there were many buildings in each sample category, it is believed

that these trends are a realistic picture of actual behavior,

Information concerning the breakdown of total damage cost was also documented. For buildings in intensity zone VI, the damage was approximately 5% structural, 5% elevators and 90% partitions and finish. For newer buildings in zone VII, these numbers were approximately 20% structural, 5% mechanical, 10% elevators and 65% partitions and finish. In zone VIII, even though the total dollars spent for repairs increased, the percentage of these repairs spent on structural damage decreased.

Many of the trends noted above have already been observed by others based on limited data (4). This detailed and extensive study of damage caused by the San Fernando earthquake has served to document these trends in probabilistic terms.

STUDIES OF OTHER EARTHQUAKES

Damage probability matrices are also being generated for other earthquakes for which adequate records of both damage and non-damage are available or can be reconstructed. Since actual damage costs are usually not available, it has been necessary to use subjective descriptions of damage. The effort of compiling these DPMs, and comparing them with those for the San Fernando earthquake, is still in progress.

CONCLUSIONS

A methodology has been described for compiling and presenting statistics concerning damage to different types of buildings as result of earthquakes having different intensities. Statistics from the 1971 San Fernando earthquake have been presented, and the trends suggested by these statistics have been noted. While the data available today are adequate, when supplemented by theoretical studies, for initial estimates of earthquake risk, it will be important to document additional data of this type during future major earthquakes.

ACKNOWLEDGEMENTS

This study was made possible by a grant from the National Science Foundation, through the offices of Dr. Michael P. Gaus and Dr. Charles C. Thiel, and by the cooperation of the Building Owners and Management Association (BOMA) of Los Angeles. Most of the collection of building and damage data was carried out by two engineering firms in Los Angeles: J. H. Wiggins Co. and Ayres, Cohen and Hayakawa (ACH). Special credit is due to Mr. Terry Sun of ACH; Professors C. Allin Cornell and Erik H. Vanmarcke of M.I.T.; and the following M.I.T. students and research assistants: Robert Czarnecki, Jorge Diaz-Padilla, Eduardo Kausel, Craig Schweinhart, and Richard Yue.

REFERENCES

1. ESSA, 1969: "Studies in Seismicity and Earthquake Damage Statistics, 1969", Coast & Geodetic Survey, Environmental Science Services Administration (now National Oceanographic and Atmospheric Administration), U.S. Department of Commerce.
2. Frazier, G. A., J. H. Wood and G. W. Housner, 1971, "Earthquake Damage to Buildings", Engineering Features of the San Fernando Earthquake, Earthquake Engineering Research Laboratory, California Institute of Technology.
3. Scott, N., 1971, "Preliminary Report on Felt Area and Intensity", The San Fernando, California Earthquake of February 9, 1971, Geological Survey Professional Paper 733, U.S. Government Printing Office.
4. Steinbrugge, K. V., E. E. Schader, H. C. Bigglestone and C. A. Weems, 1971, San Fernando Earthquake, February 9, 1971, Pacific Fire Rating Bureau (now Insurance Services Office), San Francisco.
5. Vanmarcke, E., C. A. Cornell, R. V. Whitman and J. W. Reed, 1973, "Methodology for Optimum Seismic Design", Proc. 5th World Conference on Earthquake Engineering.
6. Wiggins, J. H. and D. F. Moran, 1971, Earthquake Safety in the City of Long Beach Based on the Concept of "Balanced Risk", J. H. Wiggins Co., Palos Verdes Estates, California.

Table 1
NUMBER OF HIGH-RISE BUILDINGS
SHAKEN BY EARTHQUAKE

No.	MM Intensity					
	Pre-1933			Post-1947		
Story	VI	VII	VIII	VI	VII	VIII
5-7	36	346	0	117	321	20
8-13	21	236	0	79	231	6
14-18	2	8	0	36	37	0
19+	0	2	0	12	41	0
Total	57	592	0	244	630	26

Table 2
NUMBER OF BUILDINGS WITH DOCUMENTATION
OF BUILDING VALUES AND DAMAGE COSTS

No.	MM Intensity					
	Pre-1933			Post-1947		
Story	VI	VII	VIII	VI	VII	VIII
5-7	10	33	14	41	14	
8-13	9	78	28	70	4	
14-18	0	2	12	19	0	
19+	0	1	3	26	0	
Total	19	114	57	156	18	

Table 3
DAMAGE PROBABILITIES (%) AND MEAN DAMAGE RATIOS (%) FOR
INTENSITY VII ZONE OF SAN FERNANDO EARTHQUAKE

Date Const.	Pre-1933				Post-1947					
	5-7		8-13		5-7		8-13		14-18	19+
No. Stories	Co	St	Co	St	Co	St	Co	St	St	St
Type of Const.	Co	St	Co	St	Co	St	Co	St	St	St
Damage State										
0	16	18	16	6	21	24	27	44	43	21
1	16	9	12	13	26	28	33	31	43	54
2	26	46	28	53	16	38	32	6	0	25
3	21	27	14	16	26	5	8	16	14	0
4	11	0	21	0	11	5	0	3	0	0
5	0	0	7	9	0	0	0	0	0	0
6	10	0	2	3	0	0	0	0	0	0
7	0	0	0	0	0	0	0	0	0	0
MDR - %	4.4	1.1	2.7	2.5	1.1	6.6	4.3	5.2	4.3	2.4
No. Bldgs.	19	11	43	32	19	21	37	32	14	24

Table 4
 DAMAGE PROBABILITIES (%) AND MEAN DAMAGE RATIOS (%)
 FOR ALL BUILDINGS IN VARIOUS INTENSITY ZONES
 OF SAN FERNANDO EARTHQUAKE

Date Const.	Pre-1933		Post 1947		
	VI	VII	VI	VII	VIII
Intensity					
Damage State					
0	90	14	79	33	6
1	10	12	18	34	17
2	0	35	3	20	39
3	0	18	0	10	11
4	0	11	0	3	5
5	0	6	0	0	11
6	0	4	0	0	6
7	0	9	0	0	5
MDR - %	0.03	2.8	0.05	0.5	7.5
No. Bldgs.	19	114	57	156	18

DAMAGE STATE	STRUCTURAL DAMAGE	NON-STRUCTURAL DAMAGE	DAMAGE RATIO (%)	INTENSITY OF EARTHQUAKE				
				V	VI	VII	VIII	IX
0	None	None	0-0.05	X	X	X	X	X
1	None	Minor	0.05-0.3	X	X	X	X	X
2	None	Localized	0.3-1.25	X	X	X	X	X
3	Not noticeable	Widespread	1.25-3.5	X	X	X	X	X
4	Minor	Substantial	3.5-7.5	X	X	X	X	X
5	Substantial	Extensive	7.5-20	X	X	X	X	X
6	Major	Nearly total	20-65	X	X	X	X	X
7	Building Condemned		100	X	X	X	X	X
8	Collapse		100	X	X	X	X	X

Fig. 1 Format For Damage Probability Matrix

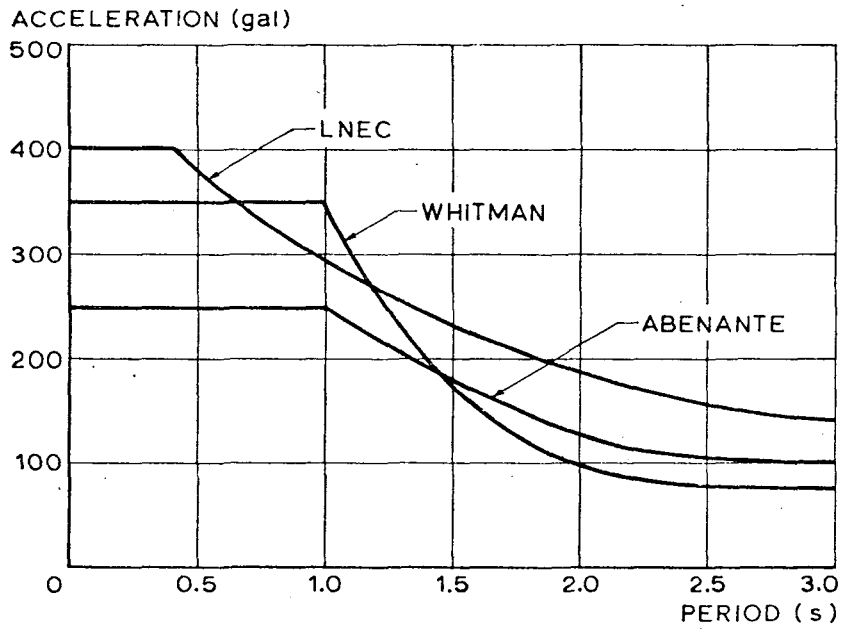


Fig. 3 - Acceleration response spectra.

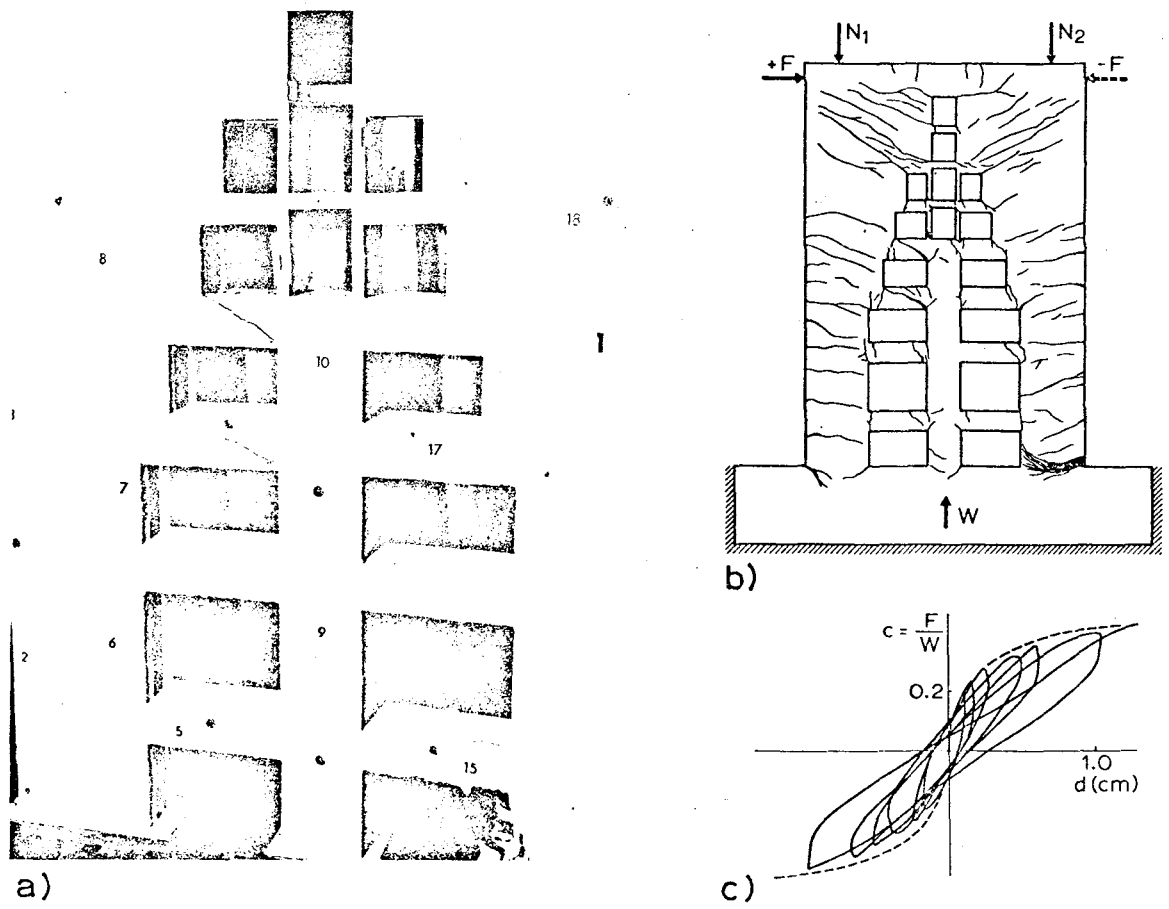


Fig. 4 - Test of reinforced concrete Model 2 (shear walls with openings)

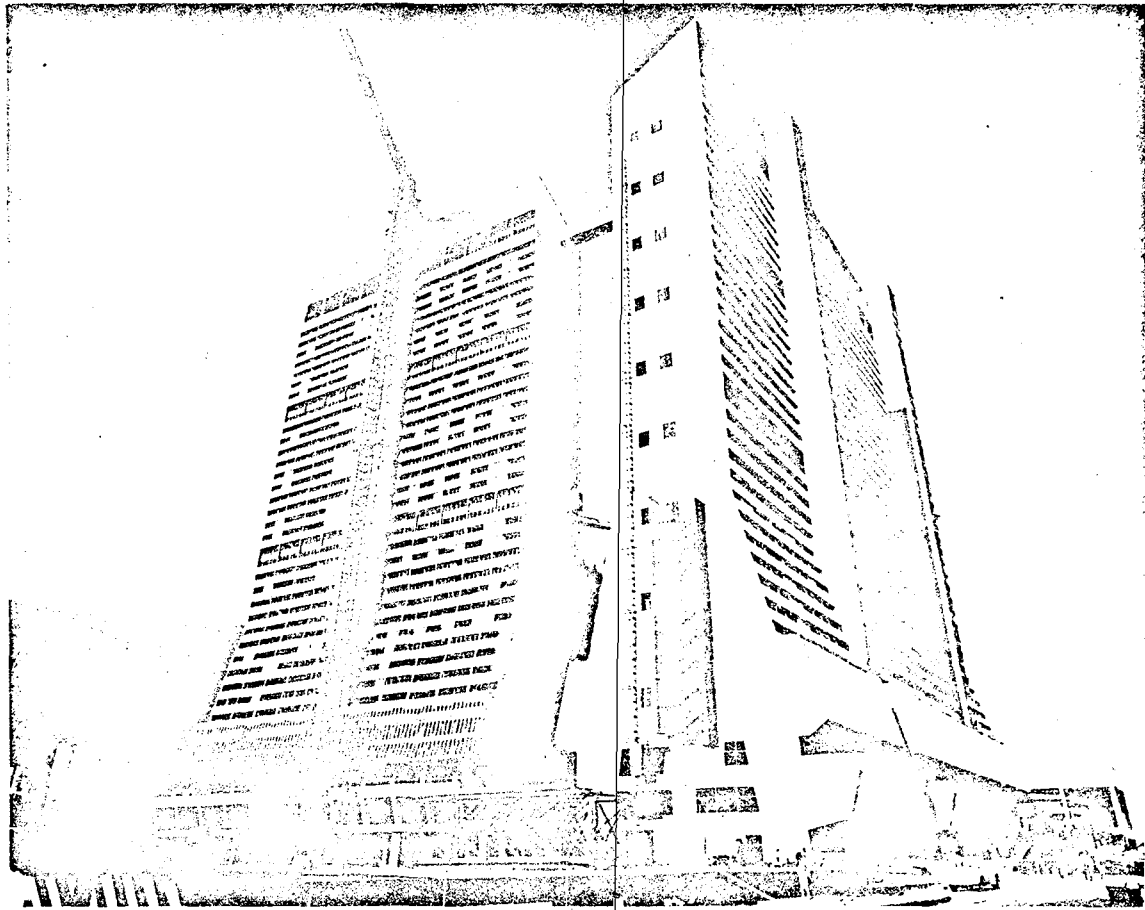


Fig. 1 - View of Parque Central Buildings, November 1972.

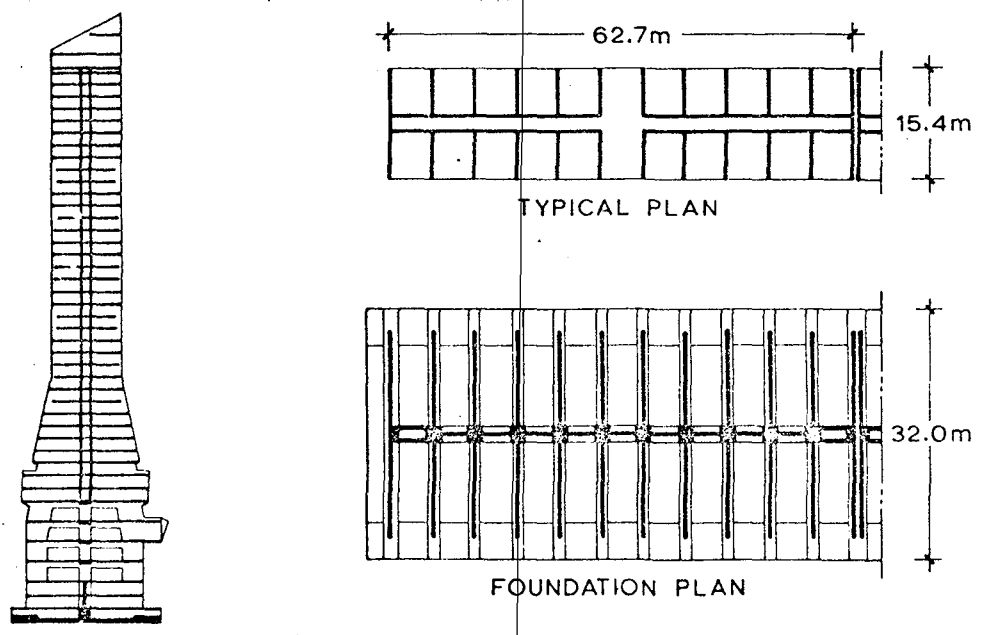


Fig. 2 - Elevation, typical plan and foundation plan of the buildings.

8 - GENERAL CONCLUSIONS

The seismic studies of Parque Central 44-story apartment buildings in Caracas performed by a multidisciplinary team of advisors coordinated by the Venezuelan engineers in charge of the structural design afforded an excellent opportunity for exchange of information and experience in the field of Earthquake Engineering. Thus useful results were obtained for the design and construction of these large reinforced concrete shear-wall buildings.

REFERENCES

- (1) - ABENANTE, F. and M. BREWER: "Recomendaciones sobre los Espectros de Diseño Derivados del Trabajo: Contribución al Analisis Sísmico de Estructuras". Caracas, 1970.
- (2) - SEED, H. B., R. V. WHITMAN, H. DEZFULIAN, R. DOBRY and I. M. IDRIS: "Soil Conditions and Building Damage in 1967 Caracas Earthquake". J. Soil Mech., Proc. ASCE, vol. 98, No. SM8, pp. 787-806, 1972.
- (3) - BORGES, J. F., J. GRASES and A. RAVARA: "Behaviour of Tall Buildings During the Caracas Earthquake of 1967". Proc. IV WCEE, Santiago de Chile, 1969.
- (4) - RAVARA, A., J. PEREIRA, C. OLIVEIRA, and P. LOURTIE: "Estudos Estruturais dos Edifícios de Parque Central - 2º. Relatório: Análise Dinâmica dos Edifícios de Apartamentos". LNEC Report, Lisbon, 1971.
- (5) - RAVARA, A., C. OLIVEIRA and P. LOURTIE: "Estudos Estruturais dos Edifícios de Parque Central - 1º. Relatório: Ensaios Sísmicos de Paredes Transversais". LNEC Report, Lisbon, 1971.
- (6) - PAPANONI, M. and S. HOLOMA: "A Model Study of Coupling Beams for the Parque Central Buildings". Tech. Comm. 24, Int. Conf. Planning and Design of Tall Buildings, ASCE-IABSE, 1972.
- (7) - CASTOLDI, A.: "Esperienze Statiche e Dinamiche su un Modello del Grattacielo Parque Central". ISMFS Report No. 827, Bergamo, 1971.
- (8) - WHITMAN, R. V.: "Dynamic Soil-Structure Interaction". Invited Discussion, Tech. Comm. 6, Int. Conf. Planning and Design of Tall Buildings, ASCE-IABSE, 1972.
- (9) - RAVARA, A. and J. PEREIRA: "Estudos Estruturais dos Edifícios de Parque Central - 3º. Relatório: Observação do Comportamento Dinâmico dos Edifícios de Apartamentos". LNEC Report, Lisbon, 1972.

Modal analysis techniques and step-by-step numerical integration (4) were used in the study of linear and non-linear seismic responses. Torsion due to the phase-lag propagation of the seismic waves was also studied (4). It was concluded that torsion could increase seismic stresses in the transverse extreme walls by about 20%.

Table II presents values of natural frequencies, as predicted in the analytical and experimental studies, and as measured after completion of the structure, in June 1972 (9).

TABLE II - Predicted and measured natural frequencies.

Type of movement	Vibration mode	Natural frequency, Hz		
		Dynamic analysis	Elastic model tests	Measured
Transverse translation	1st	0.52	0.54	0.58
	2nd	1.94	1.88	1.88
Longitudinal translation	1st	1.14	0.66	0.87
	2nd	4.00	2.12	2.44
Torsion	1st	-	0.59	0.42

Maximum horizontal displacements of 15 to 20 cm (transverse) and of 5 to 7 cm (longitudinal) were obtained at the top of the structure just below the penthouse.

The penthouse steel structure was subjected to a careful dynamic analysis since it was foreseen that whiplash effects could occur.

7 - SEISMIC DESIGN CRITERIA

The results obtained in the dynamic analysis of the structure, performed in close coordination with the structural engineers of Delpre, C. A. led to the following basic criteria.

The transverse shear walls were designed for a triangular distribution of seismic coefficients corresponding to a base shear of 14% of permanent loading. The axial seismic forces acting on the columns were reduced so as to resist the overturning moments given by the dynamic analysis.

The longitudinal frames and shear walls were designed using seismic coefficients varying linearly from 0.08 at the base to 0.16 at the top.

The penthouse was designed for a seismic coefficient of about 0.50.

These load distributions are in good agreement with the results of the dynamic analysis.

concrete. The latter solution was chosen owing to its good cracking pattern and higher ductility.

The models showed a relatively early loss of rigidity in the lintel beams. This fact required a reexamination of the structural analysis schemes, a proper reduction in the lintel rigidities being taken into account.

The confirmed reliability of the lintel performance was a basis for further redesigns of the buildings, including a substantial increase in the number of door openings.

6 - DYNAMIC LINEAR AND NON-LINEAR ANALYSES

The seismic response of the structure to translational and torsional oscillations was investigated by experimental and analytical studies. Tests on an elastic model of the whole building to a 1:40 scale were carried out at the ISMES in Bergamo (7). These tests, fully described in another paper presented at this Conference, were particularly useful for studying torsional frequencies and modes and the coupling between translational and torsional vibrations, due to a slight building asymmetry.

In the analytical studies (4) the following problems had to be considered in detail.

In the structural idealization the pseudo-frame approach (Fig. 7) proved accurate enough. It was complemented by finite element analysis for studying the longitudinal structure in the transition zone between frame and shear wall.

The influence of soil deformability upon the dynamic response was studied by including a foundation rocking spring in the pseudo-frame idealization. The values of the spring constant were estimated by using the elastic theory together with typical values of in-situ shear wave velocities for the soils of Caracas (1) and also dynamic tests in a nearby building (4). The range of spring constants covered the uncertainties inherent in such estimates (8). The resulting spring constants corresponded to values of subgrade modulus from 10 to 100 N/cm³. Since inclusion of rocking decreases the stresses but increases the displacements in the structure, the largest estimated rocking spring constant was used for computing stresses, while the smallest estimated value was used for determining total motion at the top of the structure.

It was concluded from the dynamic analysis that the soil-structure interaction could be disregarded in the longitudinal direction; in the transverse direction it was quite important, reducing seismic stresses near the base of the structure by about 20%.

Measurements during and after construction confirmed the reasonableness of the foundation design studies. The measured static settlements were, as predicted, smaller than 8 cm, while the measured dynamic foundation motion corresponded to a subgrade modulus of 60 to 100 N/cm³ (9). A viscous damping of 0.05 for the first and second modes was assumed in all the calculations.

As a result of the studies mentioned most of the dynamic analysis of the structure used as input an envelope of the three spectra proposed, with an intensity reduced to the LNEC spectrum, the variance and the maximum values of the ground acceleration being given by:

$$\overline{a^2} = \int S(f) df = 1750 \text{ gal}^2 \dots\dots\dots 1)$$

$$a_{\text{max}} \approx 3 \sqrt{1750} = 0.13 \text{ g} \dots\dots\dots 2)$$

At this level of acceleration structural behaviour is non-linear.

5 - DUCTILITY ASSESSMENT

Static rupture tests on reinforced concrete models (5, 6) were carried out to determine the ductility of the transverse walls and lintels. Two models having the same geometry but different amounts of reinforcement were used in both studies.

5.1 - Shear wall model tests

The 1:20 models of the lower portion of the transverse walls (Fig. 4) were subjected to cycles of vertical and horizontal forces combined so as to correspond to increasing values of seismic coefficients. In Model 1 most of the reinforcement was uniformly distributed as a double mesh, the total ratio of vertical reinforcement being about 1%. In Model 2 the reinforcement was distributed as a double mesh with additional bars and hoops placed at the extremes of the shear walls. The total ratio of reinforcement in this model was 2%.

The main conclusions of the tests were: in the elastic range both models exhibited cantilever behaviour; yielding started for seismic coefficients of 0.20; cracking developed at the base and around the corners of the openings and progressed uniformly in both models; the structural behaviour after yielding was little affected by cracking; rupture occurred in Model 1 due to tension in the base for a seismic coefficient of 0.36; and in Model 2 due to compression of the concrete at the base for a seismic coefficient of about 0.50.

By extrapolating the test results to the prototypes an overall ductility factor of 1.5 to 2.0 was ascribed to the transverse shear walls, within the limits of practical interest for the seismic intensity considered.

5.2 - Lintel model tests

The lintels designed was based on the testing of two reinforced concrete models, scaled to 1:2. The surrounding slabs were also taken into account in these models, in which two consecutive door openings were reproduced. The models were tested vertically.

One model was reinforced with crossed bars and another with an embedded I-beam, together with hoops placed on the surrounding

1 s for the soil.

LNEC suggested an acceleration power spectrum with a constant density of $350 \text{ gal}^2 \text{ Hz}^{-1}$ in the frequency range of 0 to 5 Hz. The maximum intensity assessed to the zone of Palos Grandes during 1967 earthquake was little above this value (3).

For the comparison of the three types of ground motion it was necessary to derive relationships between power and response spectra of acceleration. This was done at the LNEC (4) by means of a formulation and a computer program that plots acceleration response spectra produced by any type of power spectra of acceleration. Fig. 3 presents the three response spectra. It is seen from the figure that Whitman's spectrum exceeds the other two for periods near 1 s, since this was the value estimated by that author for the fundamental period of the soil at Parque Central. The incidence of this value on the seismic design of the structure is critical because it is about the same as the fundamental period of the building in the longitudinal direction. It was thus decided to perform measurements of soil vibrations in several zones of Caracas, in order to relate the predominant period of the soil and the depth of alluvium. These measurements were performed in June 1970 (4), using displacement meters to record ambient and pile-driving vibrations, the main results being presented in Table I.

TABLE I - Predominant soil periods in Caracas.

Test Site	Depth of Deposit (m)	Frequency (Hz)		Period (s) corrected
		measured	corrected	
Palos Grandes	~ 230	1.0 to 1.5	0.7 to 1.0	1.0 to 1.5
Parque del Este	~ 120	1.5 to 3.0	1.0 to 2.0	0.5 to 1.0
Parque Central	~ 70	2.5 to 5.0	1.5 to 3.5	0.3 to 0.7
Caurimare	0 (rock)	5.5 to 7.5	3.5 to 5.0	0.2 to 0.3

The "measured" values were corrected by a 50% increase of the period, in order to extrapolate microtremors to large amplitude vibrations. The value of this correction factor was selected on the basis of previous studies on the 1967 Caracas earthquake, particularly those concerning the Palos Grandes zone (1).

The soil measurement results were in some way confirmed by dynamic tests of a tall building located at Parque Central. This building, with fundamental periods of about 1 s was but little affected by the 1967 earthquake.

3 - SOIL CONDITIONS AND FOUNDATION CHOICE

The Valley of Caracas is underlain by intermingled cohesive and cohesionless soils laid down both in river flood plains and in alluvial fans emanating from the steep mountains bounding the Valley. The pattern of these deposits is erratic; at any depth at any site either clay or sand is equally likely. The depth of these soils also varies greatly over the Valley, with a maximum depth of over 300 m. At Parque Central, the depth to bedrock ranges between 40 and 100 m.

The soils within the top 10 m generally are too loose or too soft to support heavy loads directly at ground surface, and most tall buildings in Caracas are supported upon piles with a length of 10 to 20 m. However, below 10 m the soils become denser and firmer, suggesting the possibility that the Parque Central apartment buildings could be supported by rigid mats founded at that depth. Such a foundation had another potentially important advantage in connection with this unusual building: the action of a mat foundation during earthquakes is better understood than is the action of a pile foundation.

Detailed studies were made to determine the feasibility of a mat foundation. Analysis of static settlements and of resistance to overturning indicated that a mat would be adequate and safe if it had a width of about 30 m with a static bearing stress of about 35 N/cm². Soil exploration showed that the site could be dewatered economically by means of deep wells, and that there was no danger that dewatering would cause damage to nearby buildings. Thus a mat foundation placed in a deep excavation was feasible.

At the same time, other factors also indicated the desirability of deep excavation and of widening the lower part of the structure. Excavation of the entire site provided desirable underground parking space. Widening the lower part of the structure was desirable from the structural viewpoint and provided useful commercial and office space. Hence, the final solution was a mat 32 m wide founded 12 m below ground surface.

4 - INTENSITY OF GROUND MOTION FOR DESIGN

At an early stage of the project three types of seismic spectra were independently proposed by consulting engineers Abenante and Brewer, by Whitman and by the LNEC. All spectra were related to the seismic intensity of the 1967 Caracas earthquake, their main characteristics being as follows:

Abenante and Brewer (1) assumed a seismic intensity similar to the 1967 earthquake and determined a response spectrum for soft soils using Esteva and Rosenblueth propagation expression for a Richter magnitude 7, an epicentral distance of 50 km, and a focus depth of 20 km.

Whitman's response spectrum was based on a seismic intensity of about twice the 1967 earthquake (2) and on a predominant period of

What makes these studies particularly interesting from Earthquake Engineering point of view are the following points:

i) The project was started not so long after the city had suffered a severe earthquake (29th July 1967), with local codes still under discussion.

ii) The construction methods selected were developed in non-seismic countries, mostly in France, and there was no previously known experience in the full shear-wall type of construction either in the heights reached or in the lateral load requirements for design.

iii) There was no important previous local experience or trained personnel in this type of industrialized construction.

A multidisciplinary local group was assembled in a brief time and an international group of advisors was formed, once the initial ideas proposed by the developer, Delpre, C.A., a private firm, were accepted by Centro Simon Bolivar, the government institution in charge, who is at the same time the land owner and the body in charge for city renewal. This paper tries to retrace the main experiences gathered during the project stage, most of them resulting from interactions between geographically separated groups.

In terms of relative influence on the final solution, one could establish a scale of relevance by listing the main decisions which conformed the finally chosen structural solution as follows:

- i) Rejection of systems based on prefabricated panels in favour of cast-in-place type of construction, using a side sliding tunnel formwork.
- ii) Commercial use for the lower stories and office use for the intermediate stories, instead of totally separated types of buildings.
- iii) Influence of the type of soils on the intensity of ground motion.
- iv) Assessment of ductility factors.
- v) Type of foundation.

2 - GENERAL DESCRIPTION OF THE STRUCTURE

The structure of the apartment buildings consists in transverse shear walls spaced 5.70 m and two longitudinal shear walls along the central corridor as shown schematically in Fig. 2. The building height is about 125 m. Floors are 16 cm thick reinforced concrete slabs.

The total permanent load considered in the dynamic analysis amounts to about 66,000 t, including 25% of the live load according to the Venezuelan seismic code.

At the lower six stories longitudinal shear walls are replaced by frames and large openings in the transverse walls increase the overall ductility of the structure.

The buildings are directly founded on the ground by means of a ribbed mat (Fig. 2).

Concrete with a characteristic compressive strength 3500 N/cm² (5000 psi) and reinforcing steel with a characteristic 0.2 proof-stress 42000 N/cm² (60000 psi) were normally used.

SEISMIC STUDIES OF PARQUE CENTRAL BUILDINGS

by

M. Paparoni^I, J. Ferry Borges^{II}, A. Ravara^{III} and Robert V. Whitman^{IV}

Synopsis

Comprehensive seismic studies were made in connexion with the design of a group of 13 apartment and office buildings, 44 and 62 stories high, included in Parque Central project in Caracas, Venezuela. Not only were many different aspects of the expected seismic response studied in detail, but in addition these studies were closely co-ordinated with the progress of planning and design.

The subjects were: intensity of ground motion for design; relation of earthquake response to foundation design; dynamic soil-structure interaction; linear and non-linear analysis of the seismic response for translational and torsional vibrations; elastic model tests; tests of reinforced concrete models for ductility assessment; and the observation of structural behaviour during construction.

This paper describes the methods that were used during the different stages of the structural design regarding the planning and the coordination of the research involved, gives a brief account of the major results obtained in the analytical and experimental studies, and outlines the progress of design as a consequence of these results.

1 - INTRODUCTION

The Parque Central Development in Caracas, Venezuela, comprises an occupation area of approximately 130,000 m² encompassing a total of 11 residential buildings (44 stories), 2 office towers (62 stories) and several other minor buildings for a grand total of 1,200,000 m² of enclosed space.

The development is now completing its first phase, totalling 4 finished apartment buildings, and two under construction (Fig. 1). The present paper deals with the studies connected with the apartment buildings, the ones relating to the office towers being now under way.

I - DELPRE, C.A. Ingenieros Constructores, Caracas.

II - Associate Director, Laboratório Nacional de Engenharia Civil, (LNEC), Lisbon.

III - Head of the Applied Dynamics and Applied Mathematics Divisions, LNEC.

IV - Professor of Civil Engineering and Head of the Structures Division of the Dept. of Civil Engineering, M.I.T., Cambridge, Mass.

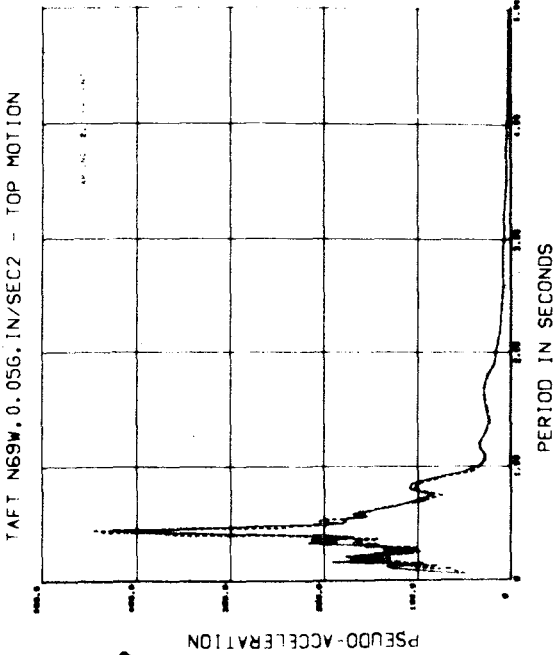


Fig. 19

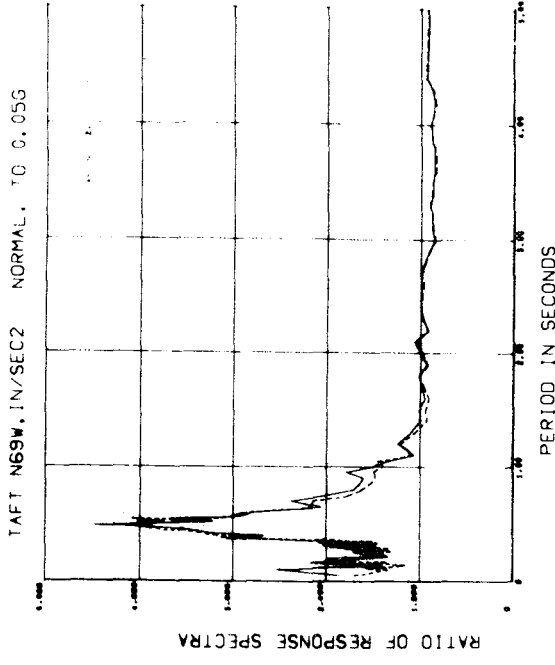


Fig. 20

Variable Profile

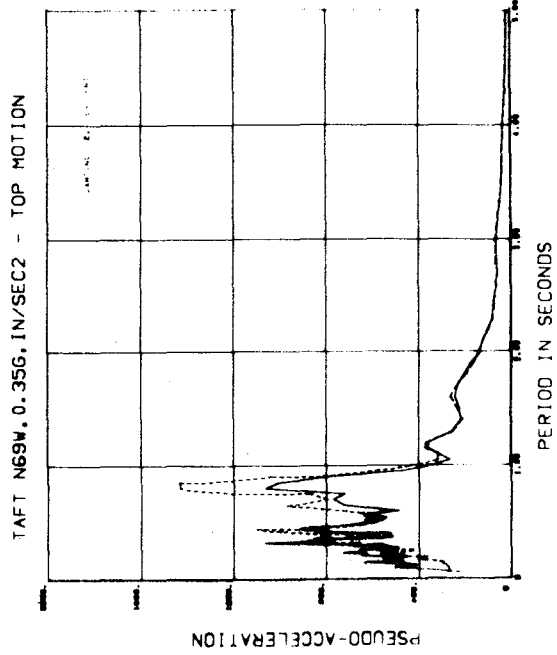


Fig. 21

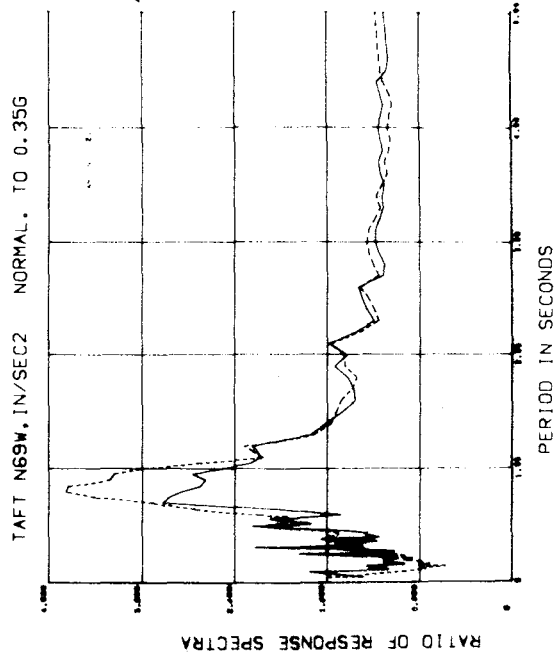


Fig. 22

TAFI N69W, 0.05G, IN/SEC2 - TOP MOTION

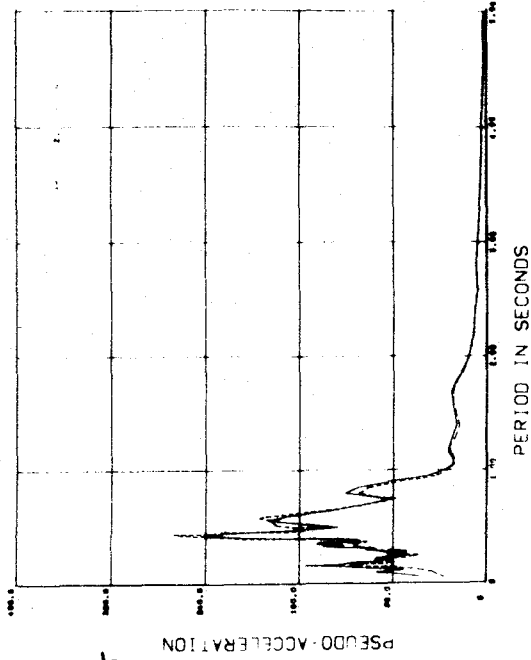


Fig. 15

TAFI N69W, 1.0/SEC2 NORMAL, IC 0.35G

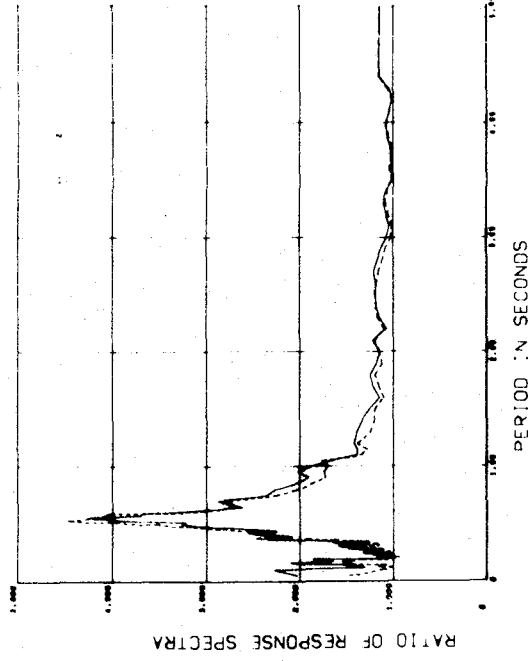


Fig. 16

Uniform profile

TAFI N69W, 0.35G, IN/SEC2 - TOP MOTION

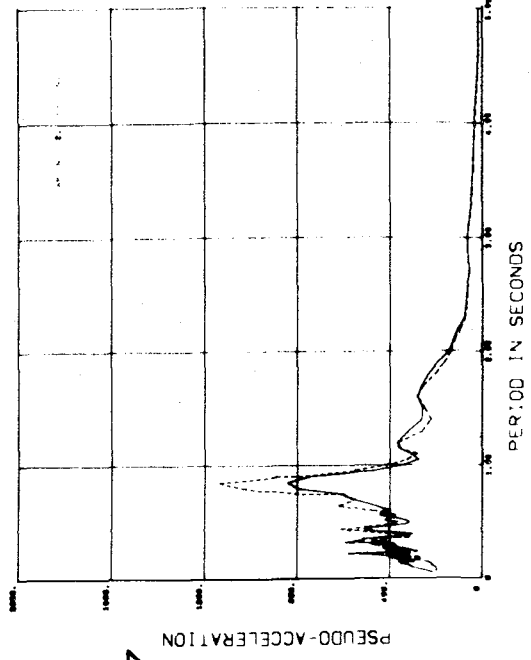


Fig. 17

TAFI N69W, 1.0/SEC2 NORMAL, IC 0.35G

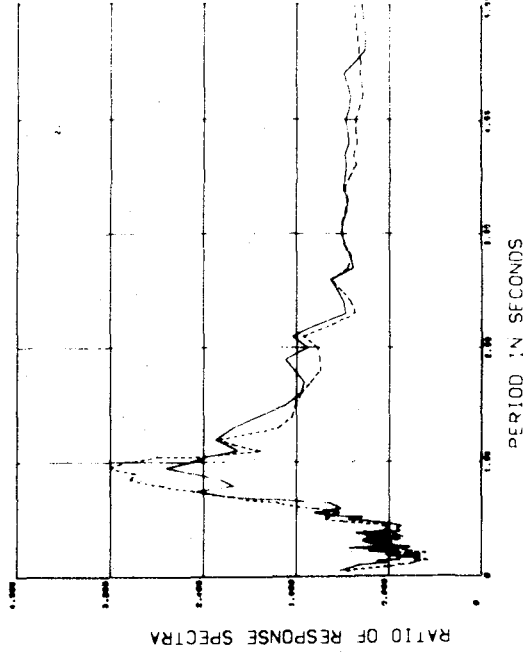


Fig. 18

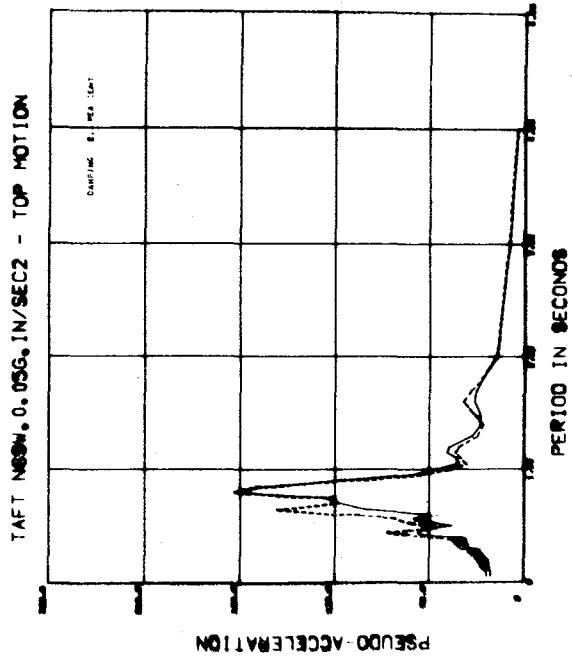


Fig. 11

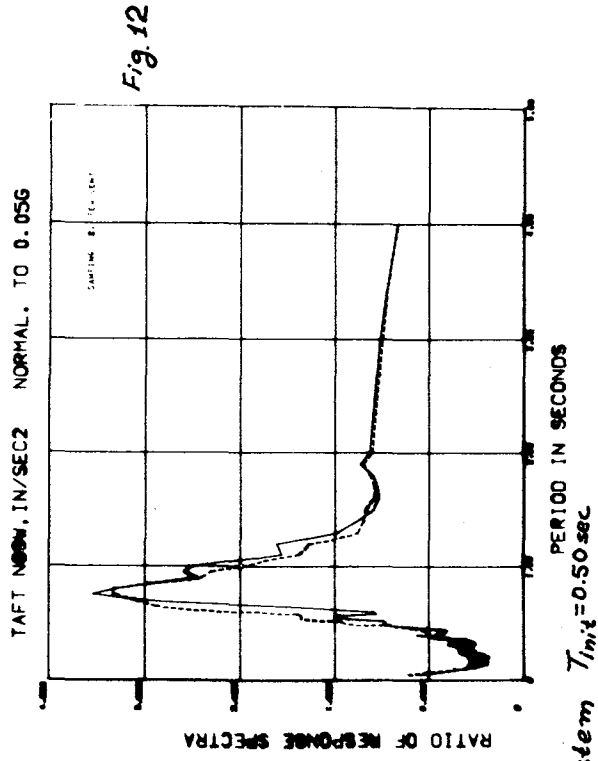


Fig. 12

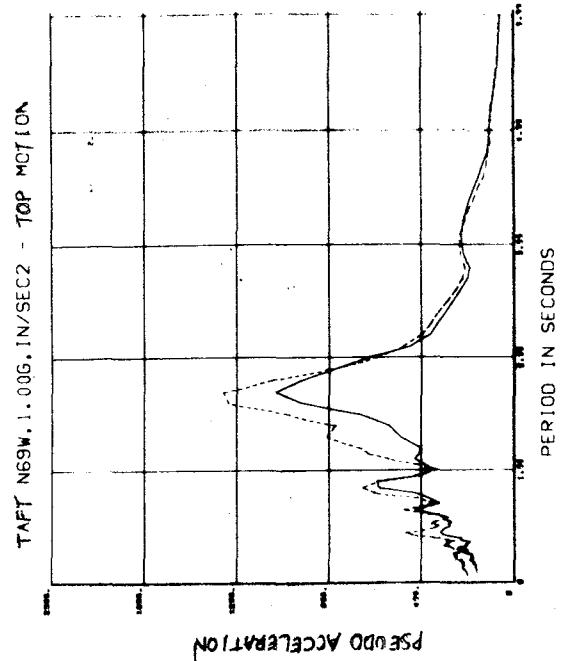


Fig. 13

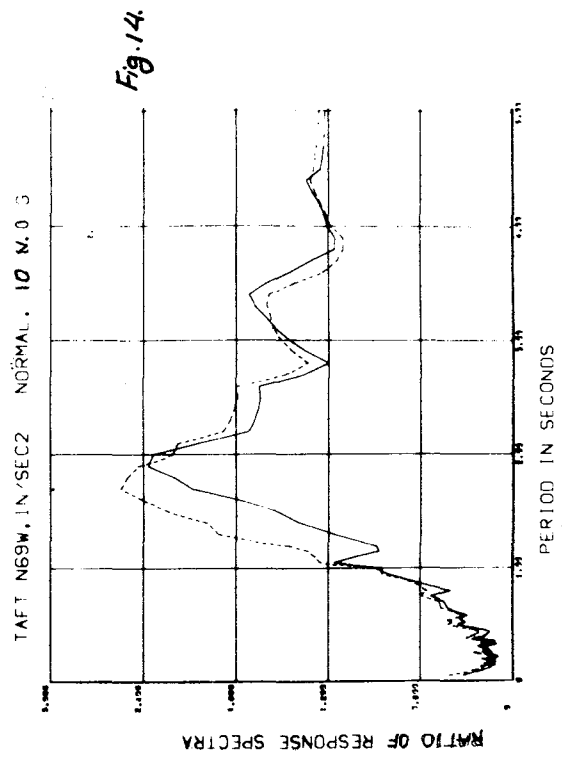


Fig. 14

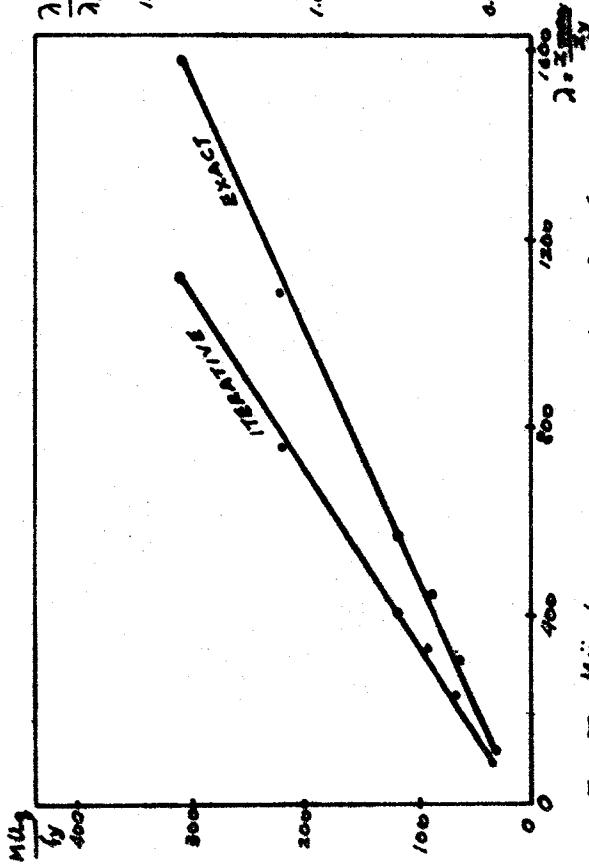


Fig. 7: Müz/ty vs corresponding λ for a SDOF system with $t_{init} = 0.50 \text{ sec}$.

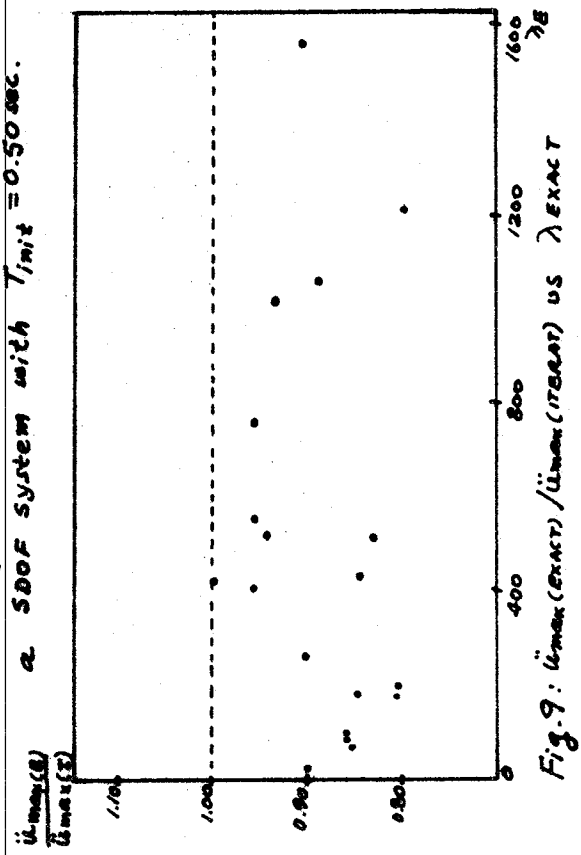


Fig. 9: $\frac{\ddot{u}_{max}(EXACT)}{\ddot{u}_{max}(ITERATIVE)}$ vs λ

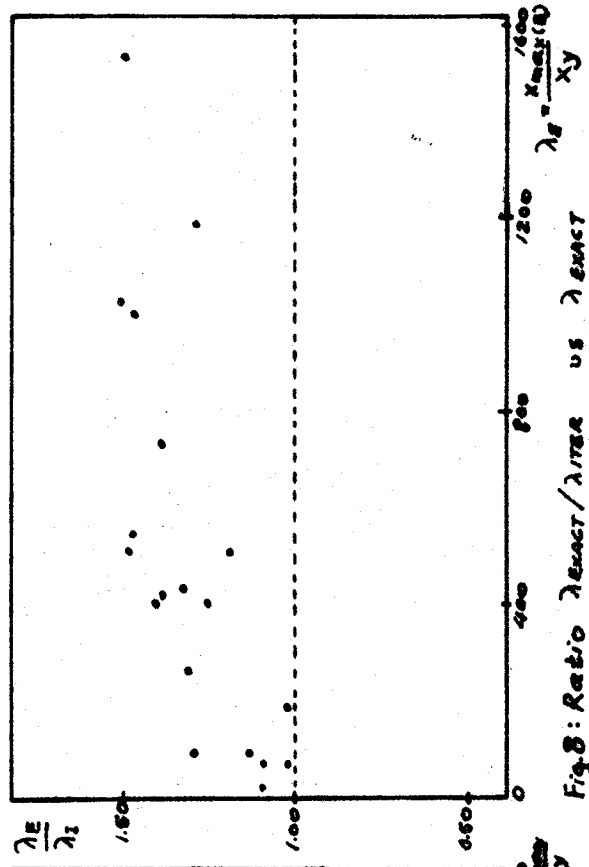


Fig. 8: Ratio $\frac{\lambda_E}{\lambda_{EXACT}}$ vs λ

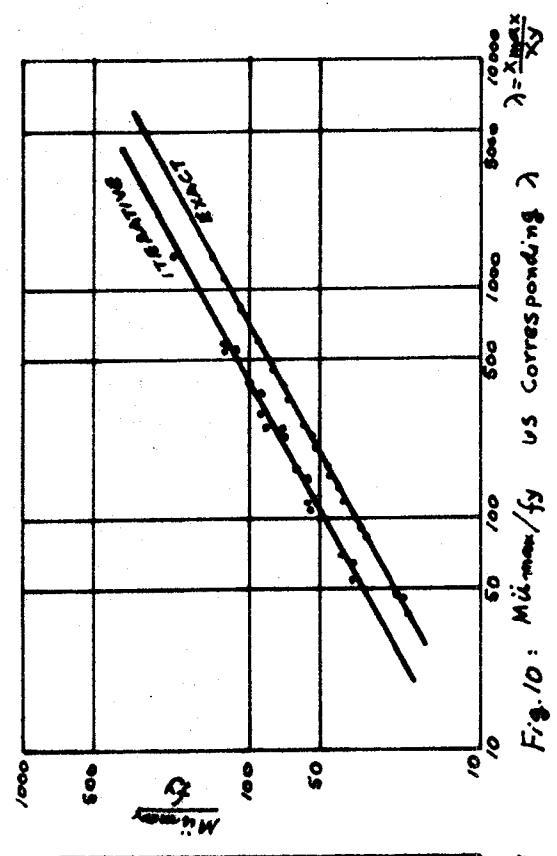


Fig. 10: Mümax/ty vs corresponding λ

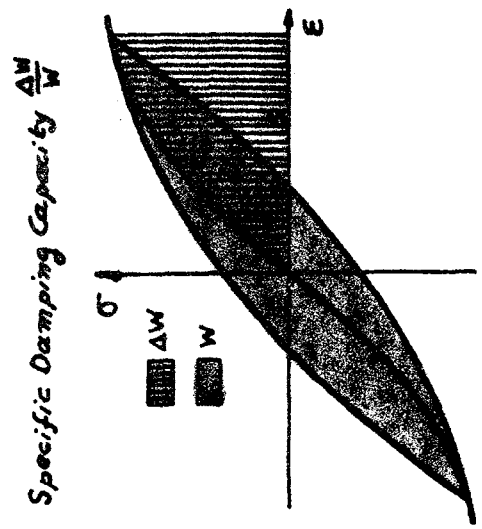
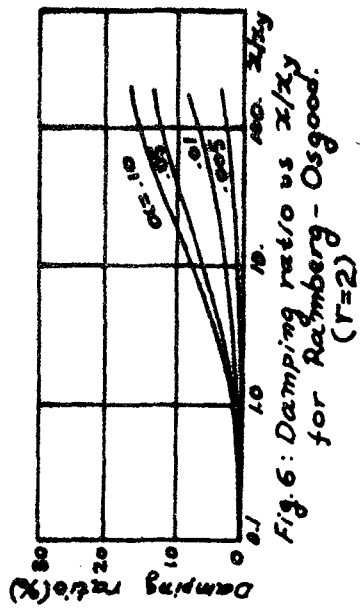
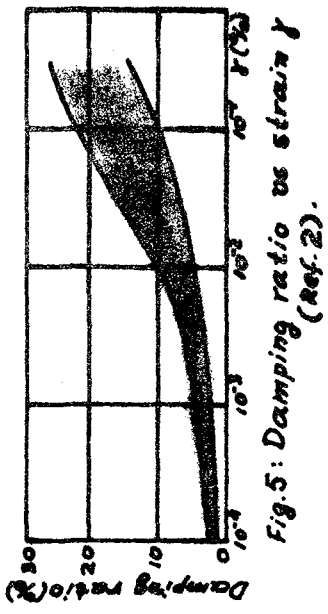
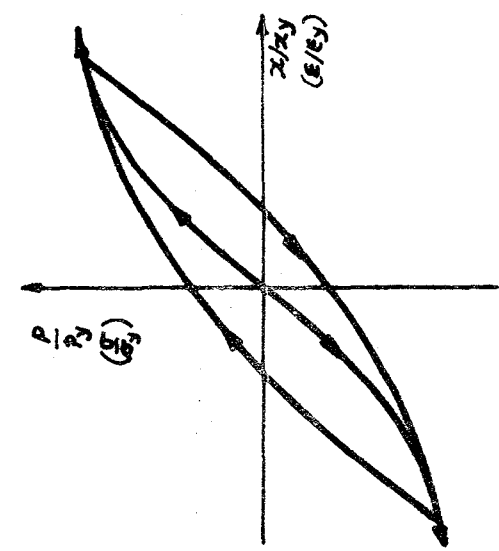
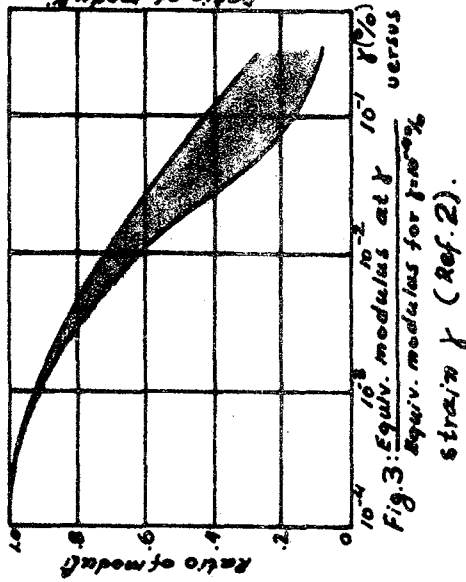
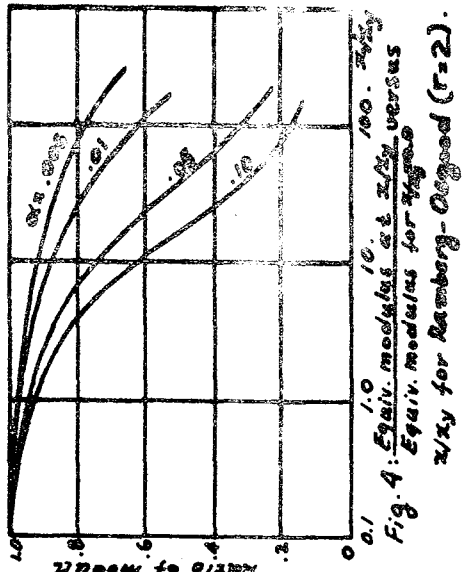


Fig. 1: Force vs Distortion for Ramberg-Osgood model under cyclic loading.

Fig. 2: Definition of Secant modulus and Specific damping.

and strains and overestimated accelerations. The agreement between both methods was much better when the nature of the damping in the individual springs was considered as hysteretic than when it was taken as viscous. The assumption of normal modes and the use of weighted modal damping seemed to introduce very little error in the cases studied.

Differences between both solutions increased again with the level of excitation and were larger for the variable than for the uniform profile. Over all, however, response spectra for the motion of the top mass and ratios of response spectra were comparable as illustrated by Figs. 15 to 22.

CONCLUSIONS

The iterative method traditionally used in soil amplification analyses cannot entirely reproduce the behavior of a nonlinear system. In general, for a characteristic strain of 2/3 of the maximum strain, it underestimates displacements (and strains), and it overestimates accelerations. The departures from the exact solution are not, however, of a large magnitude, and for moderate levels of excitation and a range of initial natural periods of 0.25 to 1 or even 2 seconds, resulting design spectra are reasonably close to the exact ones. Because of all the other uncertainties involved in usual analyses, use of this procedure within this range seems entirely appropriate. For multidegree of freedom systems it is better to assume the damping in each component to be of a hysteretic rather than of a viscous nature.

REFERENCES

1. Seed, H.B., and Idriss, I.M., "Influence of Soil Conditions on Ground Motions during Earthquakes," Journal of the Soil Mechanics and Foundations Division, ASCE, Vol. 95, SMI, 1969.
2. Seed, H.B., "The Influence of Local Soil Conditions on Earthquake Damage," Proc., 7th International Conference on Soil Mechanics and Foundation Engineering, Mexico City, Mexico, 1969.
3. Jennings, P.C., "Response of a General Yielding Structure," Journal of the Engineering Mechanics Division, ASCE, Vol. 90, EM2, 1964.
4. Dobry, R., "Soil Properties and the One-Dimensional Theory of Earthquake Amplification," M.I.T. Research Report R71-18, 1971.
5. R.V. Whitman, J.M. Roesset, R. Dobry, and L. Ayestaran, "Accuracy of Modal Superposition for One-Dimensional Soil Amplification Analysis," Proc. of the International Conference on Microzonation for Safer Construction, Research, and Application, Vol. II, 1972.
6. Constantopoulos, I.V., "Amplification Studies for a Nonlinear Hysteretic Soil Model," Sc.D. thesis, Department of Civil Engineering, Massachusetts Institute of Technology, 1973.

period of 0.5 seconds. It can be seen that the iterative procedure, with a factor of $2/3$ for the characteristic strain, consistently underestimates the maximum strain (or displacement). The ratio of maximum displacements obtained by both procedures is shown in Fig. 8 for all systems. The exact solutions are 14% to 50% higher than the approximate results, the discrepancy increasing with the ductility ratio λ (and therefore with the level of excitation and the system response).

Similar plots were obtained for the maximum acceleration. Fig. 9 shows the ratios of the exact to the approximate results for all systems. For accelerations, the iterative procedure overestimates the response, the exact value being from 80% to 100% of the approximate answer. There is not, however, a clear trend as a function of the ductility λ .

The combined effect is better illustrated by plotting f_{\max}/f_y (or \ddot{u}_{\max}/f_y) versus x_{\max}/x_y for both approaches (Fig. 10). In the exact case the resulting curve is simply given by the Ramberg-Osgood relationship and approximates closely a straight line in a log-log plot for moderate to large values of λ . Results from the iterative approach also fall essentially on a straight line, parallel to the exact one and somewhat higher and to the left.

While displacements are underestimated and accelerations overestimated by the iterative procedure, the values of natural period and damping derived from the exact response compare reasonably well with those resulting from the last cycle of iteration, except for long initial natural periods, where the estimating procedure is itself suspect (6). This would suggest that the discrepancies are not due to lack of convergence to an appropriate equivalent linear system, but rather to the impossibility of reproducing all aspects of the nonlinear response by a linear model, especially when only a few cycles of response will occur.

What is more important, response spectra and ratios of response spectra (for 2% damping) as shown in Figs. 11 to 14 for a system with an initial period of 0.5 seconds, are very similar. The differences increase again with period and level of excitation but, in view of the need to smooth these spectra for design purposes, it can be concluded in general that the approximate method gives adequate results in the calculation of response spectra.

Variations in the value of the strain factor that defines the characteristic strain, from 0.5 to 1, were also investigated. While values somewhat larger than $2/3$ seemed to improve the agreement in several cases, there was no consistent trend and it would seem that this factor itself should be a function of the system characteristics and the level of excitation. The introduction of this refinement may not be justified considering all the uncertainties involved in the estimation of soil properties and the selection of appropriate motions.

MULTIDEGREE OF FREEDOM SYSTEMS

Results for the multidegree of freedom systems confirmed the trends already reported. The iterative procedure underestimated displacements

Figs. 3 and 5 show ranges of variation of modulus and damping as functions of strain, which have been suggested as representative of typical soils (2). These ranges are indicative of the amount of scatter in experimental data. Similar curves were theoretically derived for Ramberg-Osgood systems with different values of α and r . Although a perfect match with any of the bounding curves, or an average curve, was not possible, it was found that values of α of the order of 0.05 and values of r from 2 to 2.5 provided reasonable agreement in the overall trends. Values of $\alpha = 0.05$ and $r = 2$ were selected for the study and the corresponding modulus and damping curves are shown in Figs. 4 and 6.

ORGANIZATION OF THE STUDY

The "initial natural period" of a system was defined as that period derived from the initial stiffness of the Ramberg-Osgood relation. A set of single degree of freedom systems, with initial natural periods of 0.25, 0.5, 1 and 2 seconds and Ramberg-Osgood relationships with $r = 2$ and $\alpha = 0.05$, were first analyzed under a base motion corresponding to the N69W component of the Taft record of the 1952 Kern County earthquake, scaled to different intensities. For each system, and each intensity of motion, the dynamic response was computed by direct integration in the time domain of the nonlinear equations of motion, using the fourth order Runge-Kutta method. The analysis was then repeated using the iterative procedure, assuming at each cycle a linear model with stiffness and damping coefficients obtained from the curves of Figs. 5 and 6, and a characteristic strain equal to 2/3 of the maximum strain reached in the previous cycle.

Comparison of results included time histories and maximum values of both accelerations and displacements, response spectra for the motion of the system, and ratios of the response spectra for the motion of the mass and to that for the input motion. In addition a predominant period and a damping ratio were obtained from the motion of the mass in the exact analysis (4). These values were compared to the corresponding ones resulting from the last cycle of the iterative procedure (when a tolerance of 1% in the maximum strain had been reached).

The same basic approach was applied to a set of two close-coupled multidegree of freedom systems, each one with nine masses and springs. The first system had a uniform initial stiffness with depth, while the second one had stiffness increasing with the square root of depth. In these cases the iterative linear analyses were performed in the time domain, assuming normal modes and modal dampings computed by a weighting formula (5), and in the frequency domain without any assumption as to the existence of normal modes. For each of these two cases two different hypotheses were tried: the damping in each spring was made viscous or linearly hysteretic.

SINGLE DEGREE OF FREEDOM SYSTEMS

For each system the variation of maximum displacement with earthquake intensity was plotted, using the dimensionless variables $\lambda = x_{\max}/x_y$ and $M\dot{u}_G/f_y$, where x_{\max} is the maximum displacement, M is the mass, u_G is the peak ground acceleration, x_y and f_y are the Ramberg-Osgood parameters defined earlier. Figure 7 shows a typical plot for an initial natural

Osgood relationship described in the following section, and the solution was carried out by direct numerical integration in the time domain. In the other set of analyses the iterative linear viscoelastic procedure was followed, the spring and dashpot constants being related to the strain levels directly from the Ramberg-Osgood formula. Thus, the same fundamental stress-strain relation obtained for both sets of results; the differences lay in the way the solutions were computed.

SELECTION OF PARAMETERS FOR THE RAMBERG-OSGOOD MODEL

The constitutive relations of soil are too complicated to be fully described by a single equation. Several nonlinear models, from elastoplastic to multilinear, hyperbolic, or Ramberg-Osgood relationships, have been often used, however, to approximate the stress-strain behavior of soil. For the purposes of this study, since the same characteristics will be used for both sets of analysis, the exact reproduction of any particular soil is not important. It is, however, desirable to have overall variations for moduli and damping ratios, as functions of strain, similar to those of most soils.

Ramberg-Osgood models have been extensively studied by Jennings (3). The corresponding load deflection relationship is of the form

$$\frac{x-x_i}{cx_y} = \frac{p-p_i}{cp_y} + \alpha \left(\frac{p-p_i}{cp_y} \right)^r$$

where

x is the shear distortion of the spring

p is the force developed in the spring

x_y is a shear distortion constant, characteristic of the spring

p_y is a force constant, characteristic of the spring

x_i, p_i are the distortion and force representing the most recent point at which there was a load reversal

α is a positive constant, characteristic of the spring

r is a positive number, odd and integer in the original formulation. With proper handling of the sign of $p-p_i/cp_y$ it can be however any positive real number.

$c = 1$ for virgin loading path

$= 2$ for unloading or reloading.

c has again a value of 1 if during unloading or reloading the virgin curve is reached.

Fig. 1 shows the general form of the load-deflection paths as defined by the above equation. With proper selection of the parameters α and r , a wide variety of physical behaviors can be reproduced, from that of a linear elastic to that of an elastic - perfectly plastic material. For a cyclic loading with a fixed amplitude of strain, a unique hysteresis loop is defined and a value of secant modulus and damping ratio can be obtained as illustrated in Fig. 2.

A COMPARISON OF LINEAR AND EXACT NONLINEAR
ANALYSES OF SOIL AMPLIFICATION

by

I.V. Constantopoulos,^I J.M. Roesset^{II} and J.T. Christian^{III}

SYNOPSIS

The effect of soil properties on the amplification of earthquake motions is usually studied by an iterative viscoelastic analysis. To investigate the validity of this approach direct calculations of soil amplification were made using a Ramberg-Osgood model for the soil properties. The same profiles were also studied by the iterative technique using variations of stiffness and damping derived from the same Ramberg-Osgood model. Comparison of the results of the two techniques shows that the response spectra are quite similar for the range of frequencies of engineering interest. There is, however, evidence that the iterative approach tends to underestimate the displacements and to overestimate the accelerations.

INTRODUCTION

Experimental data show that the stress-strain relationships for soils at the level of strains that might be induced by moderate to strong earthquakes are nonlinear (1). On the other hand, the great majority of the practical methods of analysis for soil amplification of earthquake motions requires the soil to be linearly viscoelastic. The difficulty of simulating nonlinear behavior with a linear analysis has been overcome traditionally by obtaining the secant moduli and damping ratios of the soil as functions of the strain level in a cyclic loading test. The linear viscoelastic analyses are then carried out iteratively, values of modulus and damping ratio being changed in successive cycles until they correspond to the levels of strain computed.

Obviously numerous questions arise as to the validity of this approach. While the process appears to converge for most practical problems, it is not clear how the characteristic strain that defines the value of the modulus and damping is to be chosen for a transient motion rather than a harmonic steady state condition. One common procedure is to use between 60 and 70% of the maximum strain. A more fundamental question is how closely the motion calculated by the iterative procedure resembles the motion predicted by an exact nonlinear analysis.

In order to investigate some of these questions the authors undertook to examine the behavior of a particular nonlinear model for soil behavior. The soil was modelled as a series of lumped masses, springs, and dashpots. In one set of analyses the springs were defined by the nonlinear Ramberg-

^I Research Assistant, Dept. of Civil Engineering, Massachusetts Institute of Technology, Cambridge, Massachusetts.

^{II} Associate Professor of Civil Engineering, Massachusetts Institute of Technology.

^{III} Associate Professor of Civil Engineering, Mass. Institute of Technology.

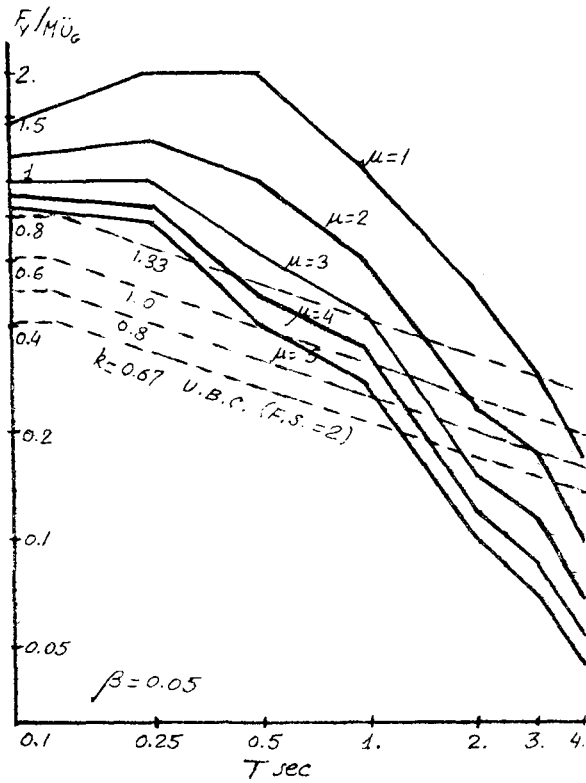


FIG 1 - ELASTO-PLASTIC

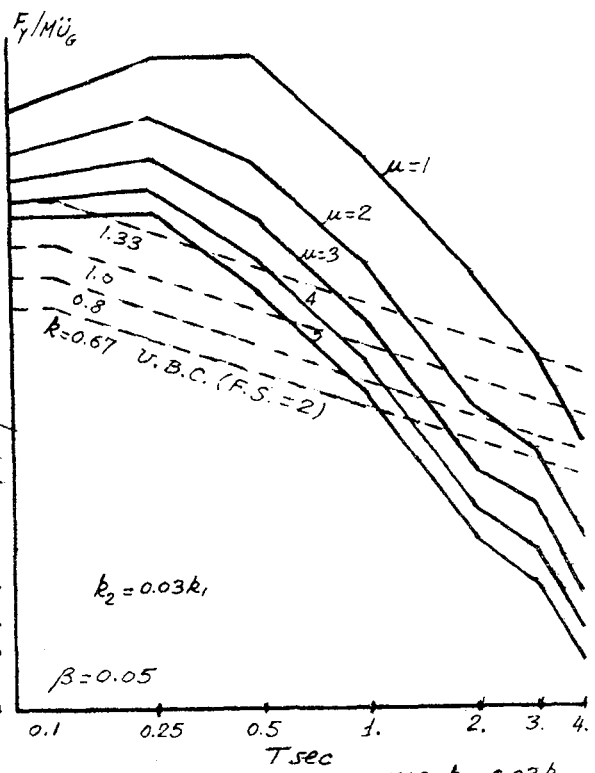


FIG 2 - BILINEAR $k_2 = 0.03k_1$

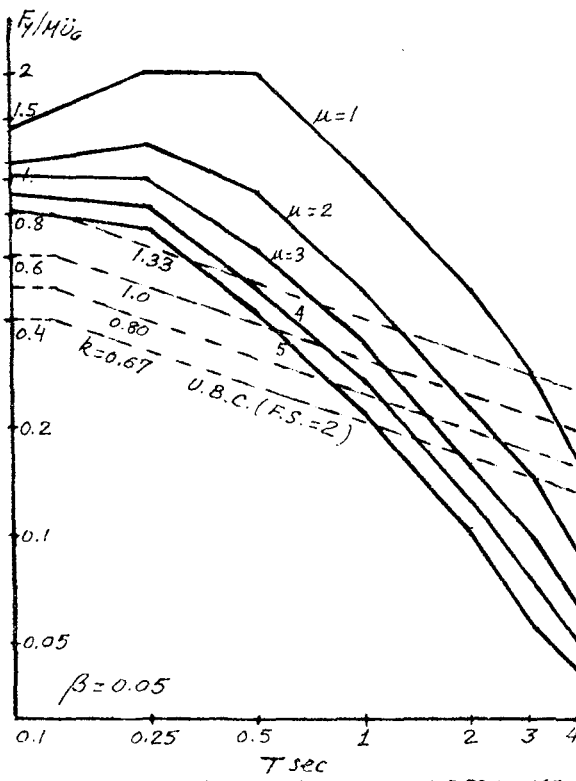


FIG 3 - STIFFNESS DEGRADING

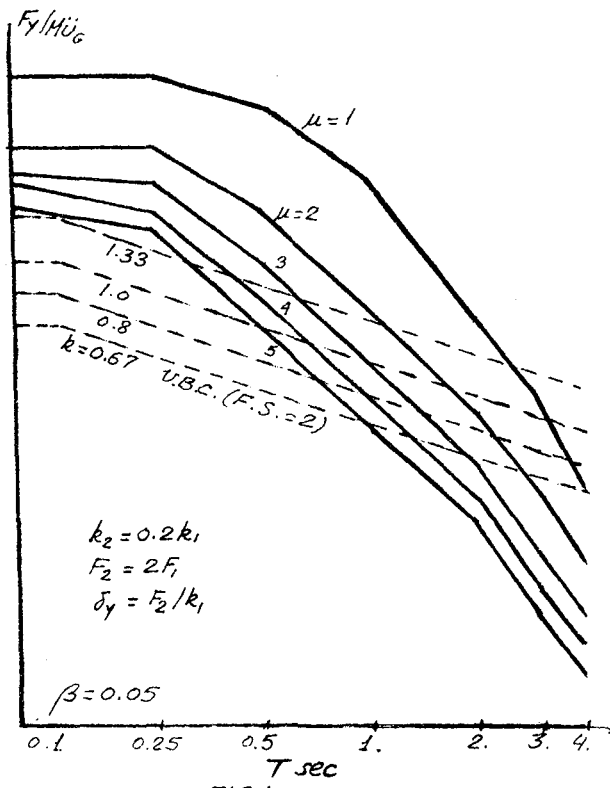


FIG 4 - TRILINEAR

d) It would seem that for single-degree-of-freedom systems, a variation of the C coefficient as suggested by the Uniform Building Code will not provide the same ductility requirements for different periods. While flexible systems designed this way are likely to remain elastic, stiff systems and particularly those with periods between 0.1 and 0.5 seconds may require very large ductilities. A variation of C inversely proportional to the period for $T > T_0$ (T_0 function of μ and β) would agree better with the constant ductility curves obtained in this study (1).

e) Extrapolation of the previous conclusion to actual structures (multi-degree-of-freedom systems) must be done with care, since higher modes are likely to be important for flexible buildings, whereas stiff buildings may entail a larger value of the K factor. Even so, analysis of different buildings seems to confirm the same overall trend. Flexible structures designed by the Uniform Building Code for zone 3 remain often elastic under an earthquake motion of the intensity of the 1940 El Centro, whereas stiff buildings require often substantial yielding.

REFERENCES

1. Anagnostopoulos, S.A., "Non-linear Dynamic Response and Ductility Requirements of Building Structures Subjected to Earthquakes," Report R-72-54, M.I.T. Department of Civil Engineering.
2. Veletsos, A.S., and Newmark, N.M., "Effect of Inelastic Behavior on the Response of Simple Systems to Earthquake Motions," 2nd World Conference on Earthquake Engineering, Vol. II.
3. Clough, R.W., and Johnston, S.B., "Effect of Stiffness Degradation on Earthquake Ductility Requirements," Japan Earthquake Engineering Symposium, 1967.
4. Kaldjian, M.J., and Fam, Wm. R.S., "Response of Steel Frames to Earthquake Forces," Steel Research for Construction Bulletin No. 11, Nov. 1968.
5. Veletsos, A.S., "Maximum Deformations of Certain Non-linear Systems," 4th World Conference on Earthquake Engineering, Vol. II.
6. Husid, R., "Gravity Effects on the Earthquake Response of Yielding Structures," California Institute of Technology, Research Report 1967.

to motion intensity and yield force (related through the variable \ddot{u}_{\max}/F_y).

3. RESULTS AND CONCLUSIONS

From the previous set of curves it was possible to obtain for any system the approximate value of \ddot{u}_{\max}/F_y which would produce a given ductility μ , and then make plots of F_y/\ddot{u}_{\max} versus critical natural period T , for different ductility levels and a specified fraction of critical damping β . Figs. 1 to 4 show these plots for elasto-plastic, bilinear, trilinear and stiffness degrading springs with $\beta = 0.05$ (based on the average of the various motions). Considering on the other hand a design shear given by a formula of the type

$$V_{\text{des}} = CZKW = CZKMg$$

and a factor of safety $F.S. = F_y/V_{\text{des}}$, one would obtain

$$\frac{F_y}{\ddot{u}_{\max}} = CK \left(\frac{Zg}{\ddot{u}_{\max}} \right) \cdot (F.S.)$$

The corresponding curves for $Z = 1$ (zone 3) and $\ddot{u}_{\max} = 0.32g$ (a motion of the intensity of the 1940 El Centro earthquake, NS component), values of K of 0.67, 0.80, 1. and 1.33, and a variation of C with natural period as suggested by the Uniform Building Code, are also plotted for comparison in figs. 1 to 4, for a safety factor of 2. Alternatively one could derive expressions for C as a function of the natural period, the initial damping, and the desired ductility level for specified values of K and of the factor of safety (1).

Results of this study tend to indicate that:

- a) As already suggested by various authors (3), (4), (5), ductility requirements for different types of springs with comparable overall force deformation characteristics, are indeed very similar. This conclusion is also valid for several slightly different models of stiffness degrading springs but may require a proper definition of the ductility factor (as for the case of the trilinear spring or Ramberg-Osgood models).
- b) Results for springs with stiffness and strength degradation showed on the other hand a much faster increase in ductility requirements as a function of motion intensity, leading rapidly to complete failure and suggesting that structural components with these characteristics should be designed to remain elastic. The results were, however, very sensitive to assumed values of the degradation parameters.
- c) Analyses were also performed including gravity effects (6). Conclusion a) did not apply to this case. On the contrary, the overall behavior seemed to be extremely sensitive to the variation of stiffness (whether a sharp, sudden, change as in elasto-plastic systems, or a smooth transition as in Ramberg-Osgood models).

DUCTILITY REQUIREMENTS FOR SOME NONLINEAR SYSTEMS SUBJECTED TO EARTHQUAKES

by

S.A. Anagnostopoulos^I, J.M. Roesset^{II}

SYNOPSIS

Following the lines of previous work, notably that of Veletsos and Newmark (2), a collection of nonlinear one-degree-of-freedom systems with different force deformation relationships were analyzed under five earthquake records, characteristic of motions on firm ground, scaled to various intensity levels. Some results of these analyses are presented, showing the yield force necessary to limit required ductility to any desired level, as a function of the elastic natural period and the intensity of motion. These forces are compared to the values that would be obtained from application of the Uniform Building Code for zone 3, and the implications of this comparison are discussed.

1. INTRODUCTION

The work described in this paper was conducted as part of an ongoing research project on optimum seismic design criteria for buildings. From published experimental results a set of nonlinear springs with different force deformation relationships were selected as representing the inter-story behavior of various structural components (1), and it was desired to assess the sensitivity of the results (ductility requirements in particular) to the models and variations in their basic parameters. Systems studied included elasto-plastic and bilinear springs representing the behavior of unbraced steel frames, stiffness degrading models representing braced steel frames or reinforced concrete frames and strength and stiffness degrading springs for infilled frames. Fractions of critical damping β in the elastic range of 0, 5, 10 and 20% were considered for each system (independently and in addition to the loss of energy by hysteresis in the inelastic range).

2. GENERAL CONSIDERATIONS

For each type of spring, systems with initial natural periods of 0.1, 0.25, 0.5, 1, 2 and 4 seconds were studied. Each one of these systems (with a given natural period and fraction of critical damping) was then subjected to base motions corresponding to the accelerograms of the NS and EW components of the 1940 El Centro earthquake, the NW and SE components of Taft (1952) and the SW component of Olympia (1949). In order to compare and average results these records were scaled so as to have for any run the same peak acceleration, the same value of Housner's intensity or the same value of Arias' intensity. It was found that this third procedure yielded the smallest variation from one motion to another, although results obtained by the second procedure were very similar. An average and an envelope curve were then obtained for each system relating ductility factor μ (defined as the ratio of the maximum strain to the yield strain)

^I Structural Engineer, Sc.D., Massachusetts Institute of Technology

^{II} Associate Professor of Civil Engineering, Mass. Institute of Technology

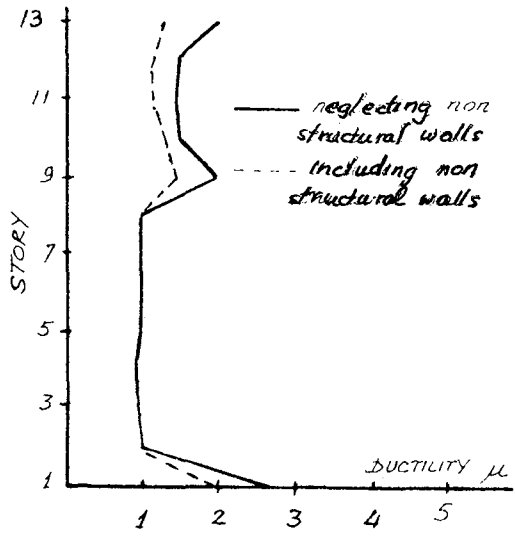


FIG 1. 13 STORY STEEL FRAME

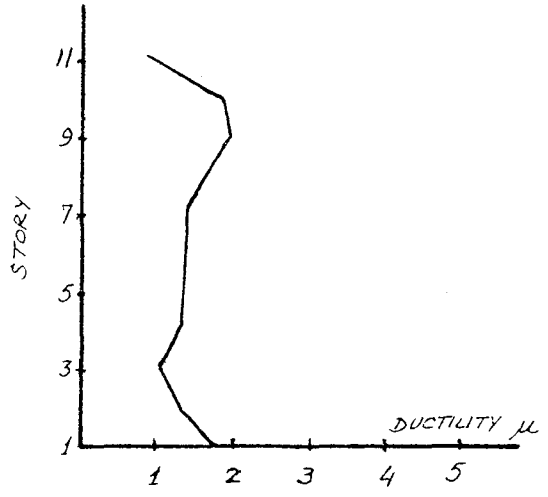


FIG 2. 11 STORY CONCRETE FRAME

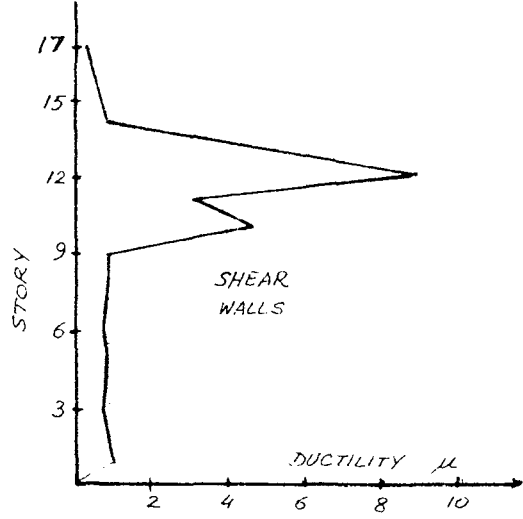


FIG 3. 17 STORY SHEAR WALLS AND CONC. FRAME BUILDING

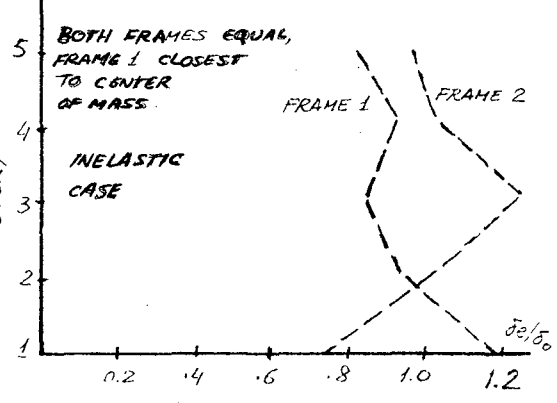
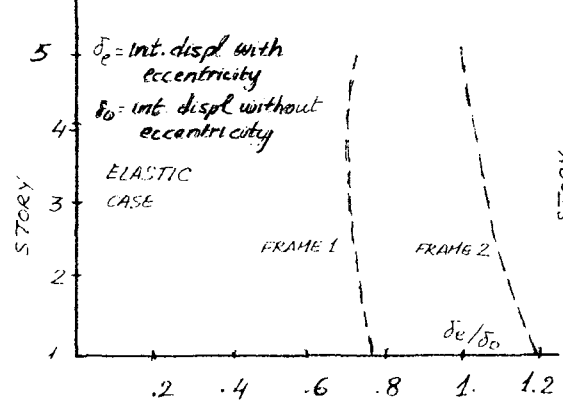


FIG 4. EFFECT OF TORSION ON INTERSTORY DISPLACEMENTS FOR 5 STORY BUILDING

permanent set for the different springs, and special flags indicating failure of any component. It is intended in the future to relate these quantities to some measure of damage in order to obtain an indication of possible economic loss as a function of earthquake intensity for a particular design.

The program was tested in the elastic range by comparing results to those obtained from a general and more accurate program for linear dynamic analysis of complete buildings developed some years ago at M.I.T. Agreement was in all cases extremely satisfactory.

Several buildings were analyzed in the inelastic range for motions of varying intensity. For similar structures, values and distribution of ductilities (1) were comparable to those reported by Clough (2). Results for a 13-story steel-frame building, an 11-story concrete-frame structure and a 17-story concrete-frame and shear-wall building are shown in figs. 1 to 3. Analysis of a five-story building with a rather large eccentricity confirmed the fact reported by other researchers that dynamic torsional effects cannot be accounted for by imposing a set of static forces with the same eccentricity. In fact for the building considered it was the frame farthest from the center of mass which had largest dynamic forces in the elastic range, contrary to what a static analysis would predict. The distribution of forces among the frames changes considerably along the height of the building as some of the elements start to yield, as shown in fig. 4.

While more work is necessary to refine and validate the selection of the spring type and characteristics for various structural components, it would seem at present that the proposed model provides an economic and reasonably accurate procedure to estimate overall behavior and ductility requirements for a wide class of practical buildings. The model is not applicable to structures where axial effects are important, but LaTona's work (5) seems to indicate that more complicated models may be equally suspect in this case. The computer program is now being used for a more complete set of parametric studies of buildings designed by different criteria.

REFERENCES

1. Anagnostopoulos, S.A., "Non-linear Dynamic Response and Ductility Requirements of Building Structures Subjected to Earthquakes," Report R72-54, M.I.T. Department of Civil Engineering.
2. Clough, R.W., and Benuska, K.L., "FHA Study of Seismic Design Criteria for High-Rise Buildings," HUD - TS-3, August 1966.
3. Goel, S.C., "Response of Multistory Steel Frames to Earthquake Forces," Steel Research for Construction Bulletin 12, November 1968.
4. Anderson, J.C., "Seismic Behavior of Multistory Frames Designed by Different Philosophies," Ph.D. Thesis, University of California at Berkeley, 1969.
5. LaTona, R.W., "Non-linear Analysis of Building Frames for Earthquake Loading," Report R70-65, M.I.T. Department of Civil Engineering.
6. Biggs, J.M., "Introduction to Structural Dynamics," McGraw-Hill 1964.

procedure was thus intended, not to give detailed information on any particular member or joint, but rather to provide average overall ductility requirements for the various components in each story.

From published experimental results a set of eight different nonlinear springs was implemented to reproduce the interstory behavior of various structural and nonstructural components such as masonry partitions or isolated block walls, unbraced, braced or infilled steel frames, open, infilled or partially infilled concrete frames, and shear walls or elevator boxes. Partitions, isolated block walls, and frames, are then assumed to act as close-coupled systems, whereas a far-coupled system is used for shear walls or boxes. The program will automatically generate, if so desired, the set of springs corresponding to a given component, determining the characteristics of each spring from the properties of columns, girders, bracing and panels. The user has, however, the option to select himself and to specify directly any set of springs. In addition, the shear capacity of each component is determined and compared at each step to the actual shear force to detect the possibility of brittle failures.

The model assumes that each floor has a slab which can act as a rigid diaphragm, leading thus to a system with three degrees of freedom per floor, (two displacements and a torsional rotation). The program computes the shear forces that have to be transmitted by the diaphragm and could therefore detect possible cracking or failure of the slab, but this option is not implemented at present.

One of the main limitations of the model is in the fact that axial deformation of the columns is neglected in order to obtain the simplified shear type behavior for the frames. This restricts its applicability to buildings with moderate slenderness ratios, but a large number of practical structures fall within this range.

The resulting differential equations of motion are written in matrix form as

$$\ddot{M}\dot{U} + C\dot{U} + F(U) = E$$

where M is a diagonal mass-inertia matrix, C a damping matrix that will yield any desired modal dampings in the elastic range, F a vector of spring forces (nonlinear function of displacements), and E the vector of excitation forces for the two principal directions. These equations are solved numerically by using a simple step-by-step integration procedure known as the "constant velocity" method (6). Extensive testing showed this method to give results comparable in accuracy, and often better, than those obtained using more complex procedures (1).

Finally, the effect of gravity loads on the deformed geometry of the building (P- Δ effect) is also included, if desired by the user.

3. RESULTS AND CONCLUSIONS

Results of the program include selectively for each floor or element time histories as well as average and maximum values of accelerations, displacements, forces and deformations, plus maximum ductility factors and

NON-LINEAR DYNAMIC ANALYSIS OF BUILDINGS WITH TORSIONAL EFFECTS

by

S.A. Anagnostopoulos^I, J.M. Roesset^{II} and J.M. Biggs^{III}

SYNOPSIS

The nonlinear dynamic response of complete buildings can be investigated using a simplified mathematical model. The masses, lumped at the floor levels, are connected with shear and bending springs whose characteristics are estimated from the properties of various structural and non-structural components. The shear springs, forming close-coupled systems, approximate the behavior of frames for which axial shortening of the columns is not important, while the bending springs, leading to far-coupled systems, are used for shear walls and boxes. Three degrees of freedom are considered per floor. Results include time histories as well as maximum and average effects.

1. INTRODUCTION

While a large number of computer programs have been developed in the last few years for the dynamic analysis of complete buildings in the linear elastic range (including braced and unbraced frames, shear walls, boxes, shear panels etc.) most of the research done on the inelastic dynamic response of buildings has been limited to the study of simple multi-story plane frames (2), (3), (4), (5), or to combinations of frames and shear walls interacting without torsion (2).

Even with models where the spreading of yielding and inelastic axial effects are neglected, analysis of a complete building by these methods becomes economically prohibitive for design purposes. Furthermore, most of these studies ignore the possibility of brittle or shear failures, being primarily intended for ductile frames. In this paper a simplified model, which incorporates space behavior and includes such factors as stiffness and/or strength degradation, nonstructural elements and possibility of brittle failures, is outlined, and results from the analysis of several buildings are discussed.

2. GENERAL CONSIDERATIONS

The mathematical model and the corresponding computer program were developed as part of an ongoing research project on optimum seismic design criteria for buildings (1). The main objective was to be able to reproduce the overall behavior of a building in the linear and nonlinear ranges at low computational costs, and to use this information for a gross estimate of damage in several types of buildings as a function of the design strategy and the intensity of the earthquake motion. The analysis

^I Structural Engineer, Sc.D., Massachusetts Institute of Technology.

^{II} Associate Professor of Civil Engineering, Massachusetts Institute of Technology.

^{III} Professor of Civil Engineering, Massachusetts Institute of Technology.

FIGURES

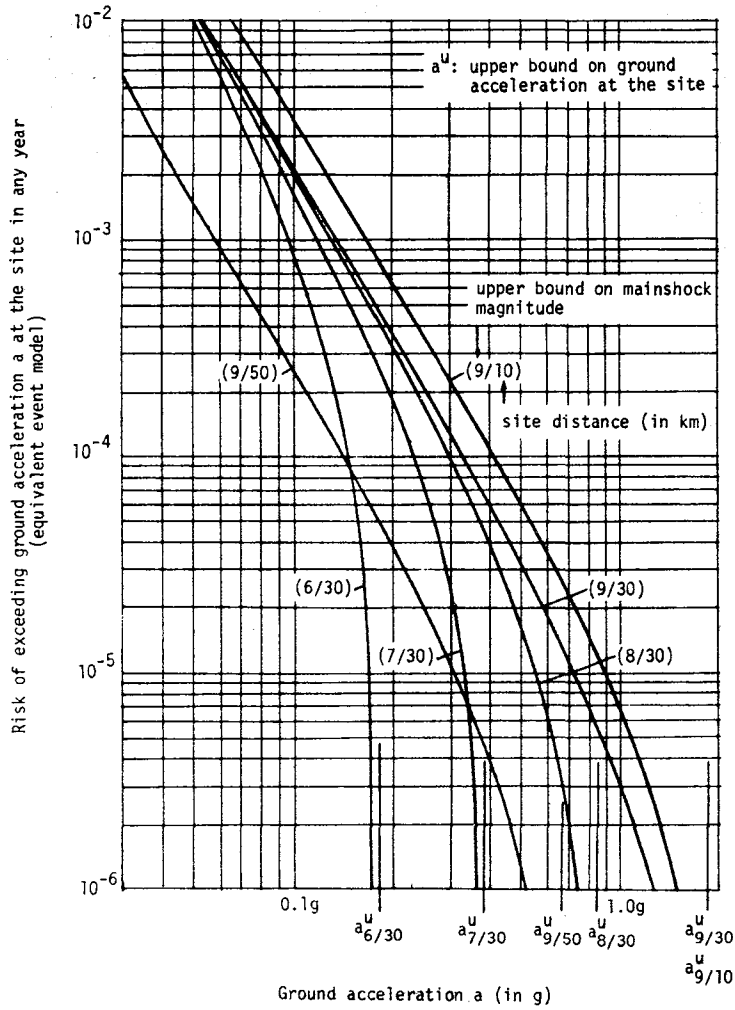


Figure 2

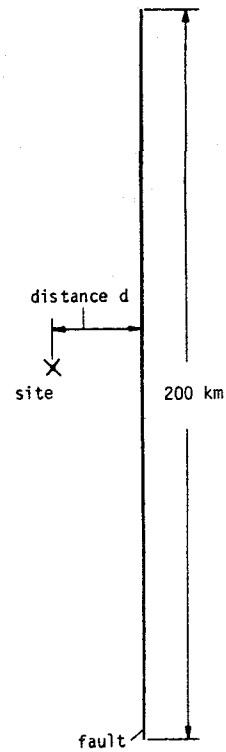


Figure 1

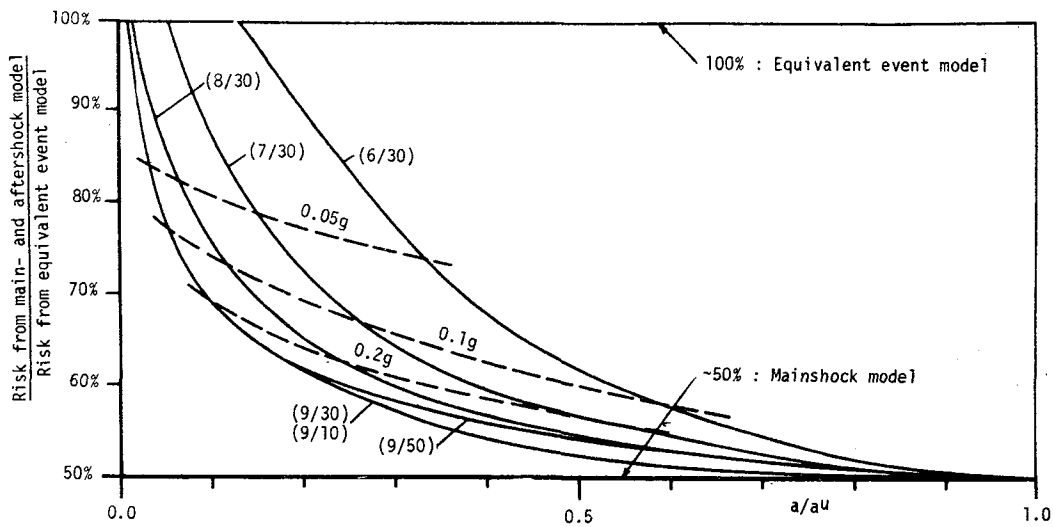


Figure 3

of the aftershocks to the total risk. It is anticipated, however, that a more realistic two-dimensional spatial assumption for aftershock locations in future analytical models will demonstrate further influences of parameters on the contributions of aftershocks.

BIBLIOGRAPHY

1. Cornell, C. A., "Probabilistic Analysis of Damage to Structures under Seismic Loads," Chapter 27 of Dynamic Waves in Civil Engineering, edited by D. A. Howells, I. P. Haigh and C. Taylor, John Wiley & Sons, 1971.
2. Esteva, L., "Seismicity Prediction: A Bayesian Approach," Proceedings 4th World Conf. Eq. Eng., Santiago, Chile, January 1969.
3. Utsu, T., "Aftershocks and Earthquake Statistics," Journal of the Faculty of Science, Hokkaido University, Japan, Ser. VII, Vol. III, No. 3, 1969.
4. Merz, H. A., "Aftershocks in Engineering Seismic Risk Analysis," Master's Thesis, Mass. Inst. of Tech., Cambridge, Mass., USA, to be published June 1973.

these relationships the empirical laws from Utsu⁽³⁾ are used. Mainshock characteristics as well as the attenuation "law" with an error term have been taken from Cornell⁽¹⁾. Based upon these assumptions, the probability p_a that the maximum seismic intensity experienced at a site in a time span of T years, caused either by a main- or an aftershock, will exceed \underline{a} units can be computed⁽⁴⁾.

An analytical model has been derived for the simplest case, where it is assumed that both the main- and the aftershock epicenters lie on the same "line" fault. Because of this simplistic assumption, the results cannot yet be generalized with confidence, however they provide new insights and understanding. Future efforts will include models with spatial assumptions that reflect more accurately the real world situation.

Example: Numerical results from an analytical model where main- and aftershocks occur only on a fault line are presented in Figures 2 and 3 for a fault-site configuration as shown in Figure 1. After dividing the fault line into many (up to 3000) smaller pieces, the risks associated with each of these pieces were computed and the total risk was obtained by addition, which is valid for the small risk levels involved. In this example the parameters in the modified Omori law were chosen such that the expected number of aftershocks greater than magnitude 4.5 in a time period of 10 years is equal to the expected number of mainshocks greater than magnitude 4.5 in 10 years; both were assumed to be 0.5. Figure 2 shows the seismic risk at the site for different upper bounds on the mainshock magnitude and for different distances d if the mean main- and aftershock rates are added and treated simply as a mean mainshock rate, i.e., aftershocks being assumed equivalent to mainshocks (equivalent event model). If mainshocks alone are taken into account (mainshock model), the risks in this example are approximately half of the ones shown in Figure 2. These risks were obtained by the analytical model described in Cornell⁽¹⁾. Because the mainshock magnitudes are truncated at an upper bound, there is also an effective upper bound on the seismic intensity at the site which depends on the upper bound on the mainshock magnitude and the distance d. In Figure 3 the risks from Figure 2 are compared with the ones obtained from the described analytical model for main- and aftershocks. It can be observed that, except for very small ground accelerations, simply treating main- and aftershocks as equivalent independent events gives conservative risk estimates, the results being especially conservative if the level of the ground acceleration is near the upper bound on the ground acceleration at the site. On the other hand, simply treating mainshocks alone as significant events in evaluating the seismic risk yields too low risk estimates. Independent of upper bounds on the magnitudes of mainshocks, the relative contribution of aftershocks to the risk at the site decreased with increasing ground acceleration, as indicated by the dashed lines. However, for a fixed level of ground acceleration, the absolute contributions are smaller for smaller upper bounds.

The most significant parameters that influence the relative contribution of the aftershocks have been found to be the ratio of the expected number of mainshocks to the expected number of aftershocks, and the upper bound on the mainshock magnitude. Other parameters, such as d, affected the absolute risk levels but not significantly the relative contribution

AFTERSHOCKS IN ENGINEERING SEISMIC RISK ANALYSIS

by

Hans A. Merz^I, C. Allin Cornell^{II}

SYNOPSIS

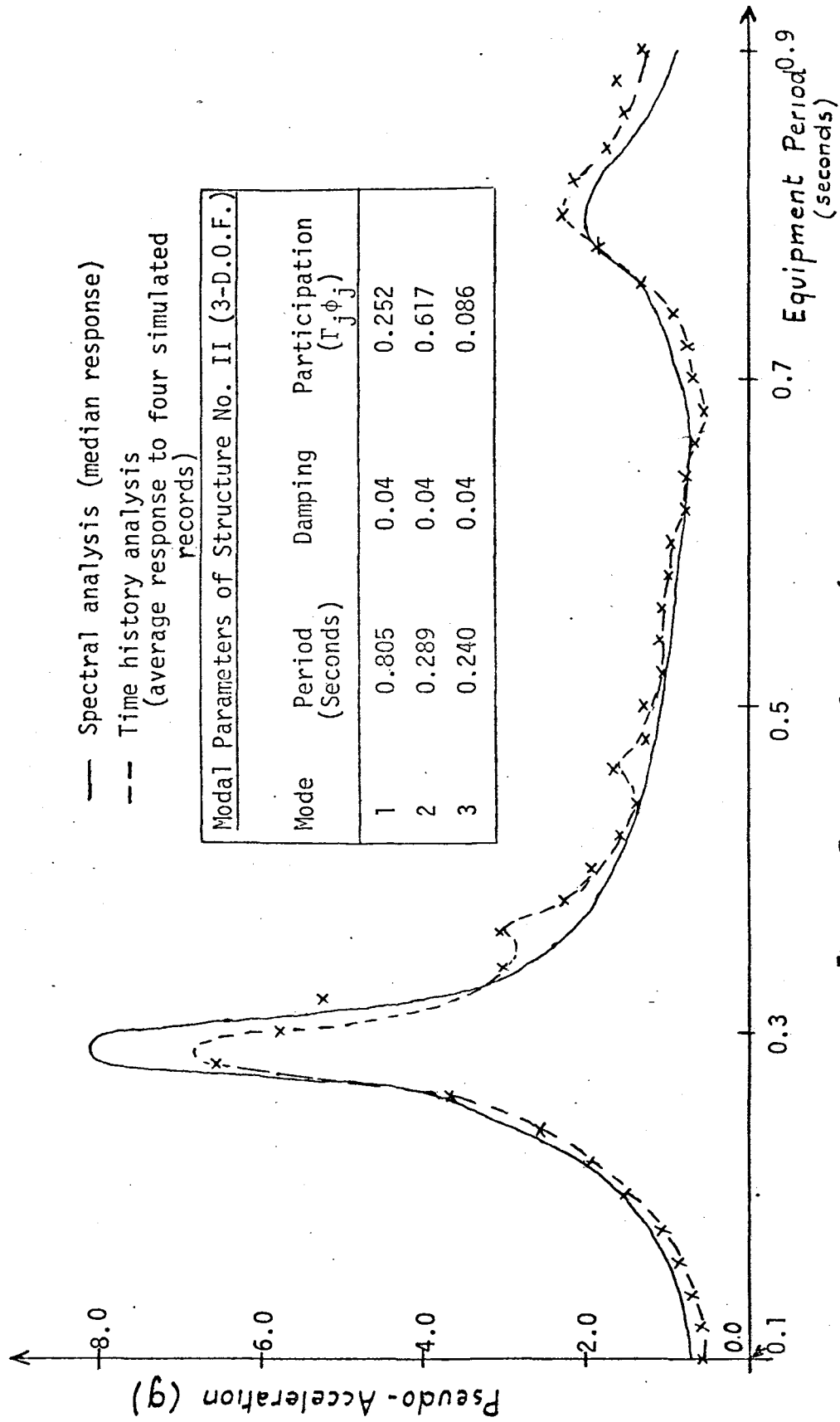
The influence of spatially distributed aftershocks on calculated seismic risks is investigated. The conclusions are that to ignore aftershocks is unconservative and that to treat all events as mainshocks is conservative.

The purpose of seismic risk analysis as defined here is to assess the probability p_a that the maximum seismic intensity experienced at a structural site in a time period of T years will exceed a units (e.g., 0.2g). Seismic risk analysis has been studied by the senior author(1), by Esteva(2) and by others for several years; reported analyses account for uncertainty in the times, locations and magnitudes of mainshocks as well as uncertainty in the attenuation "laws" (correlations) which estimate site intensity as a function of event magnitude and distance. In several historical events it has been noted that certain sites located at some distance from the mainshock epicenter have experienced more severe shaking during the temporally and spatially distributed aftershock sequence than during the larger mainshock itself. The cause is apparently the closer proximity of a particular aftershock to the site. This study is aimed at evaluating this "additional aftershock risk" and at determining under what conditions it might prove important (e.g., be of the same order as the risk due to mainshocks). The results are compared with a simple method that does not distinguish between main- and aftershocks, but treats both as mainshock events, and with a simple method that considers only mainshocks as significant events in determining the seismic risk.

Seismologists such as Omori, Utsu, Aki and Vere-Jones have studied and modeled aftershock sequences in time. Utsu(3) has, in addition, investigated the correlation between mainshock magnitude and the form and extent of the areal region around the mainshock epicenter in which aftershocks might occur. In our analysis, the temporal characteristics of aftershocks are represented as seismologists have done before, as a non-homogeneous Poisson process in time, triggered by a mainshock and with parameters dependent on the mainshock magnitude. Specifically, the modified Omori law is used to account for the decay of the rate of aftershock events in time, and the mainshock magnitude is assumed to be the upper bound on the magnitudes of the aftershocks. Furthermore, the aftershocks are assumed here to occur at random spatially in a region whose location and extent depend upon the (random) mainshock location and magnitude. For

^I Research Assistant, Mass. Inst. of Tech., Cambridge, Mass., USA.

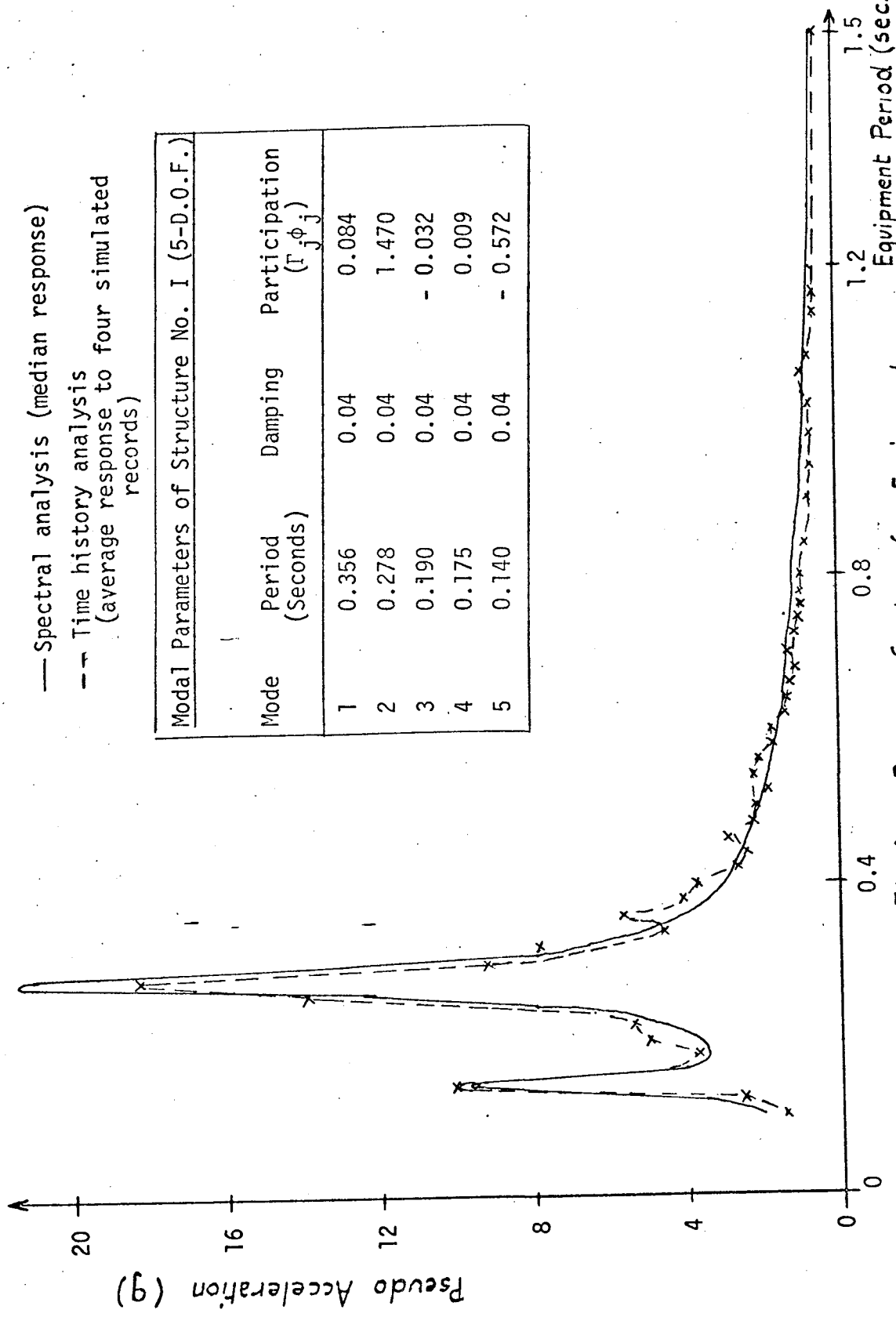
^{II} Associate Professor, Mass. Inst. of Tech., Cambridge, Mass., USA.



— Spectral analysis (median response)
 --- Time history analysis
 (average response to four simulated records)

Modal Parameters of Structure No. II (3-D.O.F.)			
Mode	Period (Seconds)	Damping	Participation ($\Gamma_j \phi_j$)
1	0.805	0.04	0.252
2	0.289	0.04	0.617
3	0.240	0.04	0.086

Fig.5 Response Spectra for Equipment in Structure No. II



— Spectral analysis (median response)
 - - Time history analysis
 (average response to four simulated records)

Modal Parameters of Structure No. I (5-D.O.F.)				
Mode	Period (Seconds)	Damping	Participation ($\Gamma_j \phi_j$)	
1	0.356	0.04	0.084	
2	0.278	0.04	1.470	
3	0.190	0.04	- 0.032	
4	0.175	0.04	0.009	
5	0.140	0.04	- 0.572	

Fig. 4 Response Spectra for Equipment in Structure No. I

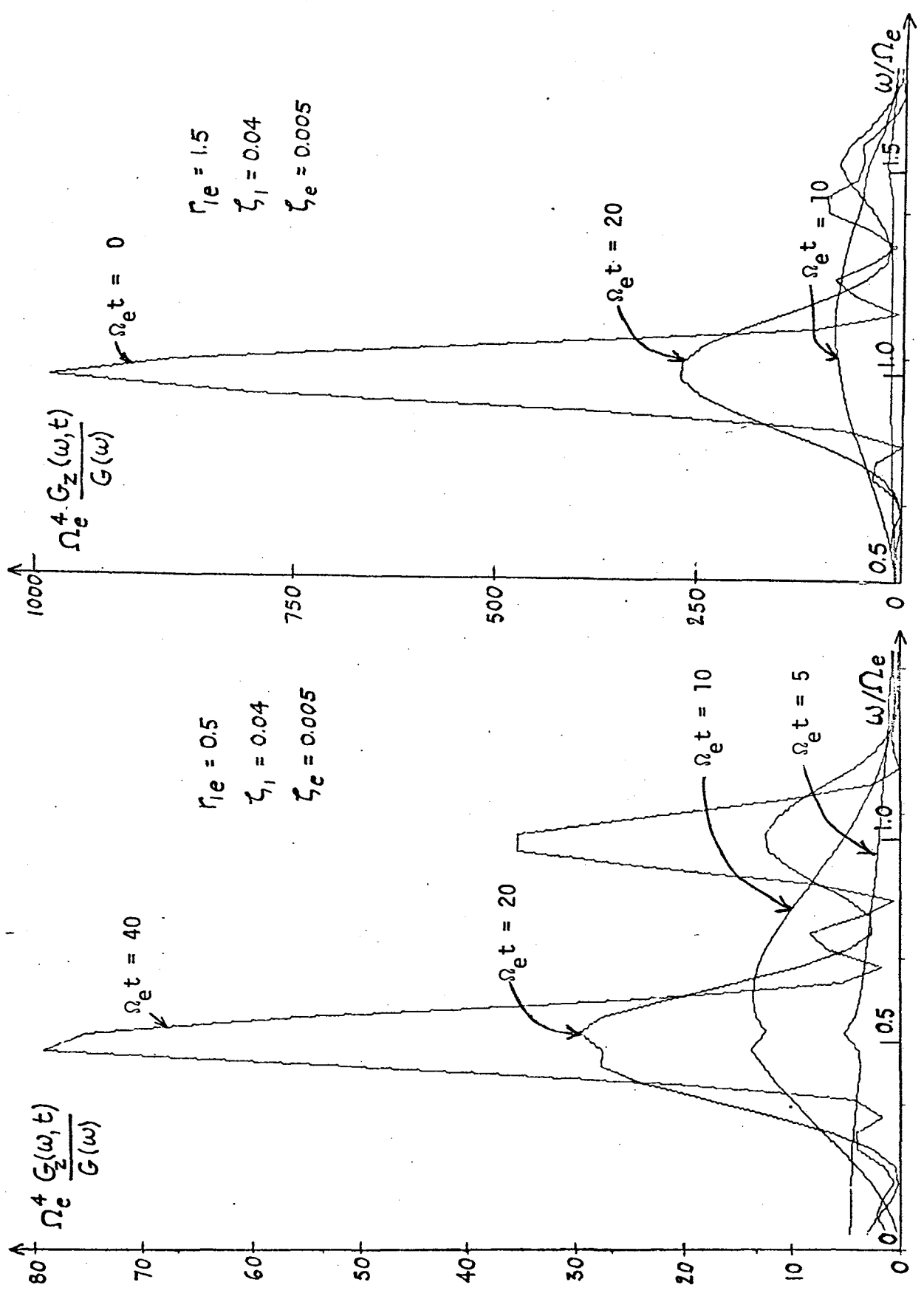


Fig 2 : Time - Dependent Spectral Density of Equipment Response

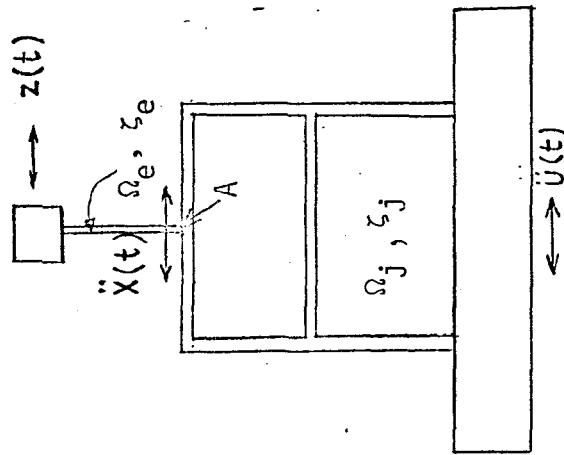


Fig. 1 System Representation

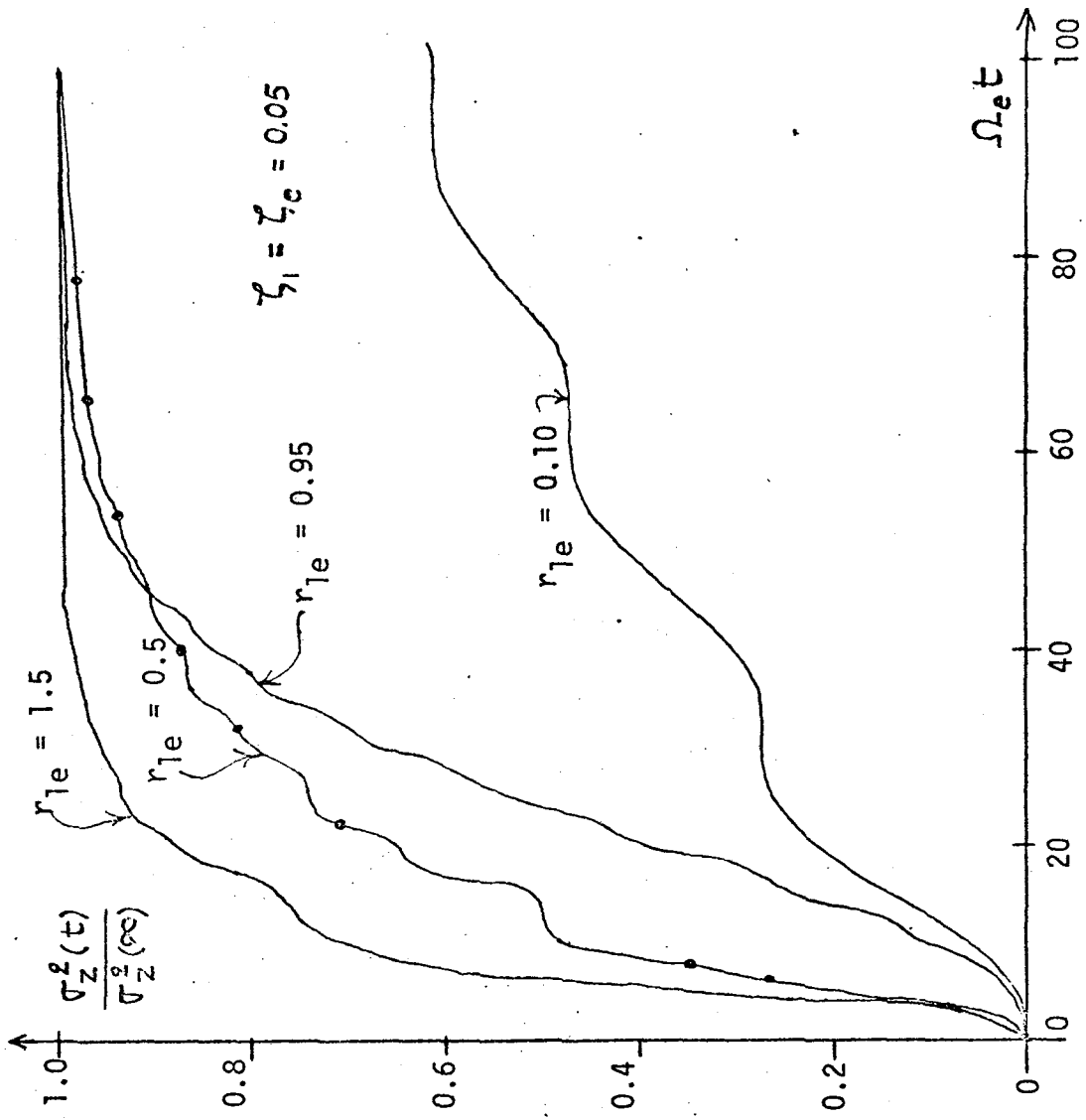


Fig. 3 Normalized Mean Square Equipment Response

from which a response spectrum is constructed; and (ii) by an extension of the response spectrum method utilizing only the peak modal responses of the structure (5). Both procedures have the same deficiencies previously attributed to time-history and response spectra-based analyses of multi-degree structures, undoubtedly amplified by extending them to two systems in series. Most of these deficiencies are not shared by the direct random vibration approach.

The validity of the proposed method was tested by making a comparison between the predicted median floor response spectra and the average of four (4) floor response spectra curves, each computed by using a time-history analysis based on a single sample function of the site ground motion process. A common spectral density function provided the input to both the artificial motion generation routine and to the probabilistic dynamic analysis. The comparison was made for two different multi-degree-of-freedom representations of the primary structure. The modal parameters of Structures I and II are listed in Figs. 4 and 5, respectively. These figures also show that the agreement between the spectra obtained by the two methods is quite satisfactory over the entire range of equipment periods considered.

REFERENCES

1. Chakravorty, M.K., "Transient Spectral Analysis of Linear Elastic Structures and Equipment Under Random Excitation," Ph.D. Dissertation, MIT Dept. of Civil Engineering Research Report R72-18, April, 1972.
2. Priestley, M.B., "Power Spectral Analysis of Nonstationary Random Processes," J. Sound and Vibration, Vol. 6, 86-97, 1967.
3. Vanmarcke, E.H., "Properties of Spectral Moments with Application to Random Vibration," J. Eng. Mechanics Div., Proc. ASCE, Vol. 98, No. EM2, April, 1972.
4. Corotis, R.B., Vanmarcke, E.H. and C.A. Cornell, "First Passage of Nonstationary Random Processes," J. Eng. Mechanics Div., Proc. ASCE, Vol. 98, No. EM2, April, 1972.
5. Biggs, J.M., "Seismic Response Spectra for Equipment Design in Nuclear Power Plants," Proc. First Conference on Reactor Technology, Berlin, 1971.

ACKNOWLEDGEMENT

This research was sponsored by the U.S. National Science Foundation under Grant No. GK-26296.

ment (1). $G_z(\omega, t)$ indicates how the mean square of $z(t)$ is distributed over different frequencies at different times, i.e., how the frequency content of the equipment response varies with time. In Reference 1, exact analytical expressions are obtained for $G(\omega, t)$. Integration over all frequencies of this function yields an algebraic expression for the time-dependent mean square value $\sigma_z^2(t)$. Other spectral moments are also computed and used in (i) a quantitative study of the variation in time of the narrowness of the frequency content of the equipment response, and (ii) an approximate evaluation of the probability distribution of the floor response spectra, i.e., a plot of the maximum value of the equipment response as a function of Ω_e for a given value of ζ_e . All results depend in a relatively simple way on the building's natural periods, modal damping ratios and participation factors, the ground motion statistics and the equipment period and damping ratio. The median maximum response is expressed as $r \sigma_x(s)$, in which s = motion duration, and r = a factor which depends upon the spectral moments $\lambda_i(t) = \int_0^\infty \omega^i G(\omega, t) d\omega$, $i = 0, 1, 2$. Note that $\lambda_0(t) = \sigma_x^2(t)$. An important related function is $q(t) = [1 - \lambda_1^2(t) / \lambda_0(t) \lambda_2(t)]^{1/2}$: it is unitless measure of the narrowness of the frequency content of $z(t)$ at time t , and ranges between 0 and 1 (3,4).

RESULTS AND APPLICATIONS

Time Dependent Spectra and Mean Square Values

Some typical time-dependent spectral densities and mean square value functions are shown in Figs. 2 through 5. The parameters employed in the study are the frequency ratio r_{1e} (ratio of structural frequency to equipment frequency), the time variable $\Omega_e t$ and the two damping ratios ζ_1 and ζ_e . In this particular computation both the structure and the equipment are treated as single-degree-of-freedom systems. The time-dependent power spectral density, $G_z(\omega, t)$ for different values of the parameters appear in Fig. 2. The shape of the spectrum during the initial stages (i.e. for low values of $\Omega_e t$) is similar to that of a wide-band process. It becomes narrower and more peaked at the resonant frequencies when time increases. This time-dependent nature of the power spectrum influences the computation of the distribution of the maximum response, through $q(t)$. When the frequency ratio $r_{1e} = \Omega_1 / \Omega_e$ is very close to 1, a strong amplification of the response spectral density due to resonance phenomenon is observed. This indicates that most of the energy is distributed around these two frequencies.

Fig. 3 shows how the mean square response, $\lambda_0(t)$, varies with time. It indicates that the time-dependent nature of the equipment response is important. In particular, the transient growth of the equipment response is quite sensitive to (i) the duration of the excitation, (ii) the frequency of the structure and the equipment, (iii) the damping ratios ζ_j and ζ_e .

Floor Response Spectra

Floor response spectra are currently generated in one of the following two ways: (i) by a time-history analysis of the structure which produces the detailed motion of the point at which the equipment is mounted

PROBABILISTIC SEISMIC ANALYSIS OF LIGHT EQUIPMENT
WITHIN BUILDINGS

by

M.K. Chakravorty^I and E.H. Vanmarcke^{II}

SYNOPSIS

Major buildings often provide support for relatively light secondary systems (equipment) whose continued performance during earthquakes is essential to safety. Presented in this paper is a nonstationary random vibration analysis which yields the statistical properties of the equipment displacement relative to the motion of the structure at the point at which the equipment is attached. It is assumed that the results of a classical modal analysis of the structure are available, and that the equipment can be modeled as a linear one-degree oscillator. The method presented herein in fact generates the probability distribution of so-called floor response spectra.

ANALYSIS

It is common to separate the seismic analysis of secondary systems (equipment) from that of the primary system (a building) and to view the structural response acceleration at a particular point A (see Fig. 1) as input for the dynamic analysis of equipment supported at that point. Thus we consider a multi-degree-of-freedom structure with an attached single-degree-of-freedom viscously damped oscillator representing equipment. The entire system is excited by a ground motion $U(t)$, which is represented by a suddenly applied weakly stationary Gaussian process whose spectral density and duration are specified. It is assumed that a classical modal analysis of the structure is possible and that the effect of the equipment vibration on the structure (i.e., interaction effect) is negligible. The structural response, $Y(t)$, at the point of attachment can be expressed in terms of the normal modes ϕ_j and the modal coordinates $\eta_j(t)$, $j=1$ to n , i.e., $Y(t) = \sum \phi_j \eta_j(t)$. Each component $\eta_j(t)$ represents the output of a single-degree-of-freedom system characterized by its modal frequency Ω_j and modal damping ζ_j , and is exposed to a modal forcing function $-\Gamma_j u(t)$, where Γ_j is the participation factor of the j th mode. The dynamic behavior of the equipment displacement, $z(t)$, relative to its point of support, will depend upon the equipment natural frequency Ω_e and damping ζ_e , and on $\ddot{X}(t)$, the absolute acceleration of the equipment support. The latter can be expressed in terms of the impulse response functions of the individual structural modes (1).

The time-dependent (or evolutionary) spectral density (2) $G_z(\omega, t)$ which characterizes the equipment response $z(t)$ can be derived from an expression of the nonstationary mean square response, $\sigma_z^2(t)$, of the equip-

^I Engineer, Stone and Webster Engineering Corporation, Boston, Massachusetts, U.S.A.

^{II} Assistant Professor of Civil Engineering, Massachusetts Institute of Technology, Cambridge, Massachusetts, U.S.A.

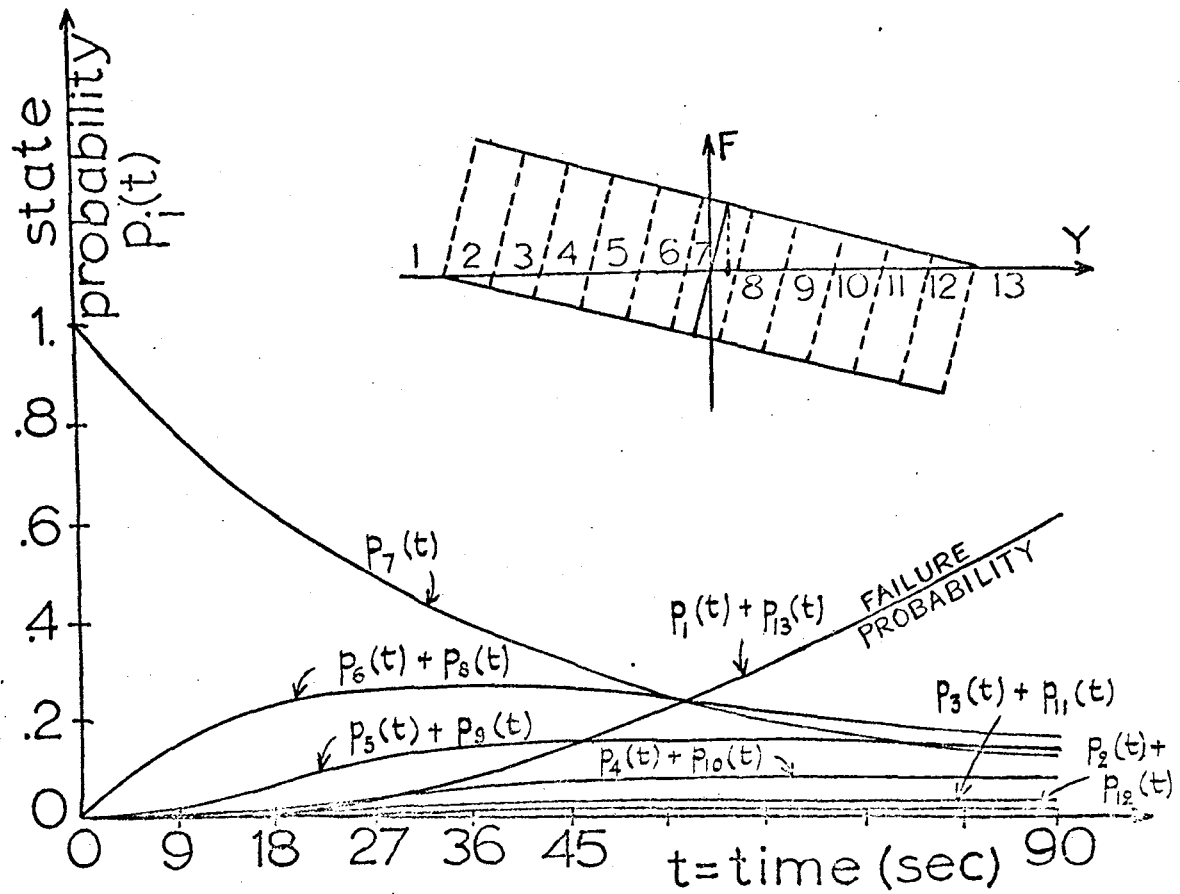


Fig. 6 The State Probabilities for Structure No. 2 (whose properties are given below).

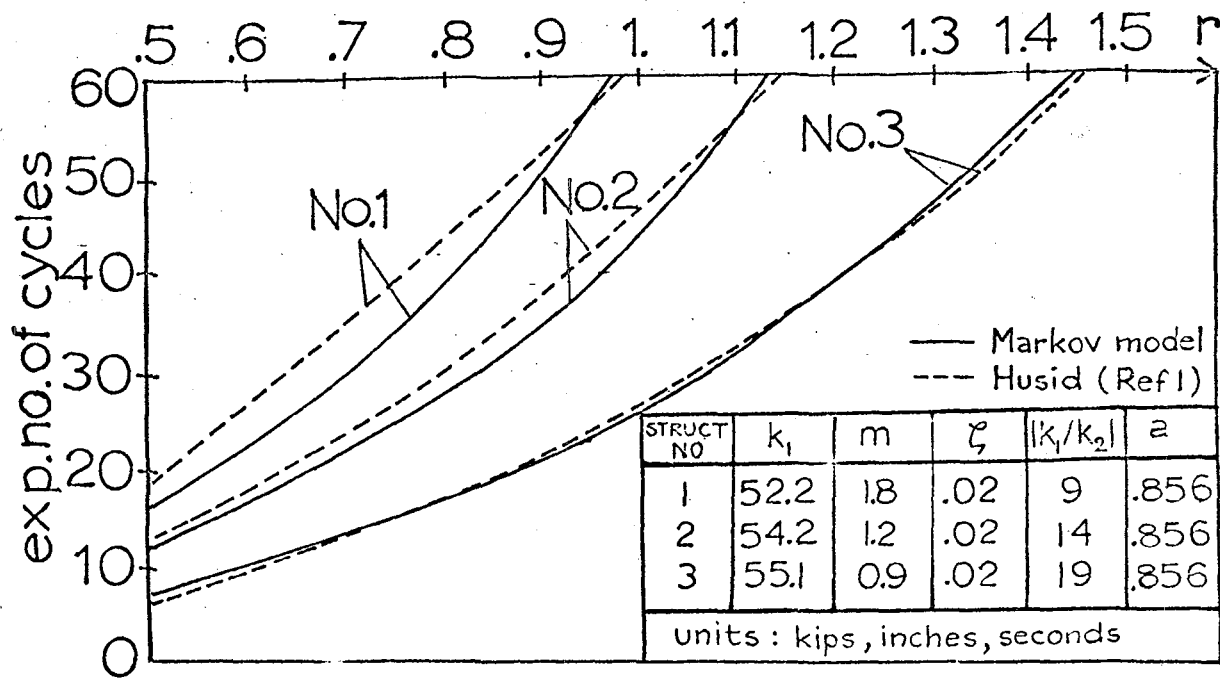


Fig. 7 The Expected Number of Cycles to Failure

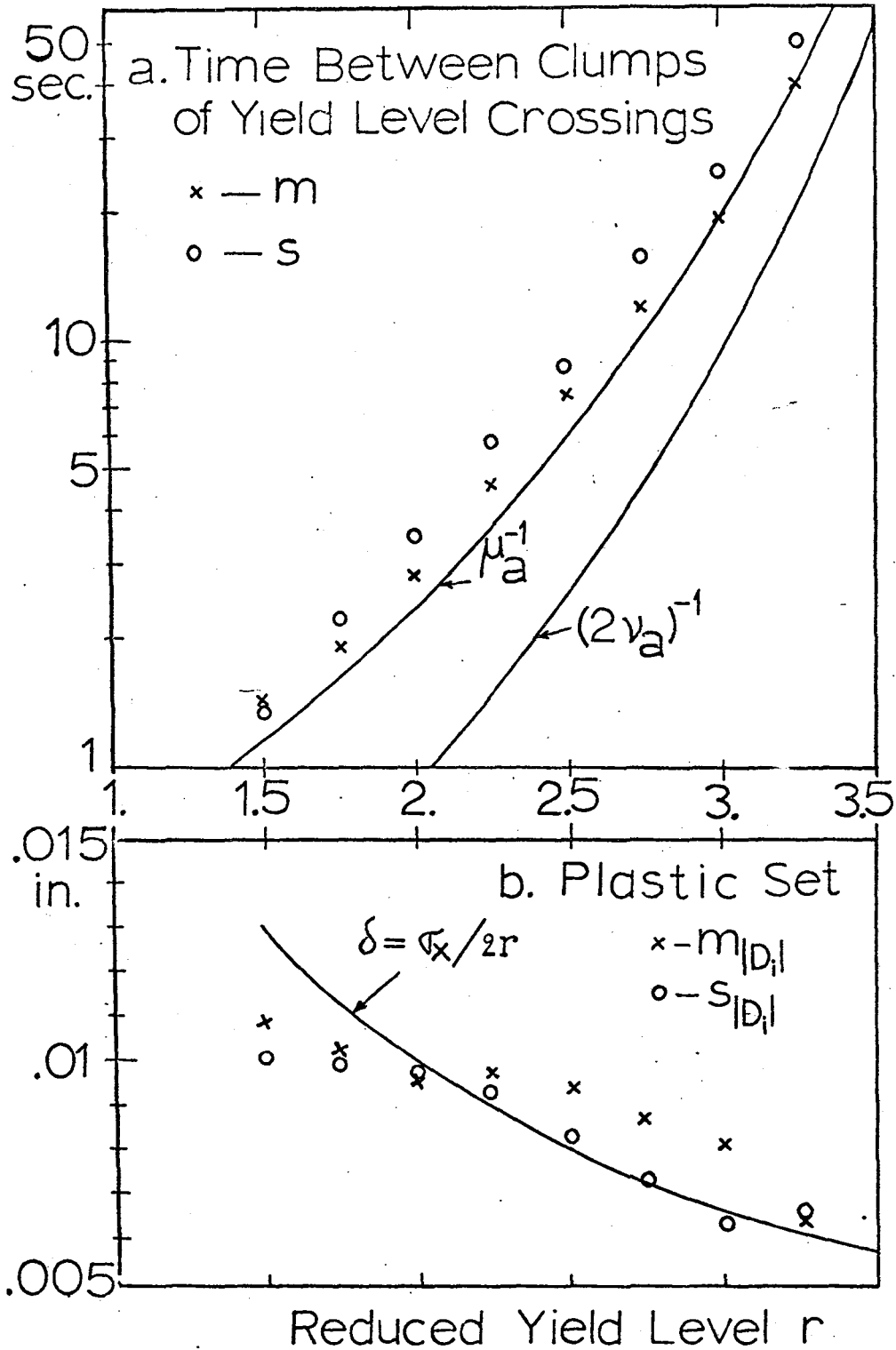


Fig. 5 Comparison of Simulated and Theoretical Values for the Mean and the Standard Deviation of (a) the Time Between Clumps of Yield Level Crossings, and (b) the Plastic Set for a Single Clump.

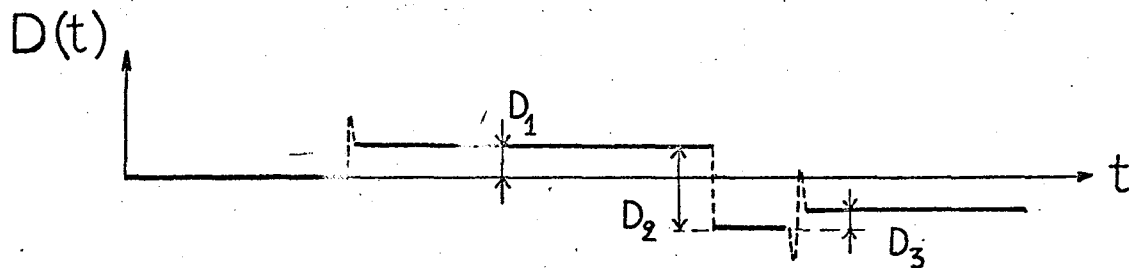
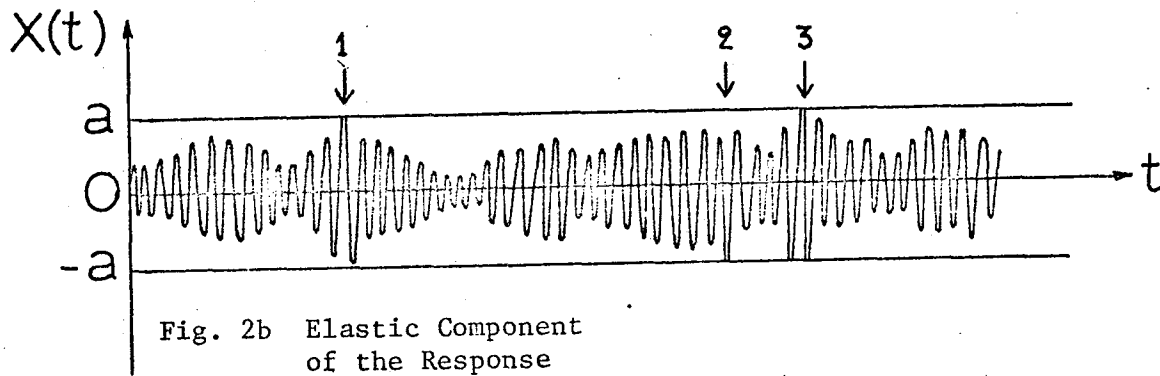
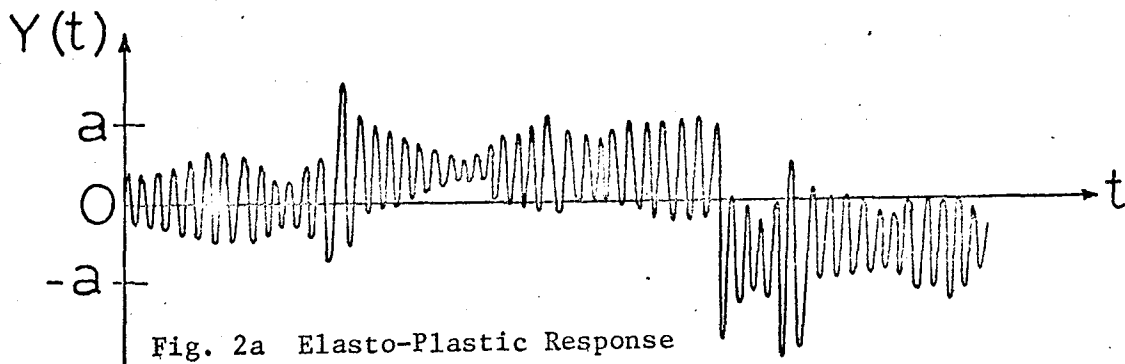


Fig. 2c Inelastic Component of the Response

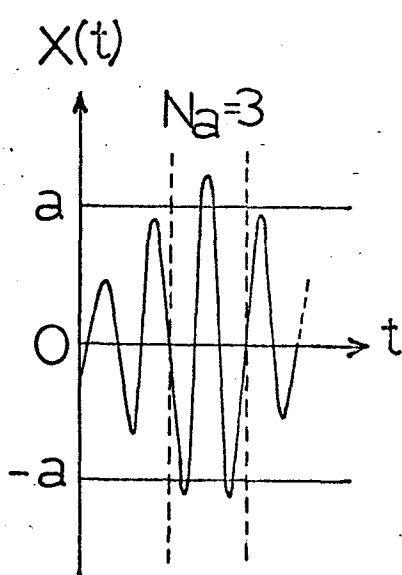


Fig. 3 A clump of Crossings Outside the Range $(-a, a)$

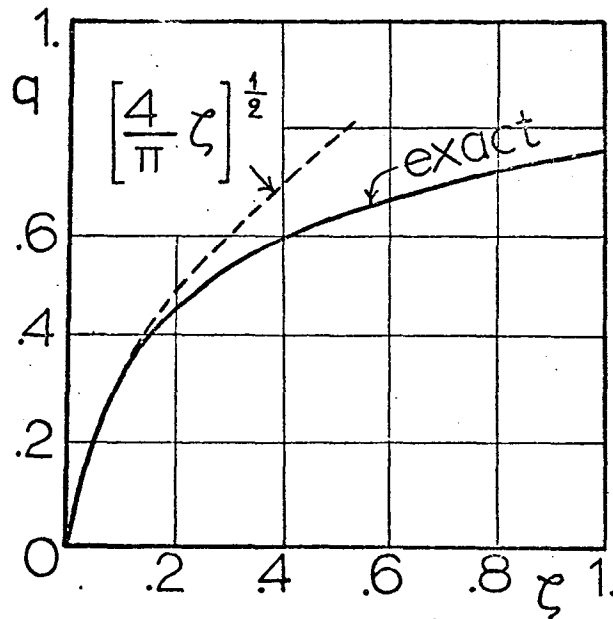


Fig. 4 The Factor q as a Function of the Damping ζ

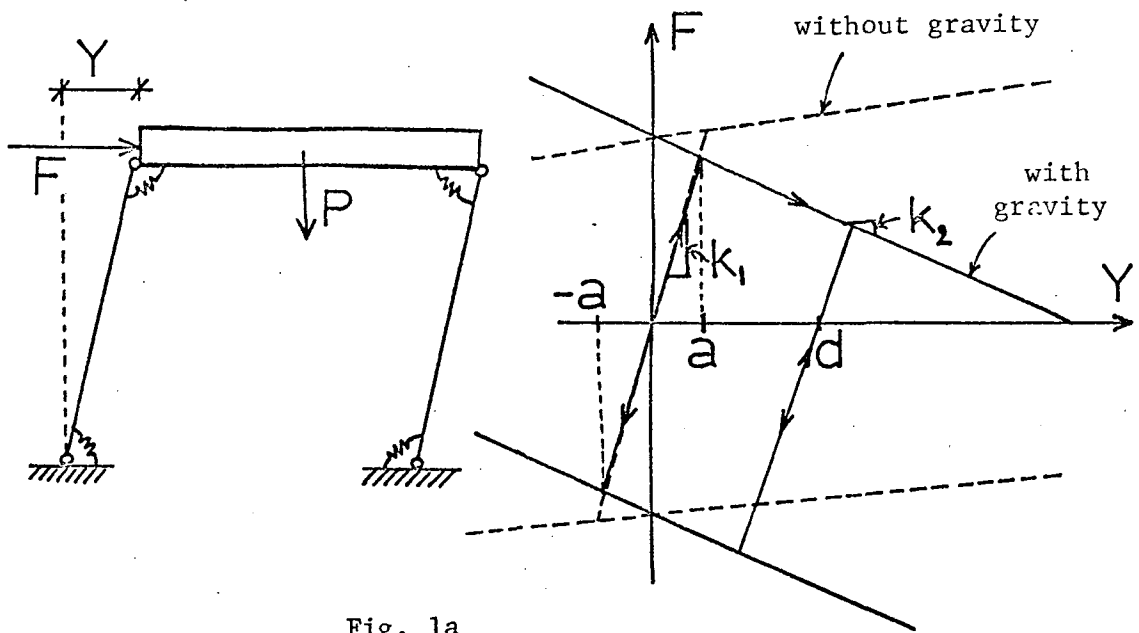


Fig. 1a

Bilinear System

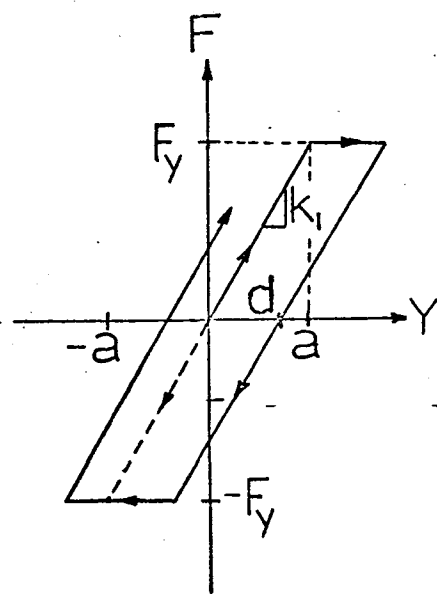


Fig. 1b

Elasto-Plastic System

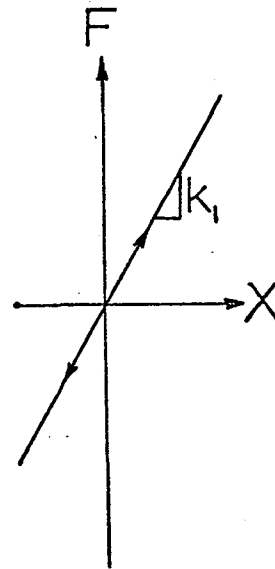


Fig. 1c

Associated Linear System

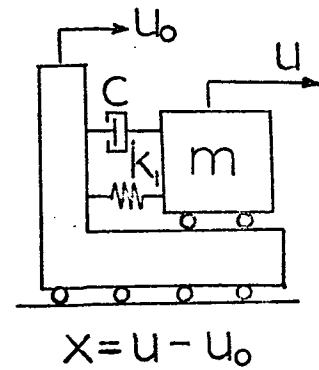


Figure 1

REFERENCES

1. Husid, R., "The Effect of Gravity on the Collapse of Yielding Structures with Earthquake Excitation," Proceedings 4WCEE, Santiago, Chile, 1969, Vol. II, A4, 31-44.
2. Penzien, J. and Liu, S. C., "Nondeterministic Analysis of Nonlinear Structures Subjected to Earthquake Excitations," Proceedings 4WCEE, Santiago, Chile, 1969, Vol. I, A1, 114-129.
3. Veletsos, A. S., "Maximum Deformation of Certain Nonlinear Systems," Proceedings 4WCEE, Santiago, Chile, 1969, Vol. II, 155-170.
4. Caughey, T. K., "Random Excitation of a System with Bilinear Hysteresis," Journal of Applied Mechanics, Vol. 27, 1960, 605-608.
5. Crandall, S. H. and Mark, W. D., Random Vibration in Mechanical Systems, Academic Press, New York, 1963.
6. Vanmarcke, E. H., "Properties of Spectral Moments with Applications to Random Vibration," Journal of the Engineering Mechanics Division, Proc. ASCE, Vol. 98, No. EM2, April 1972.
7. Rice, S. O., "Mathematical Analysis of Random Noise," Bell System Technical Journal, Part I: Vol. 23, 1944, 282-332; Part II: Vol. 24, 1945, 46-156.
8. Yanev, P. I., "Response of Simple Inelastic Systems to Random Excitation," thesis presented to the Massachusetts Institute of Technology, at Cambridge, Mass., in 1970, in partial fulfillment of the requirements for the degree of Master of Science.
9. Tajimi, H., "A Statistical Method of Determining the Maximum Response of a Building Structure During an Earthquake," Proceedings 2WCEE, Tokyo, Japan, 1960, Vol. II, 781-798.
10. Vanmarcke, E. H., Yanev, P. I. and De Estrada, M. B., "Response of Simple Hysteretic Systems to Random Excitation," M.I.T. Dept. of Civil Eng. Research Report R70-66, September 1970.
11. Karnopp, D. and Scharon, T. D., "Plastic Deformation in Random Vibration," Journal of the Acoustical Society of America, Vol. 39, 1966, 1154-1161.
12. Parzen, E., Modern Probability Theory and its Applications, Wiley, New York, 1960.
13. Benjamin, J. R. and Cornell, C. A., Probability, Statistics and Decision for Civil Engineers, McGraw-Hill, New York, 1970.
14. Veneziano, D. and Vanmarcke, E. H., "Seismic Damage of Inelastic Systems: A Random Vibration Approach," M.I.T. Dept. of Civil Eng. Research Report R73-5, January 1973.

The results of a Markov analysis of the response to Gaussian white noise of three gravity-affected hysteretic systems whose properties are listed on Fig. 7 are presented in Figures 6 and 7. Fig. 6 shows the state probabilities $p_i(t)$ as a function of the duration t of stationary motion for structure No. 2. The failure probability is $p_1(t) + p_{13}(t)$. The white noise intensity is adjusted so that the r.m.s. response σ_x of the associated linear system is equal to a , i.e., $r = a/\sigma_x = 1$. The solid lines in Fig. 7 give the expected number of cycles (expected time divided by natural period) to failure for the three structures, as a function of the ratio $r = a/\sigma_x$ (note that σ_x is a measure of the excitation intensity). Husid⁽¹⁾ used both recorded earthquakes and artificial stationary motions with Tajimi-type spectral density to develop an empirical relationship for the expected number of cycles to failure of systems of the type shown in Fig. 1. Husid's best estimates are represented by the dotted lines in Fig. 7. For purposes of comparison, an "equivalent" white noise excitation was considered by substituting G_0 by $G(\omega_n)$ in Eq. 7. The comparison appears to be quite satisfactory.

CONCLUSION

The approach outlined in this paper leads to a set of new approximate analytical results for the statistical properties of several important inelastic response measures for elasto-plastic systems undergoing steady earthquake-like random motion. The probability distributions of the peak inelastic deformation and of the time required for the inelastic deformation to cross a specified value, are expressed in terms of the yield level, the ground motion spectral characteristics and the properties (period and damping ratio) of the associated linear system. These results can be used to predict earthquake response of E-P systems when the associated linear system response, particularly σ_x , is in an approximate steady state during the intense part of the ground motion. An equivalent duration, s , of stationary associated linear system response needs to be used.

A continuous-time Markov model is also described which is used to study the response of bilinear hysteretic systems affected by gravity. Results for the expected number of cycles to failure are compared with those obtained by Husid, and they are found to be in reasonably good agreement.

ACKNOWLEDGEMENTS

This research was sponsored by the U.S. National Science Foundation under Grant No. GK-26296. The writers are grateful to Prof. C. A. Cornell for many stimulating discussions and for the helpful suggestions he provided.

There is a finite probability, $P[M_S=0]$, that no plastic action will occur. By taking $d=0$ in Eq. 13, one finds this probability to be about $\exp\{-\mu_a s\}$ when $\mu_a s \ll 1$; it becomes negligibly small for large values of $\mu_a s$. Notice that Eq. 13 has the form of a Type I Extreme Value Distribution⁽¹³⁾. A characteristic value of M_S , found by setting $P[M_S \leq d] = e^{-1}$, equals $M_S^* = \delta \ln(e^{\mu_a s} - 1)$. Recall that $\delta = \sigma_x/2r$ and that μ_a is given by Eq. 6.

Time to First Crossing of a Given Level of Plastic Deformation

The probability distribution of the time, T_d , to first crossing of a given level of plastic deformation is intimately related to the distribution of M_S . One can write

$$P[T_d > s] = P[M_S \leq d] \quad (14)$$

It suffices to view the expression for $P[M_S \leq d]$ in Eq. 13 as a function of s , with d as a known parameter.

ANALYSIS OF BILINEAR HYSTERETIC SYSTEMS

The basic model which views the total inelastic deformation $D(t)$ as a cumulative process with increments made at random "points" in time, continues to hold when the force-deformation relationship is not of the elasto-plastic type. But the statistical properties of the sizes of the increments and of the time intervals between these "points" now vary depending upon the state of the system, i.e., the level of inelastic deformation at which the system operates. In particular, at any given time t , they depend upon the values of the positive and negative yield levels corresponding to the plastic deformation $D(t)$. (For E-P systems these yield levels remain constant regardless of the value of $D(t)$.) As an example, Fig. 1a shows the force-displacement diagram of a simple frame with rigid girder and columns for which gravity loads have the effect of making the second slope k_2 negative⁽¹⁾. During the process of drift accumulation the smallest yield level ranges from zero (at $D(t) = d_m$) to a (at $D(t) = 0$).

The particular kind of "memory" and the state-dependent nature of the cumulative damage suggest a Markov process continuous in both state and time to be a suitable stochastic model. It is computationally convenient, however, to discretize the range of possible permanent deformations. Fig. 6 shows the displacement axis divided into 13 states, with states 1 and 13 signifying collapse; state 7 is the initial state. In this case, the probability of being in state i at time t is $p_i(t)$, $i = 1$ to 13, and $p_1(t) + p_{13}(t)$ is the probability of collapse. These probabilities depend upon: (i) the probabilities of transition from one state to another given the occurrence of a clump of yield level crossings, and (ii) for each state, the average value of the exponentially distributed time between clumps of yield level crossings. The first set of parameters, the transition probabilities, can be evaluated using an argument similar to that which earlier led to the distribution of the plastic set increment D . The mean times between clumps have the form of μ_a^{-1} , with μ_a given by Eq. 6. Modifications are required, however, to account for the unequal and sometimes very low yield levels⁽¹⁴⁾.

$$E[D(s)] = \mu_a s \quad E[D_i] = 0 \quad (8)$$

$$\text{Var}[D(s)] = \mu_a s (\text{Var}[D_i] + E^2[D_i]) = 2\mu_a s \delta^2 \quad (9)$$

The moment-generating function and the probability density function of $D(s)$ can also be obtained⁽¹⁰⁾. If interest focuses on the case when considerable plastic action occurs, the Central Limit Theorem could be invoked to rationalize adopting the assumption that $D(s)$ has a Gaussian distribution.

Ductility Factor

If plastic action occurs during the time interval $(0,s)$ then the ductility factor F (a random variable!) can be expressed as follows

$$F = \frac{1}{a} (\text{Max}_{0 \leq t \leq s} |D(t)|) + 1 = \frac{M_s}{a} + 1 \quad (10)$$

where M_s is the peak inelastic deformation. If no plastic action occurs, it equals the ratio of the maximum elastic deformation to the yield displacement. Eq. 9 can be used "unconditionally" when the probability of no plastic action is negligibly small.

Peak Inelastic Deformation

The peak inelastic deformation is the absolute maximum value of $D(t)$ in the time interval 0 to s . Its probability distribution can be approximated by viewing the crossings, at positive slope, by $|D(t)|$, of a fixed threshold d , as a nonstationary Poisson process with mean rate $v_d(t)$. The peak inelastic deformation M_s will be less than or equal to d if no crossing of the level d occurs in $(0,s)$. Hence,

$$P[M_s \leq d] = \exp\left\{-\int_0^s v_d(t) dt\right\} \quad (11)$$

$v_d(t)$ is proportional to μ_a , the mean rate of occurrence of jumps in the process $D(t)$, i.e., $v_d(t) = \mu_a p_d(t)$, where $p_d(t)$ is the probability that a plastic set contribution at time t results in an upcrossing of the level d . If such a contribution, D , is positive then an upcrossing will occur if $D < -d - D(t)$ and $D(t) \geq -d$. We have

$$p_d(t) = 2 \int_{-\infty}^d P[D > d-x] f_{D(t)}(x) dx \approx e^{-d/\delta} e^{\mu_a t} \quad (12)$$

The expression on the right side of Eq. 12 is approximately valid only if $\mu_a t < d/\delta$. It results from inserting $P[D > d-x] = (1/2)\exp\{-(d-x)/\delta\}$ into the integrand, expanding $\exp\{x/\delta\}$, and replacing the upper limit d by ∞ . Finally, inserting Eq. 12 into Eq. 11 yields an approximate expression for the probability distribution of the peak inelastic deformation

$$P[M_s \leq d] = \exp\left\{-\mu_a \int_0^s e^{-d/\delta} e^{\mu_a t} dt\right\} = \exp\left\{-(e^{\mu_a s} - 1)e^{-d/\delta}\right\}; d \geq 0 \quad (13)$$

3.25 in increments of 0.25. The white noise intensity is chosen so that σ_x , the r.m.s. response of the associated linear system, equals 0.04 in. Fig. 5a shows that there is good agreement between the sample averages (denoted by m) of the time between clumps of yield level crossings and the elastic inter-clump times μ_a^{-1} (see Eq. 6). Also shown in Fig. 5a is a plot of $(2v_a)^{-1}$, v_a being the mean rate of threshold up-crossings (see Eq. 5). Estimates of the standard deviation (denoted by s) of the time between clumps are very close to the corresponding sample means. This does suggest that the adoption of an exponential distribution (for which mean and standard deviation are theoretically identical) is reasonable. Other tests, described in Refs. 8 and 10, for different E-P systems subjected to excitation with both white and non-white spectra, lead to the same conclusion.

Karnopp and Scharton⁽¹¹⁾ derived a simple approximate expression for δ , the average amount of inelastic deformation (in absolute value) resulting from a single isolated crossing of the yield level a , i.e., $\delta = \sigma_x^2/2a = \sigma_x/2r$. This result follows from the argument that all the kinetic energy, $m\dot{X}^2/2$ (where m is the mass of the system; \dot{X} is the impact velocity), will be released by yielding action. The average value of the kinetic energy at impact is approximately equal to $m\omega_n^2\sigma_x^2/2 = k_1\sigma_x^2/2$. The expected plastic deformation, δ , may be obtained from the energy equation, $F_y\delta = k_1\sigma_x^2/2$, where F_y denotes the yield force (see Fig. 1b). Typical sample values, obtained by numerical simulation^(8,10), of the mean and standard deviation of $|D_i|$, the absolute value of the total plastic set during a clump of yield level crossings, are plotted in Fig. 5b. The smooth curve in Fig. 5b corresponds to Karnopp and Scharton's estimate δ . The fact that the sample means and standard deviations are nearly equal suggests that the probability distribution of $|D_i|$ is also approximately exponential (with mean value δ). Furthermore, the contributions D_i are equally likely to be positive or negative, and their probability density function is symmetrical with respect to zero. Therefore, the mean and variance of D_i will be approximately equal to 0 and $2\delta^2$, respectively.

ELASTO-PLASTIC SYSTEM RESPONSE MEASURES

Plastic Drift or Permanent Set

The total deformation $D(s)$ developed during s seconds of "steady" (constant σ_x and μ_a) elasto-plastic (E-P) response is viewed as the sum of individual (positive and negative) contributions D_i , $i = 1, 2, \dots, N(s)$. Each contribution results from a single clump of yield level crossings. On the basis of the theoretical arguments, backed up by computer simulation, presented in the preceding section, we assume that the random number of contributions $N(s)$ has a Poisson distribution with mean $\mu_a s$. Also, successive contributions D_1, D_2 , etc., are assumed to be mutually independent of the clump occurrence process $N(t)$. They are identically distributed, with a common probability density function $f_D(d) = (2\delta)^{-1} \exp(-|d|/\delta)$, $-\infty \leq d \leq +\infty$ which is symmetrical about $d=0$. Recall that $\delta = \sigma_x^2/2a$.

Under these assumptions, the expected value and the variance of $D(s) = \sum_i D_i$, where i goes from 0 to a random number $N(s)$, become⁽¹²⁾

$$E[N_a] \approx (2/\pi)^{1/2} (rq)^{-1} .$$

A well-known result in random vibration analysis, due to S. O. Rice⁽⁷⁾ is that the mean v_a of crossings with positive slope of a level $X=a$ by a stationary Gaussian process $X(t)$, is

$$v_a = \frac{1}{2\pi} (\lambda_2/\lambda_0)^{1/2} \exp\{-a^2/2\sigma_x^2\} = v_0 \exp\{-r^2/2\} \quad (5)$$

in which $v_0 = (\lambda_2/\lambda_0)^{1/2}/2\pi =$ the mean rate of zero crossings with positive slope. Also, the mean rate of excursions outside the range $(a,-a)$ equals $2v_a$. Finally, the average number, μ_a , of "clumps" per time unit is approximately

$$\mu_a = 2v_a/E[N_a] = 2v_0(1 - \exp\{-\sqrt{\pi/2} rq\}) \exp\{-r^2/2\} \quad (6)$$

If the excitation is a Gaussian white noise, then $G_X(\omega) = G_0 |H(\omega)|^2$, then^(5,6)

$$\lambda_0 = \sigma_x^2 = \frac{\pi G_0}{4\zeta\omega_n^3} \quad v_0 = \frac{1}{2\pi} \omega_n \quad q \approx \frac{2}{\sqrt{\pi}} \zeta^{1/2} \quad \text{if } \zeta \text{ small} \quad (7)$$

The factor q is plotted as a function of the damping ratio ζ in Fig. 4. It may be noted that the parameters λ_0 , v_0 and q are relatively easily obtainable for an arbitrary spectral density function $G_X(\omega)$.

THE BASIC MODEL

In the previous section it has been argued that for simple elastic systems the crossings of a relatively high threshold level are likely to occur in clumps when the viscous damping ratio ζ is small. Yield level crossings of the elasto-plastic response also tend to occur in clumps. For elastic systems, the average rate at which clumps of crossings of the level a occur equals μ_a and the average time between clumps is $1/\mu_a$. The larger the mean clump size, $E[N_a]$, the larger the average time between successive clumps. For E-P systems, $1/\mu_a$ is approximately equal to the average time between clumps of inelastic excursions. It is useful to treat these clumps as "points in time" at which inelastic action occurs, i.e., at which the permanent set $D(t)$ jumps to a different value. In fact, the total plastic deformation $D(s)$ developed in the time interval 0 to s , may be thought of as a sum of individual contributions D_i , $i = 1, 2, \dots, N(s)$, each of which is the result of a single clump of yield level crossings, i.e., $D(s) = \sum_i D_i$. $N(s)$ is the random number of contributions during the time interval $(0, s)$. For relatively high yield levels the time between clumps may be expected to have an exponential distribution with mean $1/\mu_a$. The approximate validity of this hypothesis was checked by Yanév⁽⁸⁾ through analysis of E-P system response to simulated white noise and Tajimi-filtered white noise⁽⁹⁾. Some typical results are shown in Fig. 5 for a white noise excited E-P system characterized by an initial natural period = 0.2 sec., a viscous damping ratio = 0.02, and a yield displacement $a = r\sigma_x$, where r is allowed to vary between 1.5 and

A sample function of the process $X(t)$ is shown in Fig. 2b. It is obtained by subtracting the plastic set, shown in Fig. 2c, from the total E-P response, seen in Fig. 2a. The permanent set $D(t)$ remains constant when the absolute value of $X(t)$ is smaller than the yield level a . Each time $S(t)$ exceeds the yield displacement, however, inelastic action is known to occur. The total permanent set developed in the time interval 0 to t is the sum of a number of individual contributions, each associated with a single crossing of $|X(t)| = a$. Much can be learned about the sizes of these contributions and about the length of the time intervals between yield level crossings by examining the response of the associated linear system shown in Fig. 1c. In particular, it will be useful to focus attention on the excursions of $X(t)$ outside the range $(a, -a)$.

SOME PERTINENT RESULTS FOR SIMPLE LINEAR SYSTEMS

Let the linear elastic system shown in Fig. 1c be subjected to a stochastic support motion $\ddot{u}_0(t)$. The response quantity of interest is the relative displacement $x = u - u_0$ and the equation of motion is given by Eq. 2. Assume that the support motion can be modeled as a zero-mean stationary random process characterized by a wide-band spectral density function $G(\omega)$ and an equivalent duration s . The (one-sided) spectral density function $G_X(\omega)$ of the relative displacement may then be simply expressed in terms of the input spectrum $G(\omega)$ and the transfer function of the system. We have⁽⁵⁾

$$G_X(\omega) = G(\omega) / [(\omega^2 - \omega_n^2)^2 - 4\zeta^2 \omega_n^2 \omega^2] \quad (3)$$

A typical sample function of the response of a lightly damped linear structure to wide-band random excitation is shown in Fig. 3. It has the appearance of a modulated sinusoid with a period equal to the structure's natural period. Focusing attention on a pair of fixed relatively high threshold levels $x = \pm a$, it is of interest to observe that the peaks of $X(t)$ whose values are outside of the range $(a, -a)$ tend to occur in groups or "clumps", i.e., successive peak values of $X(t)$ tend to be significantly correlated.

In Fig. 3, N_a denotes the random number of consecutive peaks whose values lie outside the range $(a, -a)$. The senior writer has recently shown⁽⁶⁾ that degree of correlation among successive peaks importantly depends on a factor $q = (1 - \lambda_1^2 / \lambda_0 \lambda_2)^{1/2}$, where $\lambda_i = \int_0^\infty \omega^i G_X(\omega) d\omega = i$ th moment of the spectral density function $G_X(\omega)$. It can be shown that q lies between 0 and 1 and that it is a measure of the spread of $G_X(\omega)$ about a center frequency. It is well-known that $\lambda_0 = \sigma_x^2$, i.e., the area under the power spectrum, equals the variance of $X(t)$. For stationary Gaussian processes, the expected value of N_a takes approximately the following form⁽⁶⁾

$$E[N_a] = (1 - \exp\{-\sqrt{\pi/2} r q\})^{-1} \quad (4)$$

where $r = a/\sigma_x$ = the threshold level normalized with respect to the standard deviation of $X(t)$. $E[N_a]$ is referred to as the average clump size. Note that for large values of $r q$, $E[N_a] \rightarrow 1$ and for $r q \ll 1$,

times when no plastic action occurs, i.e., between response excursions into the inelastic domain, the inelastic system behaves like an elastic oscillator. The total displacement then consists of (i) an oscillatory zero-mean linear elastic component, and (ii) an inelastic deformation, d , which remains constant as long as the elastic motion does not cross over into the domain bounded by the positive and negative yield levels (which may be different for different levels of plastic deformation, d). Of course, for elasto-plastic (E-P) systems, the positive and negative yield levels have the same absolute value and do not depend on the level of inelastic deformation, d .

The inelastic response is modeled as a continuous-time random process with as "state" variable the plastic deformation, d . Changes or transitions from one value of d to another can occur only at times when the elastic response component exceeds the yield level. The transition probabilities (derived from linear probabilistic analysis) are state-dependent, except in the case of E-P systems. They can be expressed in terms of the characteristics of the ground motion (intensity, parameters of the power spectrum) and of an associated linear system (period and damping ratio) described below. It is convenient to analyze E-P system response first, and then to extend the results of this analysis to bilinear systems.

THE ASSOCIATED LINEAR SYSTEM

Let $Y(t)$ represent the displacement response of an E-P structure (Fig. 1b) with a yield level $Y = a$ to a random excitation $\ddot{u}_o(t)$. At the start of the motion and until $Y(t)$ crosses the yield level for the first time, the response of the E-P system is identical to that of an associated linear system, such as that shown in Fig. 1c. It is characterized by a spring with stiffness k_1 and by a dashpot with damping coefficient c . Problems surrounding the onset of plastic deformation are equivalent to a first-crossing problem for the associated linear oscillator. Also, before plastic deformations occur, the inelastic response $Y(t)$ is described by the linear differential equation

$$\ddot{y} + 2\zeta\omega_n\dot{y} + \omega_n^2y = -\ddot{u}_o(t) \quad (1)$$

where $\omega_n = (k_1/m)^{1/2}$ is the undamped natural frequency and $\zeta = c/2m\omega_n$ is the damping ratio. In between yield level crossings, the E-P system also behaves like a linear oscillator. Suppose that at some known time t , the most recent yield level crossing brought the total plastic deformation up to the value $D(t) = d$. The total displacement at t will then consist of a permanent set d and a linear elastic component $X(t)$, i.e.; $Y(t) = d + X(t)$. The process $D(t)$ changes rather abruptly when plastic action occurs. For $d = 0$, i.e., before any plastic yield occurred, we have $Y(t) = X(t)$. The differential equation describing the elastic part, $X(t)$, of the total displacement of the E-P system, in between plastic excursions, has the form

$$\ddot{x} + 2\zeta\omega_n\dot{x} + \omega_n^2x = -\ddot{u}_o(t) \quad (2)$$

PROBABILISTIC SEISMIC RESPONSE OF SIMPLE INELASTIC SYSTEMS

by

E. H. Vanmarcke^I and D. Veneziano^{II}

SYNOPSIS

The paper presents a probabilistic dynamic analysis of the relative displacement response to earthquake-like excitation of simple elasto-plastic systems and of bilinear hysteretic systems affected by gravity. Nonlinear response measures are expressed in terms of the statistics of the response of an associated linear oscillator which is characterized by the initial properties of the hysteretic system. For elasto-plastic systems, new approximate analytical results are presented for the probability distribution of the plastic drift, the ductility factor and the time to first exceedance of a specified level of plastic deformation. A Markov model is proposed to study the response of bilinear hysteretic systems. For gravity-affected systems, results are presented for the probability of collapse and for the expected number of cycles to failure. These results are compared with those obtained by Husid⁽¹⁾.

INTRODUCTION

For many structural and mechanical systems it is permissible to allow for plastic deformation during severe but infrequent random vibratory motions such as those due to earthquakes. To take advantage of their plastic capacity often provides an efficient means of absorbing energy and limiting the oscillation amplitudes. A problem of considerable interest in the safety analysis of structures during strong-motion earthquakes, therefore, is to determine the probability distribution of important measures of inelastic behavior, e.g., the ductility factor and the time to collapse. The type of force-deformation relationship considered in this paper is a bilinear hysteretic system characterized by the initial stiffness k_1 , the slope ratio k_2/k_1 , and the yield displacement as shown in Figure 1. The effect of gravity on the inelastic response measures is given particular attention.

Several investigators (Refs. 1, 2, 3, among others) obtained response statistics of simple nonlinear hysteretic systems through time history analyses, using real and computer-generated ground motions. Other work (e.g., Ref. 4) in which it is attempted to obtain rigorous random vibration solutions, attests to the fact that the mathematical complexity of the problem is formidable.

The approach outlined in this paper is based on the idea that, at

^I Assistant Professor of Civil Engineering, Massachusetts Institute of Technology, Cambridge, Massachusetts, USA.

^{II} Research Assistant, Massachusetts Institute of Technology, Cambridge, Massachusetts, USA.

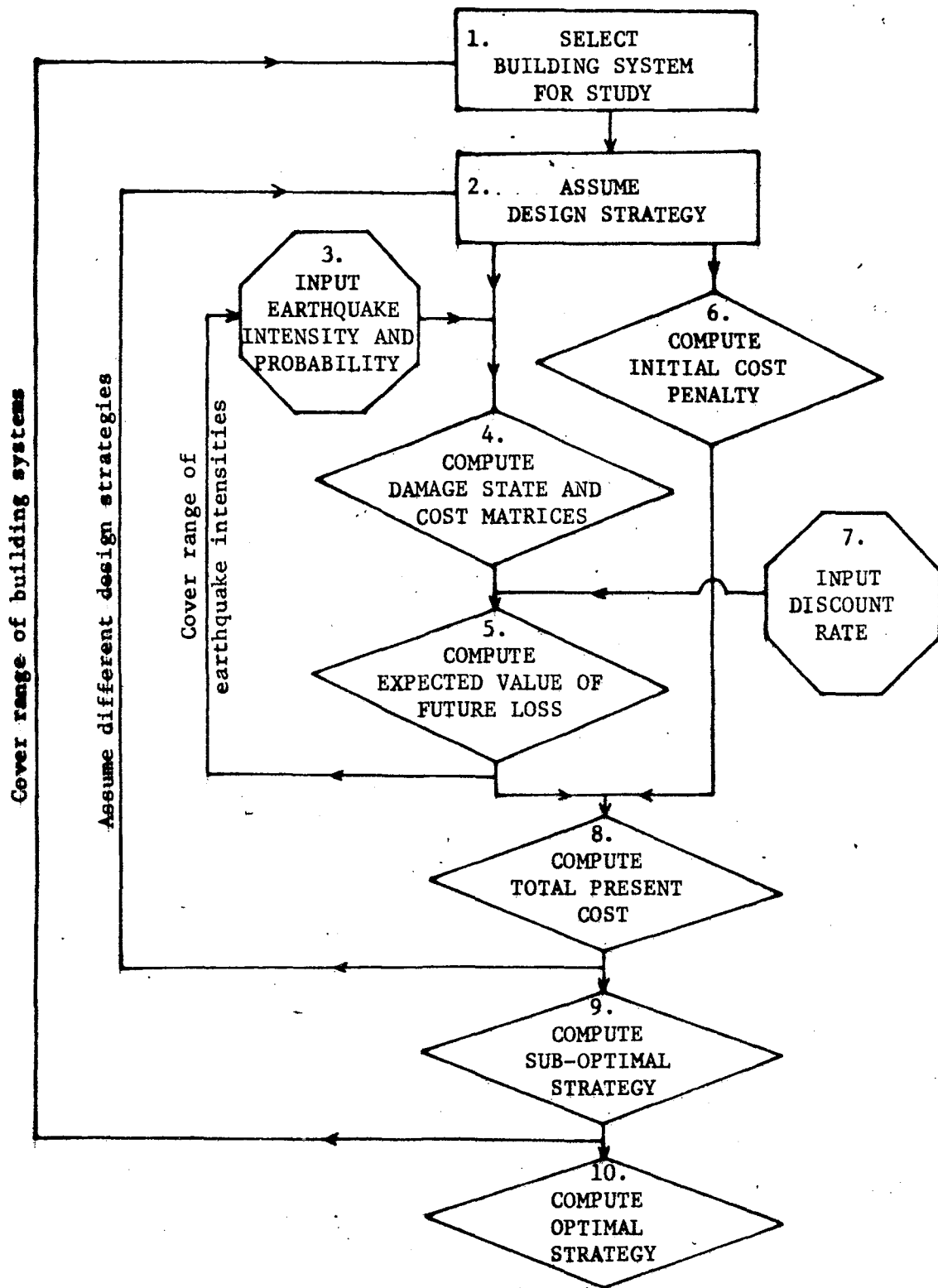
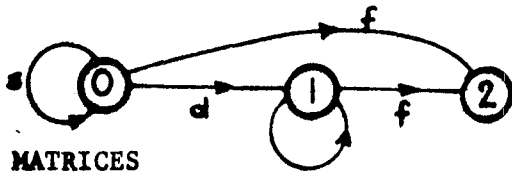


Figure 2: Flow Diagram for General Methodology

Model A



MATRICES

$$P = \begin{bmatrix} P_{00} & P_{01} & P_{02} \\ 0 & P_{11} & P_{12} \\ 0 & 0 & 1 \end{bmatrix}$$

$$C = \begin{bmatrix} c_{00} & c_d & c_f \\ 0 & c_{11} & c_f \\ 0 & 0 & 0 \end{bmatrix}$$

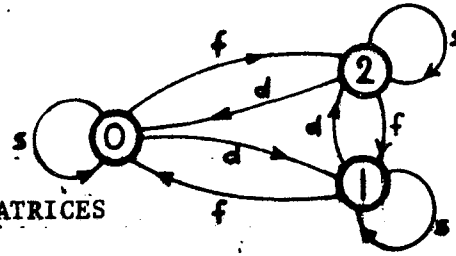
SOLUTION

$$C_0 = \frac{c_{00} + \lambda(p_{01}c_d + p_{02}c_f + p_{01}c_2)}{\delta + \lambda(p_{01} + p_{02})}$$

$$C_1 = (c_{00} + \lambda p_{12}c_f) / (\delta + \lambda p_{12})$$

$$C_2 = 0$$

Model B



MATRICES

$$P = \begin{bmatrix} P_{00} & P_{01} & P_{02} \\ P_{02} & P_{00} & P_{01} \\ P_{01} & P_{02} & P_{00} \end{bmatrix}$$

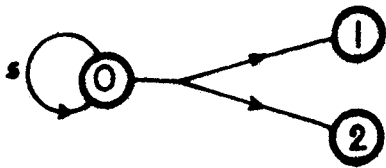
$$C = \begin{bmatrix} c_{00} & c_d & c_f \\ c_f & c_{00} & c_d \\ c_d & c_f & c_{00} \end{bmatrix}$$

SOLUTION

$$C_0 = C_1 = C_2 =$$

$$\frac{1}{\delta} [c_{00} + (p_{01}c_d + p_{02}c_f)]$$

Model C



MATRICES

$$P = \begin{bmatrix} P_{00} & P_{01} & P_{02} \\ 0 & 1 & 0 \\ 0 & 0 & 1 \end{bmatrix}$$

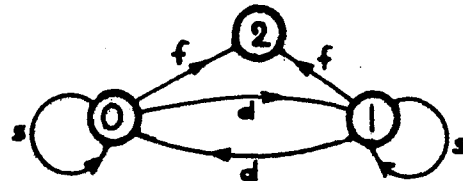
$$C = \begin{bmatrix} c_{00} & c_f & c_f' \\ 0 & 0 & 0 \\ 0 & 0 & 0 \end{bmatrix}$$

SOLUTION

$$C_0 = \frac{c_{00} + \lambda(p_{01}c_f + p_{02}c_f')}{\delta + \lambda(p_{01} + p_{02})}$$

$$C_1 = C_2 = 0$$

Model D



MATRICES

$$P = \begin{bmatrix} P_{00} & P_{01} & P_{02} \\ P_{01} & P_{00} & P_{02} \\ 0 & 0 & 1 \end{bmatrix}$$

$$C = \begin{bmatrix} c_{00} & c_d & c_f \\ c_d & c_{00} & c_f \\ 0 & 0 & 0 \end{bmatrix}$$

SOLUTION

$$C_0 = C_1 = \frac{c_{00} + \lambda(p_{01}c_d + p_{02}c_f)}{\delta + \lambda p_{02}}$$

$$C_2 = 0$$

Figure 1: Some Three State Models of Seismic Performance of Buildings

REFERENCES

1. Cornell, C. A., "Engineering Seismic Risk Analysis," Bull. Seismo. Soc. Amer., Vol. 58, No. 5, 1968.
2. Esteva, L., "Bases para la Formulación de Decisiones de Diseño Sísmico," Doctoral Thesis, Univ. Nac. Auto. de Mexico, 1968.
3. Molchan, G. M., Keilis-Borok, V. I. and Vilkevich, G. V., "Seismicity and Principal Seismic Effects," Geophys. J. R. Astro. Soc., Vol. 21, 323-335, 1970.
4. Cornell, C. A., "Probabilistic Analysis of Damage to Structures under Seismic Loads," Chapter 27 in Dynamic Waves in Civil Engineering, edited by D. A. Howells, et al., John Wiley & Sons, 1971.
5. Bellman, R. and Dreyfus, S. E., Applied Dynamic Programming, Princeton University Press, Princeton, New Jersey, 1962.
6. Howard, R. A., Dynamic Programming and Markov Processes, Wiley, New York, New York, 1960.
7. Jewell, W. S., "Markov-Renewal Programming, I: Formulation, Finite Return Models, II: Infinite Return Models, Example," Operations Research, Vol. 11, 1963.
8. Vanmarcke, E. H., "First-Passage and Other Failure Criteria in Narrow-Band Random Vibration: A Discrete-State Approach," M.I.T. Department of Civil Engineering Research Report R69-68, October 1969.
9. Shah, H. C. and Vagliente, V. N., "Forecasting the Risk Inherent in Earthquake Resistant Design," Proc. of Conf. on Microzonation, Vol. II, 693-718, Seattle, Washington, November 1972.
10. Vanmarcke, E. H. and Diaz-Padilla, J., "Markov Decision Models in Seismic Design," M.I.T. Department of Civil Engineering Research Report R71-20, December 1971.
11. Whitman, R. V., Cornell, C. A., Vanmarcke, E. H. and Reed, J. W., "Optimum Seismic Protection and Building Damage Statistics," M.I.T. Department of Civil Engineering Research Report R72-17, March 1972.
12. Whitman, R. V., Reed, J. W. and Hong, S.-T., "Earthquake Damage Probability Matrices," Proc. 5th World Conf. Eq. Eng., Rome, Italy, June 1973.
13. de Neufville, R. and Stafford, J. H., Systems Analysis for Engineers and Managers, McGraw-Hill Book Company, 1971.

7

the increase in the initial cost due to special provisions for earthquake protection. If all losses can be expressed in monetary terms, then a reasonable design objective is to minimize the total expected cost, $A_0 + C_0$. In regions of low or moderate seismicity, other design considerations, e.g., functional requirements or resistance against wind, may enable one to design buildings for sufficiently low seismic risk levels without adding to the initial cost.

The methodology is quite general and can be applied to many types of buildings and other engineered facilities. Figure 2 outlines, by means of a flow chart, the methodology as it is used in a study at M.I.T. which focuses upon seismic design criteria for a class of tall buildings to be constructed in Boston, Massachusetts. The alternative design strategies considered correspond to the four seismic zones (0, 1, 2 and 3) of the Uniform Building Code. The repair policy adopted is one whereby all damaged buildings are repaired and all unserviceable buildings are replaced immediately following each earthquake. Hence, Eq. 5 can be used to evaluate average future losses. Reference 12 gives the categorization of levels of damage. These levels of damage are described both by words and by the average damage costs $c_i = d_i A$, in which A = replacement cost, and d_i = ratio, to replacement cost, of physical damage to the building and its contents. Damage probability matrices are estimated for each particular building and its contents. Damage probability matrices are estimated for each particular building system and each design strategy. Two approaches are followed in assembling these matrices: (i) actual observed damage (and non-damage) during past earthquakes is correlated with ground motion intensity⁽¹²⁾, and (ii) theoretical predictions of dynamic response are used to interpret and extrapolate from the empirical information concerning damage and non-damage. The initial cost, in this study, is a function of the design strategy. It is expressed as the extra cost to design for, say, Zone 2 requirements as compared to making no provision for earthquake resistance.

CONCLUSION

A methodology based on Markov decision theory has been presented which evaluates the future performance of buildings under earthquakes and determines optimum seismic design levels and repair policies. To apply the analysis to a particular location, a suitable set of damage states, intensity categories and decision alternatives must be specified, and the corresponding probabilities and cost factors must be estimated.

ACKNOWLEDGEMENT

This research was sponsored by the National Science Foundation under Grant No. GK-26296 and No. GK-27955x.

Laplace transformations can be used to obtain closed-form solutions. At large values of t , however, $C_i(t)$ asymptotically approaches an upper bound $C_i = \lim_{t \rightarrow \infty} C_i(t)$. These long-range expected values are of considerable practical interest in earthquake engineering since the operational lifetimes of constructed facilities are often long and seldom predetermined. It is clear that when $t \rightarrow \infty$, the time derivative $dC_i(t)/dt \rightarrow 0$, and therefore the costs G_i can be determined from a simple system of m linear equations:

$$(\delta + \lambda)C_i = q_i + \lambda \sum_{j=0}^{m-1} p_{ij} C_j \quad i = 0, 1, \dots, m-1 \quad (3)$$

Generally only the expected total future loss C_0 will be of interest (since the building system always starts in state 0), except when the decision at hand involves questions of maintenance or condemnation of buildings.

To find C_0 for the three state models discussed earlier requires solving a set of three simultaneous linear equations. The resulting expressions are given in Figure 1. (For details, see Reference 10.) From these it is relatively easy to construct the expressions for C_0 corresponding to several important multi-state models. For example, in the multi-state extension of Model B (instantaneous repair and replacement), there are $m-1$ damage states in addition to the "no damage" state 0, m transition probabilities p_{0i} , and m transition costs $c_{0i} = c_i$ (where $c_{00} = c_0 = 0$). The resulting value for the total expected future loss C_0 is:

$$C_0 = \frac{\lambda}{\delta} \sum_{i=0}^{m-1} p_{0i} c_i \quad (4)$$

It is further worth noting that if the damage costs c_i are uncertain, it is theoretically correct to replace them by their respective average values. Inserting Eq. 1 into Eq. 4 yields

$$C_0 = \frac{\lambda}{\delta} \sum_{i=0}^{m-1} \left(\sum_{k=0}^n p_{0i|y_k} q_{y_k} \right) c_i = \frac{\lambda}{\delta} \sum_{k=0}^n \bar{c}_{y_k} q_{y_k} = \sum_{k=0}^n \bar{c}_{y_k} \lambda_{y_k}$$

in which $\bar{c}_{y_k} = \sum_{i=0}^{m-1} p_{0i|y_k} c_i$ = the mean damage ratio⁽¹²⁾ times the build-

ing replacement cost), given the intensity is y_k . In addition to direct repair costs, important human and social costs must be considered in evaluating the effects of strong earthquakes. These associated costs can be analyzed by the same method, and might be measured, for example, in number of lives lost. The conversion to equivalent monetary losses is possible only by placing a monetary value on life⁽¹²⁾.

OPTIMUM SEISMIC DESIGN

The approach just outlined combines information about earthquake risks and consequences to obtain the average values, C_0 , of the discounted future loss due to earthquakes for a building or for a class of buildings. The other major component in optimum seismic design is represented by A_0 ,

constitute the elements of the damage probability matrices whose evaluation forms the topic of another paper at this conference⁽¹²⁾.

LOSSES AND REWARDS

For any m-state model of a building an $m \times m$ cost matrix $C = [c_{ij}]$ can be constructed. The element c_{ij} , $i \neq j$, represents the loss sustained (or benefit received) if the building system makes a transition from state i to state j . The quantity c_{ii} is the cost per unit time when the system occupies state i . (Note that c_{ii} and c_{ij} , $i \neq j$, do not have the same dimensions.

Figure 1 lists the C matrices for Models A through D. For example, for Model A, the elements $c_{01} = c_d$ and $c_{02} = c_f$ are the costs associated with damage and failure, respectively. c_{11} covers operating costs (minus benefits) per unit time; it could also represent the premium for insurance against earthquakes. c_{22} is the annual cost of operating a damaged structure. Diagonal elements can be put equal to zero if one is only interested in estimating future losses resulting from actual earthquake damage.

It is realized that modifications to this format are needed when losses associated with transitions cannot be expressed in monetary value. Multi-attributed losses must then be considered, and a different "cost" matrix may be needed for each attribute.

EXPECTED FUTURE LOSSES: BASIC RELATIONS

We define the following quantities:

$C_i(t)$ = the expected discounted total loss due to earthquakes during the time interval 0 to t if the system starts in state i .

δ = the discount rate: a unit quantity of money received after a very short time interval Δt is now worth $1 - \delta \Delta t$.

$q_i = c_{ii} + \sum_{k \neq i} \lambda p_{ik} c_{ik}$ = the mean loss rate of the system when it occupies state i .

It is very important in decision making involving constructed facilities to discount future losses. The choice of an appropriate discount factor raises complex issues⁽¹³⁾, however, and this question will not be further pursued here.

The expected future losses $C_i(t)$ are governed by a set of ordinary differential equations^(6,7):

$$\frac{dC_i(t)}{dt} = q_i + \lambda \sum_{j=0}^{m-1} p_{ij} C_j(t) - (\delta + \lambda) C_i(t) \quad (2)$$

$$i = 0, 1, \dots, m-1$$

Note that it is symmetrical with respect to states 0 and 1. Repairable damage is sustained when the transition 0→1 or 1→0 occurs and transitions 0→0 and 1→1 imply no damage. But the transitions 0→2 and 1→2 signify that the system got trapped in the failure state.

It is important and rather easy to construct multi-state extensions of the models just presented. For Models A and B, for example, while preserving the respective "no repair" and "immediate repair" policies, additional intermediate damage states can be considered. In other situations, it will be appropriate to deal in a single model with both types of damage, one which is repaired and another which cannot be or is not repaired.

In an M.I.T. study aimed at evaluating tall building seismic design strategies⁽¹¹⁾, the model adopted is a direct extension of Model B: building performance is evaluated in terms of nine damage states ranging from "undamaged" to "collapse", and repair or replacement are assumed to be instantaneous.

CONDITIONAL AND MARGINAL TRANSITION PROBABILITIES

For any m-state model of a building system the uncertain effect of a single earthquake with known intensity y_k can be summarized in terms of an $m \times m$ matrix $P_{y_k} = [p_{ij}|y_k]$ of conditional one-step transition probabilities. The element $p_{ij}|y_k$ can be interpreted as the fraction of (nominally identical) buildings expected to move from state i to state j during an earthquake causing an intensity y_k at the site. The marginal one-step transition probability p_{ij} is the average of $p_{ij};y_k$ with respect to y_k , i.e.,

$$p_{ij} = \sum_{k=0}^n p_{ij}|y_k q_{y_k} \quad (1)$$

It equals the probability of transition from state i to state j under an earthquake with site intensity $\geq y_0$. The $m \times m$ matrix of marginal transition probabilities is denoted by $P = [p_{ij}]$.

All quantities of interest, e.g., the probability that the system will be in a given state at some specified future time, can be shown to depend directly on the marginal transition probabilities p_{ij} ⁽⁸⁾. In other words, the conditional probabilities $p_{ij}|y_k$ are only needed to construct the matrix $P = [p_{ij}]$ for a given site, building system and design strategy.

Figure 1 shows the P matrices for Models A through D. Note that only three elements (p_{01} , p_{02} and p_{12}) can be chosen independently in Models A and D. Also, the probability of failure will differ depending on the state the building occupies just prior to the earthquake; in particular, the ratio p_{12}/p_{02} must exceed one. In Models B and C, only the probabilities of transition out of state 0 (p_{01} , p_{02} and $p_{00} = 1 - p_{01} - p_{02}$) are needed. The same conclusion holds for the multi-state extensions of Models B and C: only the probabilities p_{0i} , $i = 0, 1, \dots, m-1$, are needed. The corresponding conditional probabilities are $p_{0i}|y_k$, and they

use λ to denote λ_{y_0} in what follows.

STATES AND TRANSITIONS

To model the uncertain effect of various levels of earthquake ground motion, a structure or a building system is idealized by a finite number of states. Between earthquake occurrences, the system always occupies one and only one state. Transitions from one state to another may take place during or immediately following an earthquake. Any particular history of seismic effects can be represented by a list of successive states starting with state 0, e.g., $0 \rightarrow 0 \rightarrow 0 \rightarrow 2 \rightarrow 2 \dots$. This particular sequence indicates that 4 seismic events occurred: the first two left the building in its original state, the third caused a "jump" from state 0 to state 2, the building remained in state 2 through the fourth earthquake, and so on. Many different multi-state models of building behavior are possible. The choice will depend on the building system under study, on the repair and replacement policy considered, and on the level of accuracy sought. The only theoretical restriction is that all transitions must be so defined that every possible sample history can be represented and interpreted in an unambiguous way in terms of a sequence of successive states.

Figure 1 shows a few of the possible three-state representations of the behavior of a constructed facility during earthquakes⁽¹⁰⁾. In these so-called transition diagrams, the states are labeled 0, 1 and 2, and the arrows indicate the direction in which transitions can take place. One always starts in state 0 and makes a transition when an earthquake occurs. Each transition diagram corresponds to a different repair and replacement policy, as explained below.

Model A: Structure Deteriorates. No Replacement Upon Failure

This model represents a simple deterioration process: the structure can be serviceable (state 0), damaged, left unrepaired, but still serviceable (state 1), or completely unserviceable (state 2). When state 2 is reached, the structure is not replaced (or, at least, replacement is not considered in the analysis).

Model B: Immediate Repair or Replacement

This transition diagram is symmetrical with respect to the three states. It indicates that whichever state is occupied at a given instant, there are exactly two paths, labeled d (for damage) and f (for failure), out of that state, and a loop labeled s (for survival) which signifies return to that state. The sample history $0 \rightarrow 2 \rightarrow 1 \rightarrow 0$ indicates that the system failed three times during successive earthquakes and was replaced (by a nominally identical one) each time.

Model C: Two modes of Failure. No Replacement Upon Failure

This model is appropriate when there are two ways in which a building may become unserviceable. For example, an earthquake may cause (i) enough structural damage that the building is declared unsafe, or (ii) actual collapse of the building.

Model D: Immediate Damage Repair. No Replacement Upon Failure

This transition diagram combines elements of both Models A and B.

tool for analyzing the performance of structures for which several levels of unserviceability (e.g., minor nonstructural damage, minor structural and major nonstructural damage, collapse) can be identified. Intermediate damage states may contribute to the total losses either directly, in terms of repair costs, or indirectly, by causing a change in the risk of collapse during subsequent strong-motion shaking. For example, the natural period of a building may significantly increase as a result of a moderate earthquake. This may have the beneficial effect of moving the structural period out of the range of predominant frequencies in the ground motion at the site, but it may also have the opposite effect.

One of the most useful properties of a Markov model is that it provides a relatively simple framework for quantifying a building's performance in terms of economic loss. This aspect of the theory of discrete state Markov processes has received wide attention in the field of control theory and operations research^(5,6,7). Basically, the building (or class of structures) is visualized to accumulate a series of benefits and costs as it proceeds through various states of damage. The method allows all future benefits and losses to be discounted. The total expected cost which forms the basis for design decisions is the algebraic sum of the discounted losses and benefits and the cost of construction. Alternative designs or design strategies can then be evaluated by comparing their total expected costs, and the optimum design or design strategy is one which minimizes total expected cost. The use of Markov models to represent earthquake damage was first proposed by Vanmarcke⁽⁸⁾. An application to structures in the San Francisco Bay Area has recently been described by Shah and Vagliente⁽⁹⁾.

EARTHQUAKE OCCURRENCE CHARACTERISTICS

Methods of seismic risk analysis⁽¹⁻³⁾ allow one to make reasonable estimates for the probability of exceeding a given site intensity say, MMI scale in any one year, by appropriate analysis of local historical records and of geological information. It is generally assumed that within a given seismically active area, strong earthquakes occur independently according to a Poisson process, and that earthquake occurrences and sizes in non-overlapping seismically active areas are independent. Under further mild assumptions relative to the laws governing intensity attenuation it can be shown that earthquakes causing a site intensity in excess of a high level y also follow a Poisson process with average annual occurrence rate λ_y . This mean rate λ_y , viewed as a function of the threshold intensity y , defines the risk-versus-intensity curve which characterizes the site seismicity.

It is often appropriate to discretize the intensities. If y_0 denotes the intensity below which associated building damage is negligibly small, one may choose to evaluate λ_y for a discrete set of y values, i.e., $y = y_0, y_1, \dots, y_n$. Of particular interest in subsequent analysis are the related quantities $q_{y_k} = (\lambda_{y_{k+1}} - \lambda_{y_k}) / \lambda_{y_0}$, $k = 0, 1, \dots, n-1$ in which q_{y_k} = the probability that the site intensity equals y_k given an event in which it is at least y_0 . Also, $q_n = \lambda_{y_n} / \lambda_{y_0}$ = the probability that the site intensity is at least y_n given that it is at least y_0 . Note that $\sum_{k=0}^n q_k = 1$ and $\lambda_{y_k} = \lambda_{y_0} \sum_{j=k}^n q_j$. It will be notationally convenient to

METHODOLOGY FOR OPTIMUM SEISMIC DESIGN

by

E. H. Vanmarcke^I, C. A. Cornell^{II}, R. V. Whitman^{III} and J. W. Reed^{IV}

SYNOPSIS

The paper introduces a method based on Markov decision theory to describe the effects and evaluate the performance of building systems subjected to strong-motion earthquakes. The effect of a single earthquake is described in terms of (i) a matrix of probabilities of transition from one state of system serviceability to another, and (ii) a matrix of associated losses and benefits. Average discounted future costs are computed for various multi-state models of a building. Throughout the paper reference is made to a major study in which this methodology is applied to the evaluation of seismic design criteria for tall buildings in U.S. eastern metropolitan areas.

INTRODUCTION

In seismic design of buildings a fundamental trade-off between costly higher protection levels and higher risks of various levels of social and economic losses must be made. A rational formulation of seismic design decisions requires combining the uncertainties and the values and losses involved. The uncertainties entering into the computation of expected future losses due to earthquakes are of two types: first, the uncertainty in the occurrence characteristics of earthquakes of various intensities, secondly, the uncertainty in the effect each earthquake has on the building or the class of buildings being studied.

Methods of evaluation of seismic risk which aim at obtaining intensity-versus-return period curves have been developed⁽¹⁻³⁾. They basically rest on the assumption that the times between successive exceedances of relatively high intensity levels at a given site are independent and exponentially distributed. The effect on structures of earthquakes with various intensities is more difficult to model. A number of recent papers^(2,3,4) consider damage models in which the effects of successive earthquakes are stochastically independent. It is well-known, however, that previous damage may significantly influence future behavior. The model studied here allows the incremental damage at any stage to be stochastically dependent on the damage to date. It provides an excellent

^I Assistant Professor of Civil Engineering, Massachusetts Institute of Technology, Cambridge, Massachusetts, USA.

^{II} Associate Professor of Civil Engineering, Massachusetts Institute of Technology, Cambridge, Massachusetts, USA.

^{III} Professor of Civil Engineering and Head of the Structural Engineering Division, Massachusetts Institute of Technology, Cambridge, Massachusetts, USA.

^{IV} Senior Research Engineer, URS/John Blume Associates, Las Vegas, Nevada, USA.

- 0 No Damage
- 1 Minor non-structural damage--a few walls and partitions cracked, incidental mechanical and electrical damage
- 2 Localized non-structural damage--more extensive cracking (but still not widespread); possibly damage to elevators and/or other mechanical electrical components
- 3 Widespread non-structural damage--possibly a few beams and columns cracked, although not noticeable
- 4 Minor structural damage--obvious cracking or yielding in a few structural members; substantial non-structural damage with widespread cracking
- 5 Substantial structural damage requiring repair or replacement of some structural members; associated extensive non-structural damage
- 6 Major structural damage requiring repair or replacement of many structural members; associated non-structural damage requiring repairs to major portion of interior; building vacated during repairs
- 7 Building Condemned
- 8 Collapse

FIG. 3 DESCRIPTION OF DAMAGE STATES

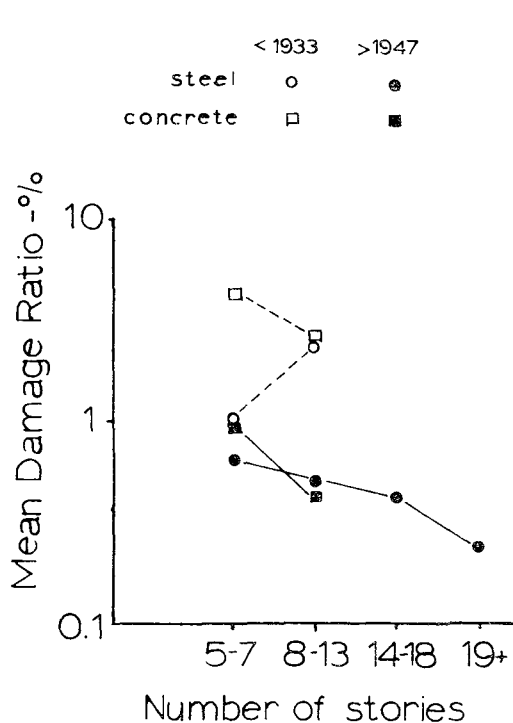


FIG. 4 VARIATION OF DAMAGE WITH BUILDING HEIGHT FOR INTENSITY VII

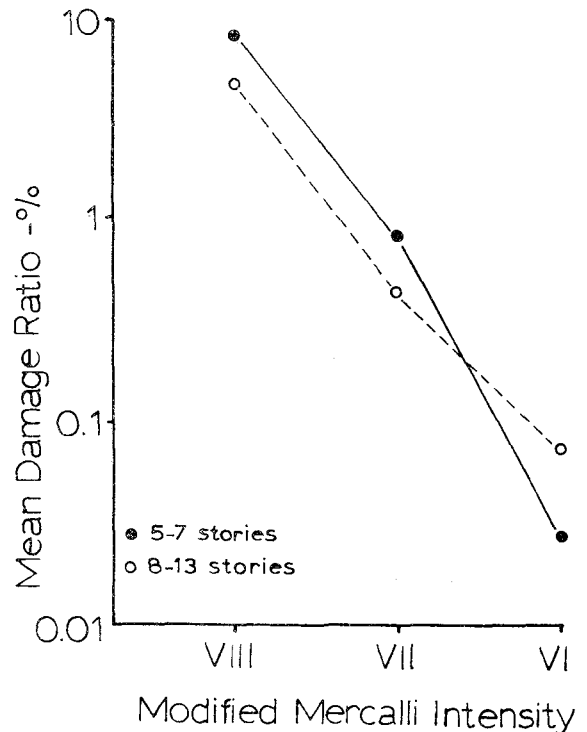


FIG. 5 VARIATION OF DAMAGE WITH INTENSITY FOR POST-1947 BUILDINGS

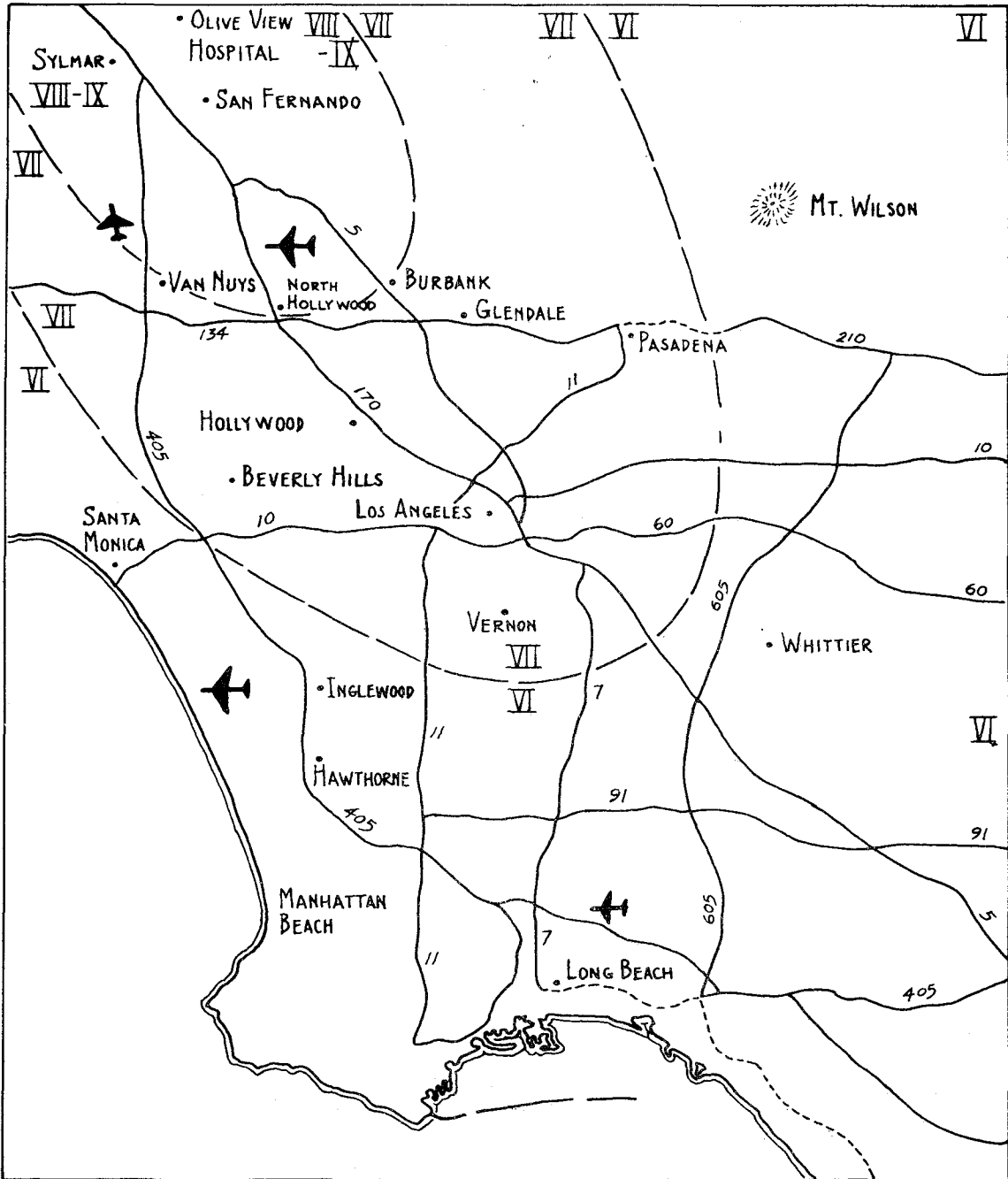


FIGURE 2 GEOGRAPHICAL AREA OF STUDY
 SHOWING FREEWAYS, AIRPORTS
 AND ISOSEISMALS